



# Review of the *Merodon natans* group with description of a new species, a key to the adults of known species of the *natans* lineage and first descriptions of some preimaginal stages

Ante Vujić<sup>1</sup>, Tamara Tot<sup>1</sup>, Andrijana Andrić<sup>2</sup>, Jelena Ačanski<sup>2</sup>, Ljiljana Šašić Zorić<sup>2</sup>, Celeste Pérez-Bañón<sup>3</sup>, Andrea Aracil<sup>3</sup>, Sanja Veselić<sup>1</sup>, Maja Arok<sup>1</sup>, Ximo Mengual<sup>4</sup>, André van Eck<sup>5</sup>, Santos Rojo<sup>3</sup>, Snežana Radenković<sup>1</sup>

- 1 University of Novi Sad, Faculty of Sciences, Department of Biology and Ecology, Trg Dositeja Obradovića 2, 21000 Novi Sad, Serbia; Ante Vujić [ante.vujic@dbe.uns.ac.rs]; Tamara Tot [tamarat@dbe.uns.ac.rs]; Sanja Veselić [sanja.veselic@dbe.uns.ac.rs]; Maja Arok [maja.arok@dbe.uns.ac.rs]; Snežana Radenković [snezana.radenkovic@dbe.uns.ac.rs]
- 2 University of Novi Sad, BioSense Institute, Dr Zorana Đinđića 1, 21000 Novi Sad, Serbia; Andrijana Andrić\* [andrijana.andric@biosens.uns.ac.rs]; Jelena Ačanski [acanski@biosense.rs]; Ljiljana Šašić Zorić [ljsasic@biosense.rs]
- 3 Department of Environmental Sciences and Natural Resources, Faculty of Sciences III, Campus of San Vicente, University of Alicante, Alicante, Spain; Celeste Pérez-Bañón [celeste.perez@ua.es]; Andrea Aracil [and.aracilgisbert@gmail.com]; Santos Rojo [santos.rojo@ua.es]
- 4 Zoologisches Forschungsmuseum Alexander Koenig, Adenauerallee 160, D-53113 Bonn, Germany; Ximo Mengual [x.mengual@leibniz-zfmk.de]
- 5 BioMongol Foundation, Korte Hoefstraat 30, 5046 DB Tilburg, The Netherlands; André van Eck [andrevaneck@biomongol.org]

<http://zoobank.org/F4545213-9C35-4104-A97E-14A8D1AC8029>

Corresponding author: Andrijana Andrić (andrijana.andric@biosens.uns.ac.rs)

Received 12 March 2021

Accepted 2 July 2021

Published 10 August 2021

Academic Editor Bradley Sinclair

**Citation:** Vujić A, Tot T, Andrić A, Ačanski J, Šašić Zorić L, Pérez-Bañón C, Aracil A, Veselić S, Arok M, Mengual X, van Eck A, Rojo S, Radenković S (2021) Review of the *Merodon natans* group with description of a new species, a key to the adults of known species of the *natans* lineage and first descriptions of some preimaginal stages. *Arthropod Systematics & Phylogeny* 79: 343–378. <https://doi.org/10.3897/asp.79.e65861>

## Abstract

*Merodon natans* group (Diptera, Syrphidae) taxa are reviewed using an integrative taxonomic approach combining morphological, morphometric and molecular techniques. The approach substantiates recognition of the three species: *M. calcaratus* (Fabricius, 1794), *M. natans* (Fabricius, 1794) and *M. pulveris* Vujić & Radenković in Radenković et al. 2011, and reveals the existence of a new species, *M. makrissi* Vujić, Radenković & Tot **sp. nov.**, which is described. It also highlights the existence of a series of *natans* group populations, especially on some of the Mediterranean islands, in the Levant and in the Afrotropical Region, for which more comprehensive data are required to clarify their status. A key is provided to the *natans* lineage species currently recognised, and preimaginal stages of some *natans*-group species are described for the first time. Redescriptions for *M. calcaratus* and *M. natans* are provided. A neotype is selected for *M. natans*. Lectotypes are designated for *M. annulatus* (Fabricius, 1794) and *M. melancholicus* (Fabricius, 1794). *Merodon annulatus* is recognised as a synonym of *M. natans*.

## Key words

distribution, flower flies, geometric morphometrics, immature stages, integrative taxonomy, *Merodon makrissi* sp. nov., mtDNA COI gene, nuclear 28S rRNA gene

## 1. Introduction

The phytophagous hoverfly genus *Merodon* Meigen, 1803 (Diptera, Syrphidae) contains 234 species distributed in the Palaearctic and Afrotropical regions, and introduced into North America and New Zealand (Vujić et al. 2021). Adults feed on flowers, ingesting pollen and nectar, whereas their larvae feed on bulbs and other underground storage organs of geophytes (i.e., Asparagaceae, Amaryllidaceae and Iridaceae). Several species-specific associations between *Merodon* species and geophyte host-plants have been confirmed; e.g., through records of oviposition behavior (Reemer and Goudsmits 2004), direct bulb-feeding (Popov 2010; Djan et al. 2020), and captive rearing of larvae (Pehlivan and Akbulut 1991; Stepanenko and Popov 1997; van Eck 2016). However, the larval food-plants and natural history remain unknown for the great majority of *Merodon* species and the immature stages have been described for only nine species within this genus so far (Heiss 1938; Stuckenberg 1956; Ricarte et al. 2008, 2017; Andrić et al. 2014; Preradović et al. 2018; Vujić et al. 2020a).

The *Merodon* fauna of the Balkan Peninsula, Aegean Islands, Turkey and the Iberian Peninsula are the most comprehensively explored (Marcos-García et al. 2007; Radenković et al. 2011, 2018a, 2020; Veselić et al. 2017; Vujić et al. 2011, 2020a, 2020b, 2020c, 2020d). The taxonomic status and identification of many *Merodon* species are still under scrutiny as the genus contains a high number of species groups comprising taxa with very subtle morphological differences. In various recent publications, an integrative taxonomic approach combining morphological and molecular information has been useful in resolving taxonomic problems in hoverflies (e.g., Marcos-García et al. 2011; Nedeljković et al. 2013, 2015, 2020; Vujić et al. 2013, 2020b, 2020c; Haarto and Ståhls 2014; Popović et al. 2015; Ačanski et al. 2016; Šašić et al. 2016; Kočiš Tubić et al. 2018; Šašić Zorić et al. 2018, 2020; Radenković et al. 2018a, 2020; Arok et al. 2019; Djan et al. 2020).

Based on the mitochondrial cytochrome c oxidase I (COI) and nuclear 28S rRNA gene sequences of *Merodon* species from Europe and Turkey, three well supported clades within the genus *Merodon* were established (Vujić et al. 2012): *M. aureus*, *M. nigritarsis* (corresponding to the *M. avidus* group of Mengual et al. (2006)) and the *M. albifrons*+*M. desuturinus* groups. Radenković et al. (2018b), based on phylogenetic analyses with additional taxa, recognized four lineages (putative subgenera) within *Merodon*; besides the three previously established ones (*albifrons*+*desuturinus*, *aureus* (sensu lato) and *avidus-nigritarsis*), one new lineage named *natans* was distinguished. Vujić et al. (2019), summarising previously published data (Šašić et al. 2016; Radenković et al. 2018b), cited five monophyletic lineages in *Merodon*, dividing the *albifrons*+*desuturinus* lineage sensu Vujić et al. (2012) into two lineages, *M. albifrons* and *M. desuturinus*. Thus, the current evolutionary lineages in *Merodon* are *albifrons*, *aureus*, *avidus-nigritarsis*, *desuturinus*, and *natans*.

The *Merodon natans* lineage contains the *M. natans* group and *M. segetum* (Fabricius, 1794) as an individual taxon. The *Merodon natans* group contains medium sized species with distinct pollinose ornamentation, vittae and fasciae on the scutum, and terga 2–4 with broad pollinose fasciae. This group includes three already known species, *M. calcaratus* (Fabricius, 1794), *M. natans* (Fabricius, 1794) and *M. pulveris* Vujić & Radenković in Radenković et al. 2011, recently revised by Radenković et al. (2011). In addition to marked morphological and molecular (5'-end COI sequence) differences between *M. natans* and *M. pulveris* (Radenković et al. 2011), Arok et al. (2019) provided geometric morphometric evidence for these species delimitation based on wing parameters. In the present work, a fourth species belonging to this group is described. The overall morphological similarity of these four taxa and the availability of the mentioned datasets prompted us to use an integrative approach to decipher the taxonomy of this species group.

The aims of the present study are: 1) to review specimens of this group deposited in several entomological institutions and private collections; 2) to define and describe a new taxon of the *Merodon natans* species group, with geographical distribution map of all species presented; 3) to infer the species diversity within this species group using molecular and geometric morphometric data; 4) to present the first data about the preimaginal morphology of some species of this group; and 5) to discuss biological data about the host plants of the *M. natans* group.

## 2. Material and methods

### 2.1. Taxonomic research

**Institutional acronyms.** The present study was based on examination of specimens belonging to the *Merodon natans* group deposited in the following entomological collections (abbreviations mentioned in the material citations are given in bold): Axel Ssymank collection, Bonn, Germany (AS coll.); André van Eck collection, Tilburg, The Netherlands (AvE coll.); Dieter Doczkal collection, München, Germany (DD coll.); Daniele Sommaggio collection, Bologna, Italy (DS coll.); Miroslav Barták collection, Prague, Czech Republic (MB coll.); Michael de Courcy Williams collection, Alexandroupoli, Greece (MCW coll.); Jeroen van Steenis collection, Amersfoort, The Netherlands (JvS coll.); Natural History Museum, London, United Kingdom (BMNH); Colección Entomológica de la Universidad de Alicante, Alicante, Spain (CEUA); Entomological Museum of Isparta, Isparta, Turkey (EMIT); Department of Biology and Ecology, Faculty of Sciences, University of Novi Sad, Novi Sad, Serbia (FSUNS); The Melissotheque of the Aegean, University of the Aegean, Mytilene, Greece (MAegean); Koninklijk Belgisch Instituut voor Natuurwetenschappen, Brussels, Belgium (KBIN); Finnish Museum of Natural History, University of Helsinki, Helsinki, Finland (MZH); Muse-

um of Zoology Lund University, Lund, Sweden (MZLU); Università di Firenze, Museo Zoologico “La Specola”, Firenze, Italy (MZUF); Muséum National d’Histoire Naturelle, Paris, France (MNHN); Naturalis Biodiversity Center, Leiden, The Netherlands (NBCN); Naturhistorisches Museum Wien, Vienna, Austria (NHMW); Natural History Museum of Montenegro, Podgorica, Montenegro (PMCG); Tel Aviv University, Tel Aviv, Israel (TAUI); Zoologisches Museum of the Humboldt University, Berlin, Germany (ZHMB); National Museum of Bosnia and Herzegovina, Sarajevo, Bosnia and Herzegovina (ZMBH); Zoologisches Forschungsmuseum Alexander Koenig, Bonn, Germany (ZFMK); Zoological Museum, Natural History Museum of Denmark, University of Copenhagen, Copenhagen, Denmark (ZMUC); World Museum Liverpool, Liverpool, United Kingdom (WML).

**Examined material.** During our detailed investigation of the *Merodon natans* group in the collections mentioned above, we examined more than one thousand specimens ( $n=549$  *M. natans*;  $n=426$  *M. pulveris*;  $n=89$  *M. makrissi* Vujić, Radenković & Tot sp. nov.;  $n=60$  *M. calcaratus*) collected over a 158 year period (1862–2020) from Algeria, Bulgaria, Croatia, Cyprus, France, Greece, Israel, Italy, Kenya, Libya, Montenegro, Morocco, North Macedonia, Portugal, Serbia, Somalia, Spain, Tunis and Turkey. Most of the captured adult specimens were collected using entomological nets, except for some specimens from Miroslav Barták’s collection and ZFMK collected with Malaise traps.

During three different field investigations of the localities where large populations of adult *Merodon* were previously recorded, two *Merodon* pupae were found (on Cyprus in February and in Serbia in September) and a larva (on Lesbos in April), all in the bulbs of *Prospero autumnale* (L.) Speta (Asparagaceae). Pupae were collected with the bulbs and reared at an ambient temperature until adults emerged. The larva was kept frozen ( $-20^{\circ}\text{C}$ ) for several days and preserved in 70% ethanol. The studied material of the immature stages has been deposited in the collection of FSUNS.

**Type material.** All types of the known species of *Merodon natans* group were examined by Ante Vujić, except for the type material of *M. natans* because the type specimen is destroyed (Zimsen 1964; Vujić A., pers. obs.). Only the name label with number 193.20 for this type specimen exists in the collection of ZMUC. For holotypes, neotype, paralectotype and lectotypes, the original label data have been given verbatim; quotation marks (“ ”) were used to indicate separate labels, a slash (/) has been used to indicate separate lines within a label.

**Morphological study of adults.** External morphological features of adults and characters of the male terminalia were observed using a Nikon SMZ 745T (Nikon Corporation, Tokyo, Japan) stereomicroscope. For studying the male terminalia structure, specimens were first relaxed in a humidity chamber and then their terminalia were ex-

tracted with a hook-tipped entomological pin. The terminalia were cleaned by boiling in a 10% solution of potassium hydroxide (KOH) for 3–5 minutes. This was followed by brief immersion in glacial acetic acid ( $\text{CH}_3\text{COOH}$ ) to neutralize the KOH, and then by immersion in ethanol ( $\text{C}_2\text{H}_5\text{OH}$ ) to remove the acid. Terminalia were examined and dissected in several drops of glycerin under stereomicroscope and finally, were stored in plastic microvials and pinned with the source specimens. Measurements of specimen size were made with the same stereoscope using an eyepiece graticule. Body length was measured from the frontal prominence, excluding the antenna to the tip of the abdomen. The length of the basoflagellomere was measured from its base to the apex (Fig. 2A:bl), and its width was measured in the widest part between its dorsal and ventral margins (Fig. 2A:bw).

**Morphological study of the immature stages.** Puparia were cleaned before morphological analysis. To do so, they were immersed in water for several hours. Soil and debris were removed from the surface using pins and brushes, and puparia were placed in an ultrasonic cleaner for five minutes, until adherent material had fallen off the integument. The head skeleton was removed from the antero-ventral margin of the puparium using entomological pins, then soaked in 10% potassium hydroxide (KOH) and heated for 15 minutes in order to remove the remaining tissue. It was then soaked in acetic acid to neutralize the KOH, followed by 70% ethanol to eliminate the acid, for a few minutes each. The skeleton was then preserved and examined in glycerin. The larva was frozen ( $-20^{\circ}\text{C}$ ) and preserved in 70% ethanol; no special preparation for the analysis was conducted.

Morphological studies on the puparium were conducted using a Hitachi SEM (Scanning Electron Microscope) S3000N (Hitachi Ltd, Tokyo, Japan) at 20 kV at variable-pressure (or low vacuum) mode and a Leica DFC 320 digital camera attached to a Leica MZ16 stereomicroscope (Leica Microsystems, Wetzlar, Germany). A Leica M205C stereomicroscope (with Leica DFC450 camera) (Leica Microsystems, Wetzlar, Germany) was used for the examination of the larva and for a general view of the puparium. Olympus SZX16 (with Olympus U-TVO.5XC-3 camera) (Olympus Corporation, Tokyo, Japan) and Nikon SMZ 745T (with Nikon Coolpix D7100 digital camera) (Nikon Corporation, Tokyo, Japan) stereomicroscopes were used for the examination of the head skeletons. Puparium dimensions were measured using an eyepiece micrometer attached to the stereomicroscope. Maximum puparial length, including the posterior respiratory process (prp), and maximum puparial width were recorded.

**Morphological terminology.** The adult morphological terminology used in descriptions and drawings follows Thompson (1999), except for terms “fossette” and “sensory pit” from Doczkal and Pape (2009), “proepimeron” from McAlpine (1981) and those proposed in Marcos-García et al. (2007) for structures of the male terminalia.

The general terminology for hoverfly immature stages follows Rotheray (1993) and Rotheray and Gilbert (1999) with characters of the head (= cephalopharyngeal) skeleton following Courtney et al. (2000), Rotheray and Gilbert (2008) and Rotheray (2019). Our descriptions of morphological characters are based on previous preimaginal descriptions of the genus *Merodon* (e.g., Ricarte et al. 2008, 2017; Andrić et al. 2014; Preradović et al. 2018).

**Abbreviations.** Abbreviations for antenna are shown in Fig. 2: **bl** – length of basoflagellomere, **bw** – width of basoflagellomere, **f** – fossette. Abbreviations for male genitalia structure are shown in Figs 8, 10, 14: **a** – anterior surstyle lobe, **aa** – aedeagal apodeme, **ae** – aedeagus, **ea** – ejaculatory apodeme, **c** – cercus, **la** – lateral sclerite of aedeagus, **n** – notch on theca to which is attached the aedeagal apodeme; **p** – posterior surstyle lobe, **v** – triangular prominence on ventral margin of posterior surstyle lobe. Abbreviations for puparial head skeleton are shown in Fig. 15: **c** – cibarium, **db** – dorsal bridge, **dc** – dorsal cornu, **is** – intermediate sclerite, **m** – mandibles, **mo** – mortar, **p** – pestle, **vc** – ventral cornu, **vp** – vertical plate; and for the other preimaginal morphology features in Figs 16, 17, 19: **am** – antenno-maxillary organs, **as** – anterior spiracle, **cs** – central scar, **eat** – external accessory teeth, **iat** – internal accessory teeth, **is** – inter-spiracular setae, **lp** – lappets, **mh** – mouthhooks, **pps** – primordia of pupal spiracles, **prp** – posterior respiratory process, **so** – spiracular opening, **tu** – tubercle.

**Drawings and photos.** Drawings were made with a FSA 25 PE drawing tube attached to Leica MZ16 stereomicroscope. Leica DFC 320 digital camera (Leica Microsystems, Wetzlar, Germany) attached to Leica MZ16 stereomicroscope was used to take photos for Figures 1, 3, 13. Figures were processed with CombineZ5 (Hadley 2006) software and edited with Adobe Photoshop CS3 version 10.0 (Adobe Systems Incorporated, San Jose, California, USA, 2007).

**Distribution map.** The geographical distribution map of all species of the *Merodon natans* group was produced with the aid of DIVA-GIS version 7.5 (Hijmans et al. 2012) software.

## 2.2. Geometric morphometric analysis of adults

Geometric morphometric analysis of wing shape, based on measurements of the venation, was conducted using 285 specimens (209 specimens from Arok et al. (2019), marked with \* in the Supplementary file 1: Table S1) of three species from the *Merodon natans* group. Out of the 111 specimens of *M. natans* analysed, three specimens were new including two specimens from Greece and one specimen from Italy (Sicily) providing a broader geographical analysis than given in Arok et al. (2019). A total of 36 specimens of *M. pulveris* were new for the analysis

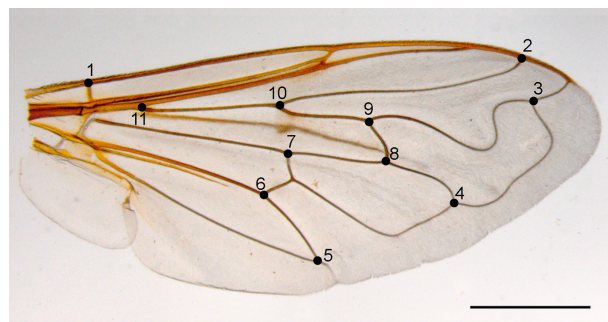


**Figure 1.** The location of 11 landmarks on the right wing in the *Merodon pulveris* selected for geometric morphometric analysis. Scale bar: 1 mm.

including two from Cyprus (Limassol) and 27 from Turkey again providing a broader geographical analysis than given in Arok et al. (2019). All 38 specimens of *M. calcaratus* were new to the analysis. *Merodon makrisi* Vujić, Radenković & Tot sp. nov. was excluded from geometric morphometric analysis due to an insufficient number of available specimens. For the population level analysis 270 specimens, from 54 different localities, grouped into 15 populations based on geographical proximity were used (Supplementary file 1: Table S1). Specimens from Algeria, Bulgaria, Cyprus, Italy, Portugal and Tunisia were not included in population level analysis due to small sample size.

Three separate geometric morphometric analyses were conducted. Two analyses for species level identification were carried out separately on males and females due to sexual dimorphism (Arok et al. 2019), and a third to explore phenotypic differentiation among populations.

The geometric morphometric analyses were based on right wings which were dissected using micro-scissors under Nikon SMZ 745T stereomicroscope and mounted on a microscopic slide using Hoyer's medium. Each wing was labeled with a unique code for the FSUNS collection, together with other data relevant to the specimens, and photographed using a Leica DFC320 camera attached to a Leica MZ16 stereomicroscope.

Eleven homologous landmarks, evenly distributed across the wing, were digitized using TpsDig 2.05 (Rohlf 2017a) (Fig. 1). Generalised least squares Procrustes superimposition on the raw coordinates was done using TpsRelw v1.68 (Rohlf 2017b) to minimize non-shape variations in location, scale and orientation of wings, and to superimpose the wings in a common coordinate system (Rohlf and Slice 1990; Zelditch et al. 2004).

To explore wing-shape variation among specimens without *a priori* defined groups, a principal component analysis (PCA) was carried out. Next, the discriminant function analysis (DA) and canonical variate analysis (CVA) were employed to analyse the shape differences among species and populations. Phenetic relationships among the species and populations were characterised using an unweighted pair group method with arithmetic Mahalanobis distances computed from the discriminant function analysis. Superimposed outline drawings were

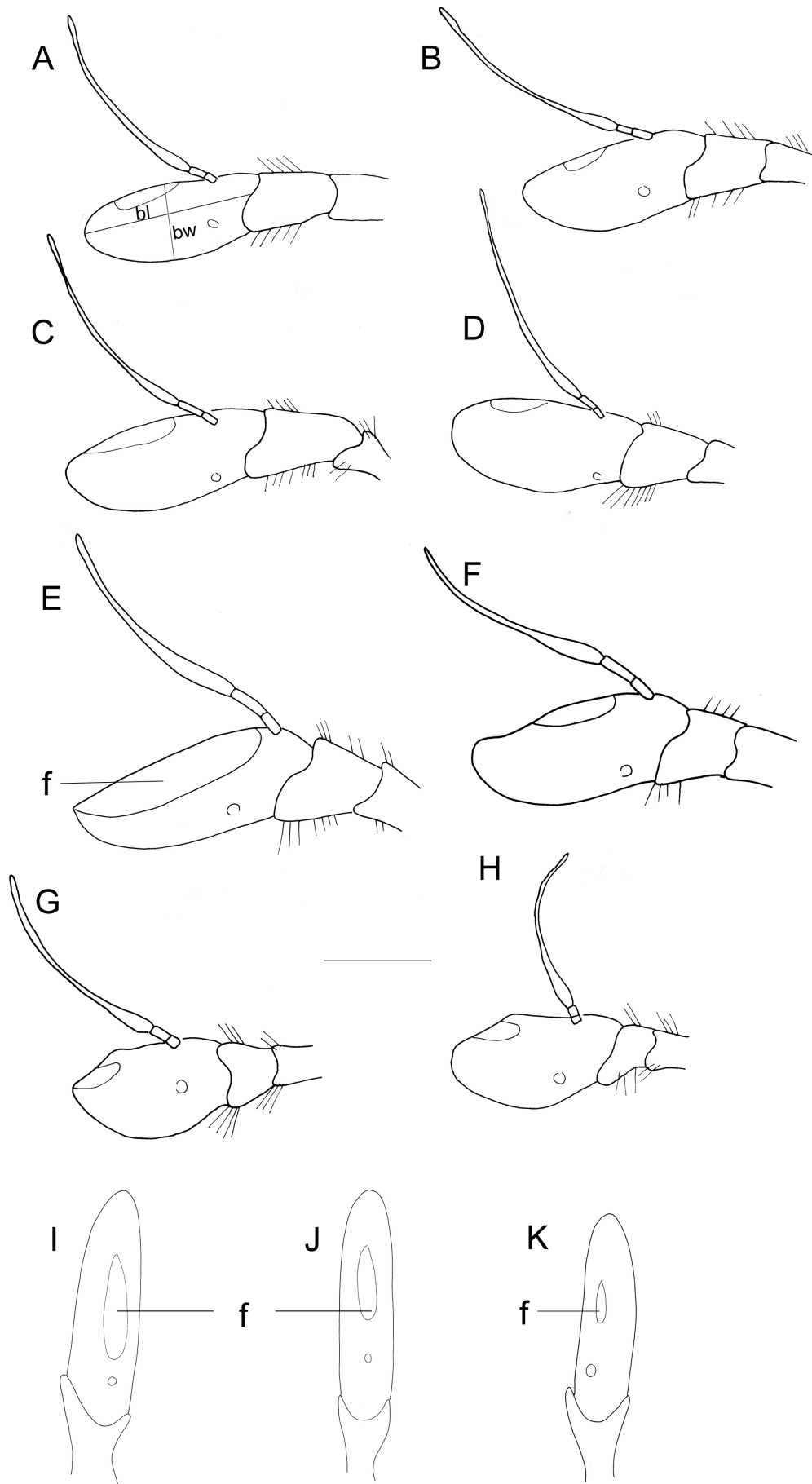


**Figure 2.** Antenna. **A, B, J** *Merodon natans* **C, D, K** *M. pulveris* **E, F, I** *M. makrissi* Vujić, Radenković & Tot sp. nov. **G, H** *M. calcaratus*; **A, C, E, G** male **B, D, F, H–K** female; **A–H** lateral view **I–K** dorsal view; **A** Greece (Olimp) **B** Greece (Achaia) **C, D** Turkey **E, F, I** Cyprus **G, H** Spain **J** Greece (Alexandroupoli) **K** Turkey. Scale bar: 0.2 mm.

produced using MorphoJ version 2.0 (Klingenberg 2011) to visualise differences in mean wing shape among species. All statistical analyses were calculated using Statistica for Windows version 13 (TIBCO Software Inc. 2018).

## 2.3. Molecular analysis

Genomic DNA of 42 adult hoverfly specimens was obtained for the present study. For specimens processed at FSUNS, DNA was extracted from meso and metalegs using the sodium dodecyl sulfate (SDS) extraction protocol (Chen et al. 2010). The same protocol was applied for DNA extraction from the mid body part of a larva (specimen AU 1590). The DNA vouchers are deposited at FSUNS. For specimens deposited at ZFMK (identified as ZFMK-DIP numbers in the Supplementary file 1: Table S1), the extraction protocol by Mengual et al. (2018) was followed. Detailed information on analysed specimens is provided in the Supplementary file 1: Table S1.

For sequences obtained at ZFMK, polymerase chain reaction (PCR) amplification protocol follows Rozo-Lopez and Mengual (2015). For sequences obtained at FSUNS, PCRs were carried out in 25 µl reaction volumes. The PCR mixture contained 1x reaction buffer (Thermo Scientific, Vilnius, Lithuania), 2.5 mM MgCl<sub>2</sub>, 0.1 mM of each nucleotide, 1.25U Taq polymerase (Thermo Scientific, Vilnius, Lithuania), 5 pmol of each primer, and 50–100 ng of template DNA. The amplification conditions were as follows: 95°C for 2 min; 29 cycles of 94°C for 30 s, 49°C (for the 3' end of the COI gene) for 30 s or 50°C (for the 5' end of the COI gene and D2-3 region of the 28S rRNA gene), and 72°C for 2 min; with a final extension at 72°C for 8 min. We used C1-J-2183 (also known as Jerry) and TL2-N-3014 (also known as Pat) primer pair for amplification and sequencing of the 3'COI (Simon et al. 1994), LCO1490 and HCO2198 (Folmer et al. 1994) for the 5' COI, and F2 and 3DR (Belshaw et al. 2001) for the D2-3 region of the 28S rRNA gene. PCR products were purified using Exonuclease I and FastAP Thermosensitive Alkaline Phosphatase (Thermo Scientific, Vilnius, Lithuania) following the manufacturer's instructions. ZFMK specimens were sequenced bidirectionally at Macrogen Europe (Amsterdam, The Netherlands), while FSUNS specimens were sequenced in forward direction by the Sequencing Laboratory of the Finnish Institute for Molecular Medicine (Helsinki, Finland) and Macrogen Europe (Amsterdam, The Netherlands).

### 2.3.1. Sequence processing

The COI and 28S rRNA gene sequences were edited for base-calling errors using BioEdit 7.0.9.0. (Hall 1999). The COI gene sequences were aligned manually, while 28S rRNA gene sequences were aligned using MAFFT version 7 (Kato and Standley 2013) and the Q-INS-i algorithm. We prepared two sequence matrices, one which

contained concatenated non-continuous 5' and 3' COI sequences and the other with combined COI and 28S rRNA gene sequences. In order to assess the monophyly of the *Merodon natans* species group that belongs to the *M. natans* lineage, we included additional sequences of representatives of all *Merodon* lineages (sensu Vujić et al. 2019): (1) *M. avidus-nigritarsis* lineage (*M. avidus* (Rossi, 1790), *M. italicus* Rondani, 1845, *M. testaceus* Sack, 1913, *M. nigritarsis* Rondani, 1845, *M. ottomanus* Hurkmans, 1993); (2) *M. aureus* lineage (*M. aureus* Fabricius, 1805, *M. cinereus* (Fabricius, 1794), *M. chalybeus* Wiedemann in Meigen, 1822); (3) *M. desaturinus* lineage (*M. desaturinus* Vujić, Šimić & Radenković, 1995); (4) *M. albifrons* lineage (*M. albifrons* Meigen, 1822, *M. geniculatus* Strobl in Czerny & Strobl, 1909, *M. luteofasciatus* Vujić, Radenković & Stähls, 2018 in Vujić et al. 2018a, *M. papillus* Vujić, Radenković & Pérez-Bañón, 2007, *M. armipes* Rondani, 1843, *M. constans* (Rossi, 1794), *M. triangulum* Vujić, Radenković & Hurkmans, 2020 in Vujić et al. 2020b) and (5) *M. natans* lineage (*M. segetum* (Fabricius, 1794)). For GenBank accession numbers of all analysed sequences see Supplementary file 1: Table S1. Maximum Parsimony (MP) analysis was performed in NONA version 2.0 (Goloboff 1999) spawned with the aid of ASADO (Nixon 2008) using the heuristic search algorithm with 1,000 random addition replicates (mult\*1,000), holding 100 trees per round (hold/100), maxtrees set to 100,000 and applying tree-bisection-reconnection (TBR) branch swapping. The bootstrap support values for clades were calculated with 1,000 replicates. The Maximum Likelihood (ML) trees were constructed in RAxML 8.2.8 (Stamatakis 2014), using the CIPRES Science Gateway web portal (Miller et al. 2010) under the general time-reversible (GTR) evolutionary model (only available model of nucleotide substitution in the RAxML) with a gamma distribution (GTRGAMMA) (Rodríguez et al. 1990). For combined COI+28S rRNA gene sequences ML analysis was done with partitioning by genes. Nodal supports were estimated using rapid bootstrapping with 1000 replicates. The trees were rooted on *Eumerus pulchellus* Loew, 1848. The average uncorrected *p* distances between species of the *M. natans* group were estimated using the COI gene sequence matrix in MEGA 7 software (Kumar et al. 2016).

## 2.4. Correlation among wing shape, genetic, spatial differentiation

To test pairwise correlations between morphometric, genetic, and geographical distances among species, simple two-tailed Mantel tests were performed (Mantel 1967) with 10 000 permutations in PaSSaGe version 2 (Rosenberg and Anderson 2011). Morphometric distances were represented as a matrix of pairwise squared Mahalanobis distances, and genetic distances as a matrix of uncorrected *p* distances. Geographical distances were calculated as the minimum distance between two species using QGIS (Quantum GIS Development Team 2012).

### 3. Results

#### 3.1. Taxonomy

Species belonging to the *Merodon natans* lineage, including *M. segetum*, share the following characters: posterior side of mesocoxa with less than 10 pile; pile on anterior anepisternum reduced; anterior lobe of surstylus in its inner side well developed, oval, rounded, pilose, without curved distal prolongation (Figs 5A–G, 8A, B, 10A–D); basoflagellomere elongated, 1.75 to 2.4 times as long as wide, narrowed in apical third (Fig. 2A–H) (shorter in *M. calcaratus*); tergum 2 with inconspicuous reddish anterolateral maculae, always absent in *M. calcaratus* and may be absent in some specimens of other species of *M. natans* group. In *M. segetum*, scutum with indistinct white pollinose vittae; terga 2–4 with or without narrow white pollinose fasciae.

The *Merodon natans* species group (Fig. 3) contains medium sized, black, short pilose species characterized by the following diagnostic features: scutum with distinct white pollinose ornamentation, vittae and fasciae (less developed in males of *M. calcaratus*); terga 2–4 with broad white pollinose fasciae, which may be interrupted in the middle; legs black, except reddish-brown tibiae darkened in the middle and reddish-brown first and second tarsomeres of pro-, meso- and metalegs (in *M. calcaratus* all tarsomeres of pro-, meso- and metalegs black); in some specimens the base and apex of femora yellowish.

#### *Merodon calcaratus* (Fabricius, 1794)

*Syrphus calcaratus* Fabricius, 1794: 301.

**Diagnosis.** *Merodon calcaratus* is a medium sized (8–11 mm) black species. It can be easily distinguished from other members of the *M. natans* group by its shorter antenna; curved dorsal margin of basoflagellomere; small fossette near apex of basoflagellomere (Fig. 2G, H); narrow metafemur (Fig. 4G, H); black tarsomeres; completely black tergum 2. Narrow, fingerlike posterior surstyle lobe of male genitalia (Fig. 5A–G).

**Type material. Holotype:** NORTH WEST AFRICA: 1 ♂, original labels: “Zywan Africae”, “*E. calcaratus*”, “type” [red label] in J.C. Fabricius collection (ZMUC) [examined; in good state, but without male genitalia]. — **Other studied material.** Published in van Eck (2016) and van Eck et al. (2020a). — **Additional material examined.** ALGERIA: 1 ♀; Tlencen, 20 km N from Maghnia Babtaza; 34.9667°N, 1.75°W; 9 Apr. 1983; NBCN 1 ♂; Alger, Daly Ibrahim; 36.7533°N, 2.985°E; 15 Mar. 1910; MNHN 1 ♂; Fraïss Vallon env d’Alger; 36.7763°N, 3.0350°E; 30 Oct. 1892; P. Lesni leg.; MNHN. — KENYA: 1 ♂; Taita distr., Surroundings of Voi; 3.3616°S, 38.5677°E; 31 May–3 Jun. 1994; L. Bartolozzi, B. Cecchi, A. Sforzi leg.; “num. mag. 1561”; MZUF. — LIBYA: 1 ♂; Tripolitania, Garyan hills; 32.1928°N, 13.0190°E; 5–16 Nov. 1958; K.M. Guichard leg.; BMNH. — MOROCCO: 1 ♂; 38 km SW of El Jadida; 32.9723°N, 8.7508°W; 600 m a.s.l.; 2 Jan. 2003; J.H. Stuke leg.; ZFMK-DIP-00069620 (ZFMK) 2 ♀♀; same data as



**Figure 3.** *Merodon natans* male, dorsal view (Greece (Argalasti)). Scale bar: 1 mm.

for preceding; ZFMK-DIP-00072941, ZFMK-DIP-00072942 (ZFMK) 10 ♀♀; Mountain de Beni-Snassen, Garbouz; 34.918°N, 2.052°W; 526 m a.s.l.; 14 Oct. 2017; A. Vujić, S. Radenković, N. Kočič Tubić, N. Veličković leg.; FSUNS 4 ♀♀; near Nador; 35.1408°N, 2.9853°W; 13 Oct. 2017; A. Vujić, S. Radenković, N. Kočič Tubić, N. Veličković leg.; FSUNS. — SPAIN: 1 ♂; Grazalema; 36.7254°N, 5.3293°W; 813 m a.s.l.; 30 Sep. 2016; A. Vujić, S. Radenković, A. Juslén leg.; FSUNS ID 10853 (FSUNS) 13 ♂♂; Grazalema 2; 36.7671°N, 5.3575°W; 825 m a.s.l.; 30 Sep. 2016; A. Vujić, S. Radenković leg.; FSUNS ID 10810 to 10822 (FSUNS) 11 ♀♀; same data as for preceding; FSUNS ID 10823 to 10833 (FSUNS) 1 ♂; Grazalema 3; 36.7730°N, 5.3595°W; 1 Oct. 2016; A. Vujić leg.; FSUNS ID 10793 (FSUNS) 1 ♀; same data as for preceding; FSUNS ID 10794 (FSUNS). — TUNIS: 1 ♂, 1 ♀; [locality and date unknown].

**Redescription. MALE. Head:** *Antenna:* short, dark brown to blackish; basoflagellomere about 1.75 times as long as wide with curved dorsal margin; small fossette positioned near apex of basoflagellomere. *Face:* black, white pollinose; covered with long white pile as long as pedicel; ventral part of face and anteroventral part of gena black, shiny; frontal triangle black, white pollinose, covered with dense, long white pile as long as pedicel; eyes holoptic, covered with white pile as long as scape; vertical triangle isosceles black, shiny, except for anterior part to anterior ocellus and posterior part to posterior ocelli white pollinose; vertical triangle covered with intermixed long white and black pile as long as pile on frontal triangle; ocellar triangle equilateral; occiput blackish white pollinose covered with white pile as long as pile on vertical triangle. *Thorax:* Scutum black, with less developed white pollinose vittae; covered with yellow erect pile as long as pile on occiput, in some specimens black pile present on area between transverse suture and scutellum; area above wing base with short black bristles; scutellum black covered

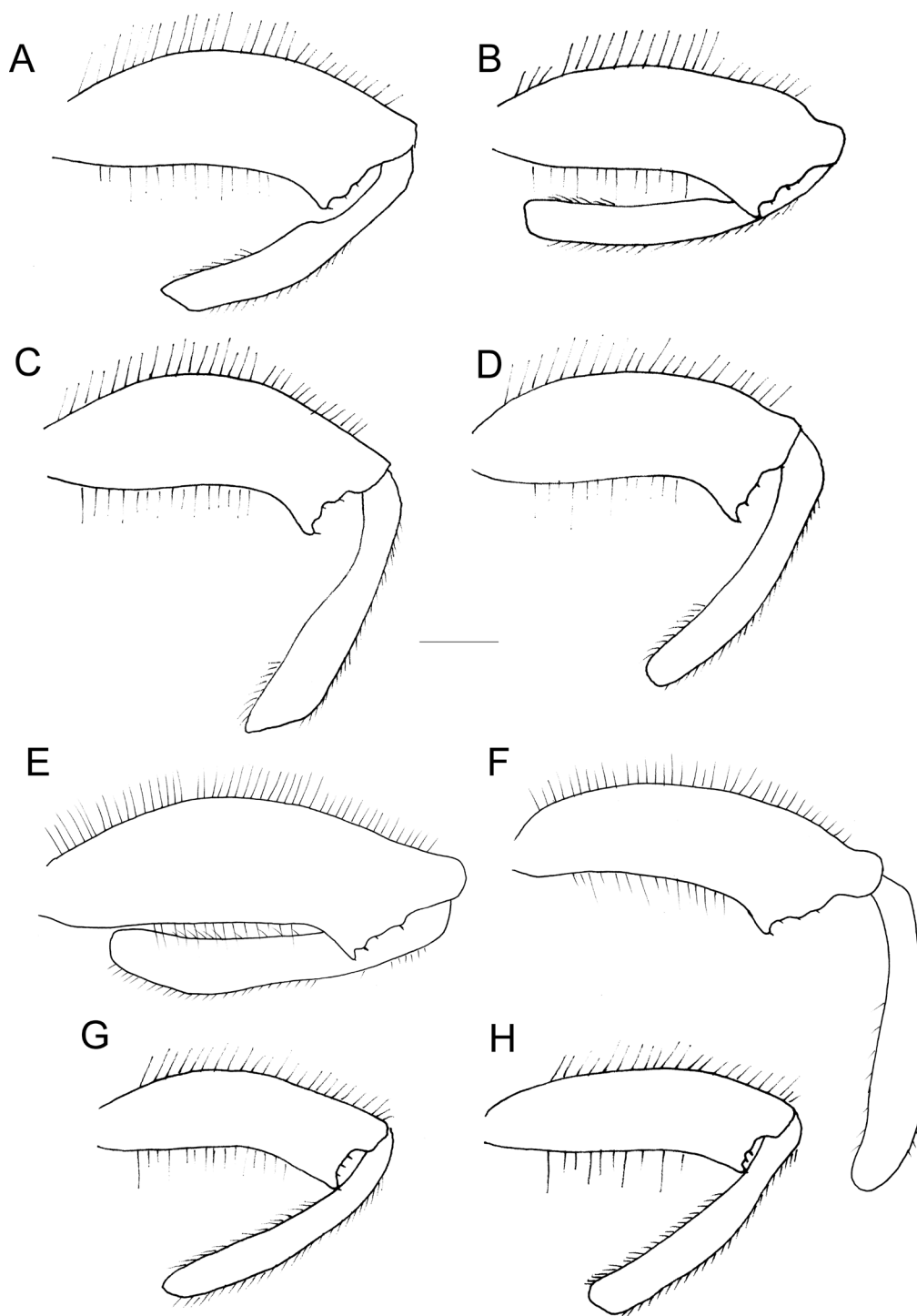


**Figure 4.** Metaleg without tarsomeres, lateral view. **A, B** *Merodon natans* **C, D** *M. pulveris* **E, F** *M. makrasi* Vujić, Radenković & Tot sp. nov. **G, H** *M. calcaratus*; **A, C, E, G** male **B, D, F, H** female; **A** Italy (Sicily) **B** Croatia **C, D** Turkey **E, F** Cyprus **G** Algeria **H** Tunis. Scale bar: 1 mm.

with long yellowish pile as long as pile on scutum; pleura black, white pollinose; dorsal part of anterior anepisternum, posterior anepisternum, anterior anepimeron, dorso-medial part of anepimeron with long, dense white pile as long as pile on scutum; long white pile on katepisternum broadly separated with bare area between; proepimeron and katatergum with some white pile. *Legs*: femora black, yellow only at apex; metafemur narrowed (Fig. 4G), with serrated triangular lamina in its apical part; tibiae black, yellow only at base and apex; tarsomeres dorsally black,

ventrally yellow; legs covered with mainly whitish pile, black pile present on apex of femora and on tarsomeres dorsally; tarsomeres ventrolaterally with bristle, which color varies from black to yellowish. *Wing*: hyaline, covered with microtrichia, except for some bare areas in first and second basal cells; stigma light yellow; wing veins dark brown; halter and calypter yellowish. *Abdomen*: Black, slightly tapering; terga 2–4 with white pollinose fasciae; pollinose fasciae on terga separated, not reaching lateral margin; terga 2–3 covered with black adpressed

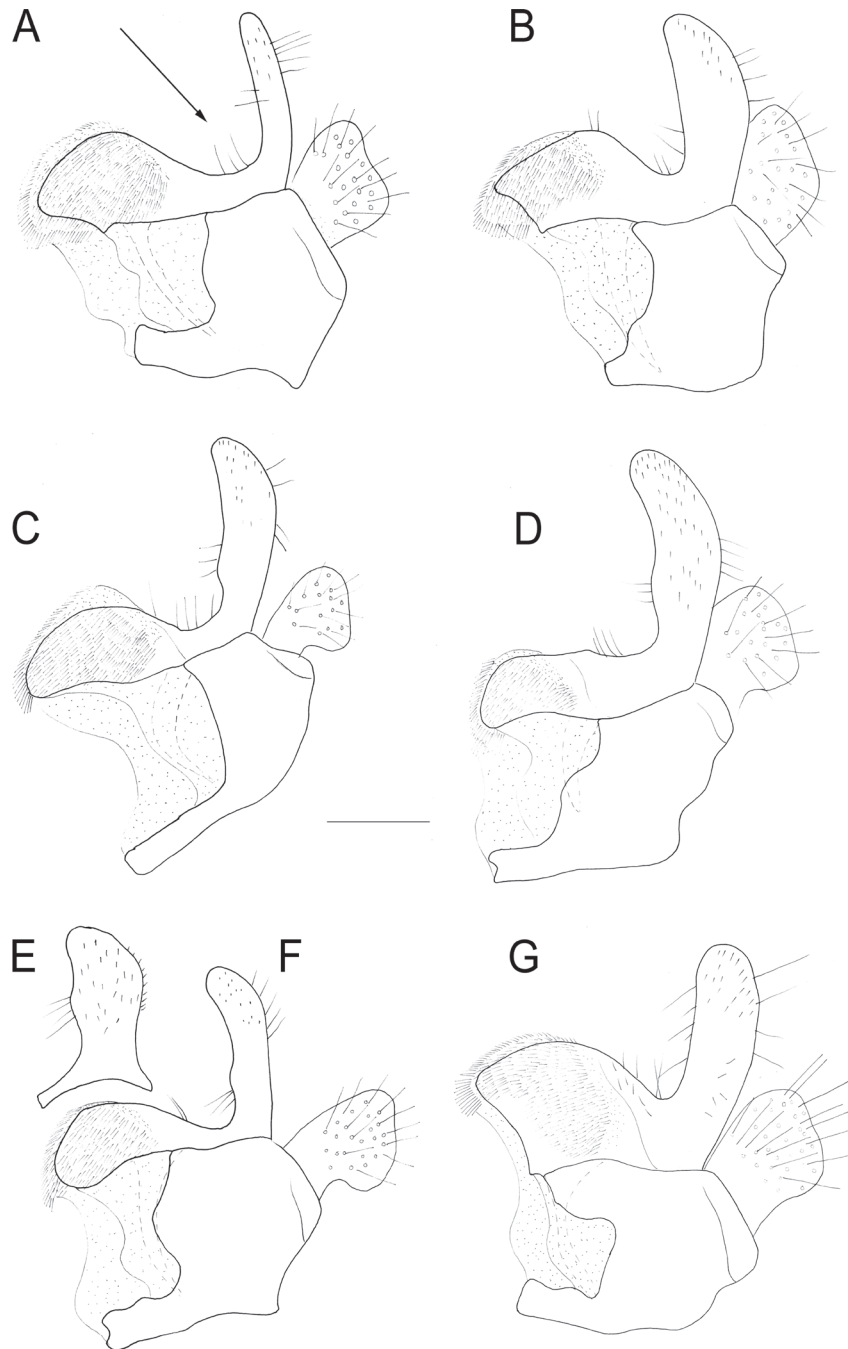


**Figure 5.** *Merodon calcaratus* epandrium, lateral view. **A** Morocco **B, D** Algeria **C** Tunis **E** left surstyle of specimen from Kenya **F** Kenya **G** Spain. Arrow marks invagination on ventral margin of surstyle. Scale bar: 0.2 mm.

pile medially and white pile laterally; tergum 4 covered with intermixed black and white pile; sterna blackish covered with white erect pile in some specimens pile on sternum 4 shorter than those on sterna 2–3. **Male genitalia:** *Epandrium:* posterior surstyle lobe of male genitalia narrow, fingerlike; anterior surstyle lobe on inner side oval shaped, covered with dense, short white pile (Fig. 5A–G); cercus square-like to rounded; *Hypandrium:* as in other members of *Merodon natans* group, medially broadened. **FEMALE:** Similar to male, except for normal sexual dimorphism and by following character: well developed white pollinose vittae present on scutum (in males scutum with less developed white pollinose vittae).

**Variability.** *Merodon calcaratus* is characterized by its easily recognizable narrow and long posterior surstyle lobe which however, is highly variable in its shape amongst specimens from different geographical populations: very narrow in width in specimens from Morocco (Fig. 5A); broader in width, medioventrally with a protuberance in specimens from Algeria (Fig. 5B, D); in specimens from Tunisia similar to specimens from Algeria, but narrower in width (Fig. 5C); in specimens from Spain apically rounded, similar to specimens from Morocco, but broader in width (Fig. 5G); the specimen from Kenya is unique, because of the asymmetry of the left (Fig. 5E) and the right posterior surstyle lobe (Fig. 5F). This vari-

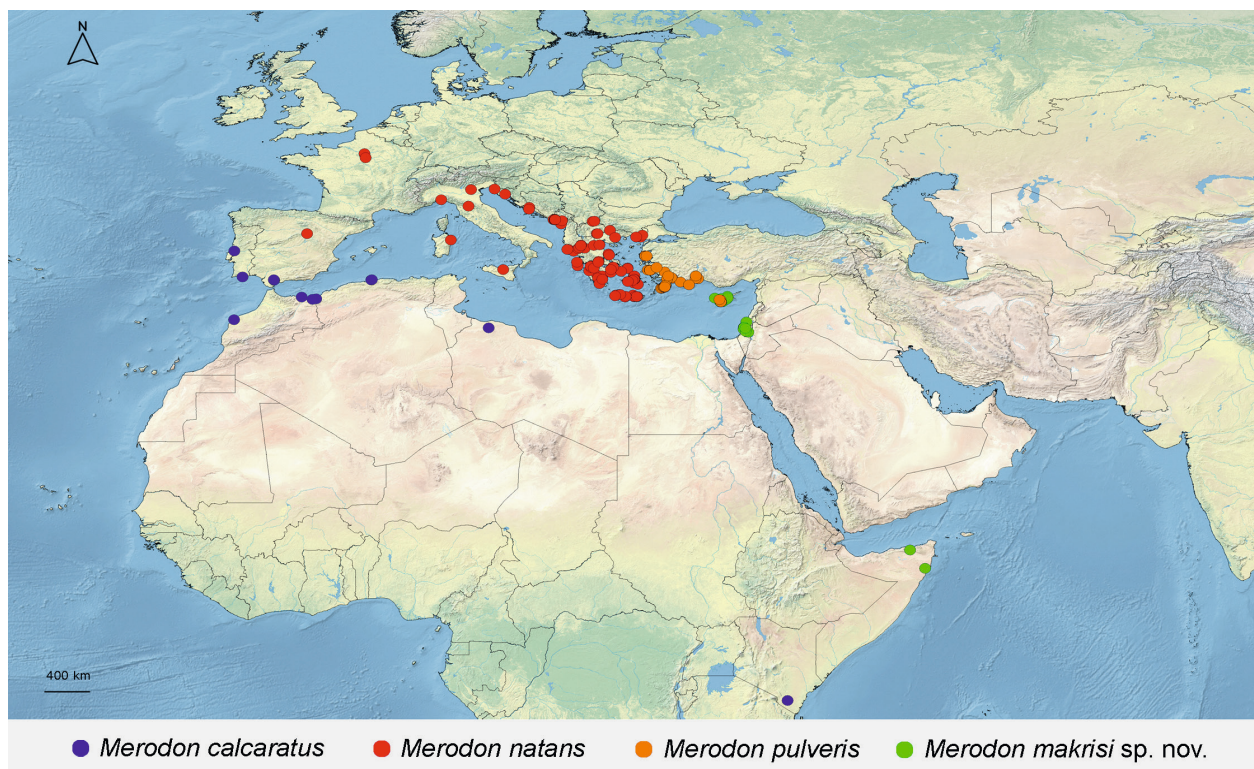


**Figure 6.** Distribution map of the species of *Merodon natans* group.

ability of surstyle lobe is unusual among most of the species of the genus *Merodon*, but shape of basoflagellomere connects all these populations in one taxon. Genetic data clearly connect populations from Spain and Morocco in spite of differences in the shape of surstyle lobe. Lack of genetic data and small number of specimens in African populations prevents use of an integrative approach. We decided to keep all these populations under the name *M. calcaratus* until future research.

**Distribution.** *Merodon calcaratus* occurs in the southern part of the Iberian Peninsula (Spain, Portugal), in North Africa (Morocco, Algeria (Haffaressas et al. 2017), Tunisia, Libya) and one isolated record present in East Africa (Kenya) (Fig. 6).

**Biology.** The preferred environment of the species is semi-arid, sandy calcareous grasslands with scattered *Pinus pinea* L. in Portugal (van Eck 2016), thermophilic and ancient pastures of a limestone massif, also in Portugal (van Eck et al. 2020a); and *Pinus* forest on low mountains in Morocco with large populations of potential host plant *Prospero autumnale* (Vujić A. pers. obs.). Flowers visited: *Drimia maritima* (L.) Stearn, in Portugal (van Eck 2016; van Eck et al. 2020a) and *Prospero autumnale* in Morocco and Spain (Vujić A. pers. obs.). Flight period on the Iberian Peninsula and in North Africa is usually Autumn or exceptionally early spring (Algeria). Preimaginal stages are not described.

### *Merodon makrиси* Vujić, Radenković & Tot sp. nov.

<http://zoobank.org/D37E323B-C715-488D-A28A-E1904E037CA8>

Fig. 7A, B

*Merodon* aff. *natans* in van Steenis et al. 2019: 139.

**Type locality.** CYPRUS: Limassol, Platres, Trooditissa Picnic Site, 4 Oct. 2017, X. Mengual leg.

**Type material.** *Holotype*: 1 ♂, pinned, with genitalia in a separate microvial with glycerine. Left metaleg glued to the locality label. Original labels: “Cyprus: Limassol, Platres, / Trooditissa Picnic Site, 1340m., / 34.914736°N 32.842261°E, / 4 Oct. 2017. X. Mengual leg.”, “DNA voucher specimen / ZFMK, Lab code / D363 / Bonn, Germany”, “ZFMK DIP / 00028063 [QR code]”. *Paratypes*: CYPRUS: 1 ♂; Mia Milia; 2 Nov. 1926; S.J. Curry leg.; “Anti Locust Res. Centre Reg. No. 453”; FSUNS ID 04973 (TAUI) 1 ♀; same data as for preceding; FSUNS ID 04965 (TAUI) 1 ♀; Limassol, Eftagonya; 550 m a.s.l.; 25 Oct. 1951; G. Mavromoustakis leg.; KBIN (R.I.Sc.N.B. 24.236) 3 ♂♂; Paramali; 34.6754°N, 32.8043°E; 1 Nov. 2013; C. Makris leg.; AvE coll. 1 ♀; Limassol, Fasouri; 34.63°N, 32.92°E; 9 Nov. 2013; C. Makris leg.; AvE coll. 5 ♂♂; Episkopi; 34.87°N, 32.87°E; 4 Nov. 2014; C. Makris leg.; AvE coll. 1 ♂; Episkopi, Kourion; 34.6699°N, 32.8754°E; 7 Feb. 2016; A. van Eck leg.; collected bulbs of *Prospero autumnale* (*Scilla autumnalis*), 1 male emerged 21 Oct. 2016; CEUA 1 ♀; Episkopi; 34.8754°N, 32.8754°E; 30 Oct. 2016; A. van Eck leg.; AvE coll. 2 ♂♂; Lefkara; 34.9026°N, 33.3392°E; 31 Oct. 2016; A. van Eck leg.; on low hanging branches and leaves of carob tree; AvE coll. 1 ♀; Episkopi; 34.8754°N, 32.8754°E; 2 Nov. 2016; A. van Eck leg.; on bare ground, in *Pinus bru-*



**Figure 7.** *Merodon makrisi* Vujić, Radenković & Tot sp. nov. **A** male in Cyprus, photo: C. Makris, 14 Nov. 2016 **B** female in Cyprus, photo: C. Makris, 24 Oct. 2013 **C** typical habitat in Cyprus where *M. makrisi* Vujić, Radenković & Tot sp. nov. can be collected. Bulbs of *Prospero autumnale* were collected in the patch in the front, from which one male specimen was reared. Photo: A. van Eck, 7 Feb. 2016.

*tia* / *Cistus*-vegetation; AvE coll. 1 ♂; same data as for preceding; on the ground, in more open vegetation 1 ♀; Neo Chorio, Akamas; 35.0259°N, 32.3508°E; 200 m a.s.l.; 2 Nov. 2016; A. van Eck leg.; AvE coll. 1 ♂; Kakopetria; 34.9746°N, 32.9132°E; 3 Nov. 2016; A. van Eck leg.; AvE coll. 2 ♂♂, 2 ♀♀; Agios Sozomenos; 35.0496°N, 33.4406°E; 5 Nov. 2016; C. Makris leg.; AvE coll. 1 ♂, 3 ♀♀; Lemesos; 34.66°N, 32.87°E; 4 Oct. 2017; C. Makris leg.; near *Prospero autumnale*; AvE coll. 1 ♂; Limassol, Platres, Trooditissa Picnic Site; 34.9147°N, 32.8422°E; 1340 m a.s.l.; 4 Oct. 2017; X. Mengual leg.; ZFMK-DIP-00028063 (DNA-voucher D363) (ZFMK) in van Steenis et al. (2019) as *Merodon* aff. *natans*; 1 ♂; Episkopi, near Ancient Kourion stadium; 34.6709°N, 32.8745°E; 112 m a.s.l.; 7 Oct. 2017; X. Mengual leg.; ZFMK-DIP-00028064 (DNA-voucher D367) (ZFMK) in van Steenis et al. (2019) as *Merodon* aff. *natans*; 1 ♀; Paphos, Paphos Forest, Appides stream; 34.9913°N, 32.647°E; 747 m a.s.l.; 6–12 Oct. 2017; X. Mengual leg.; double-head Malaise trap; ZFMK-DIP-00027887 (DNA-voucher D395) (ZFMK) 1 ♂; Kyrenia, Lapithos; 35.3477°N, 33.1504°E; 5 m a.s.l.; 14–28 Oct. 2018; Ö. Özden leg.; Malaise trap in garden; AvE coll.; (*Merodon* sp. in van Eck et al. (2020b)). — **Additional material examined.** ISRAEL: 2 ♂♂; Mount Carmel; 32.7430°N, 35.0475°E; 30 Sep. 1971; A. Freidberg leg.; det. W. Hurkmans as *Merodon natans*; TAUI 1 ♀; Tel Aviv country club; 32.0780°N, 34.8128°E; 16 Nov. 1974; M.

Yakubowski leg.; det. W. Hurkmans as *Merodon natans*; TAUI 12 ♂♂, 7 ♀♀; Nahal Poleg; 32.2452°N, 34.8580°E; 7 Nov. 1977; M. Kaplan leg.; det. W. Hurkmans as *Merodon natans*; TAUI 4 ♂♂; same data as for preceding; FSUNS ID 04892, 04893, 04950, 04951 (TAUI) 4 ♂♂, 8 ♀♀; same data as for preceding; A. Freidberg leg.; TAUI 1 ♀; same data as for preceding; FSUNS ID 04955 (TAUI) 6 ♂♂; Yarihiv; 32.1490°N, 34.9674°E; 3 Nov. 1977; M. Kaplan leg.; det. W. Hurkmans as *Merodon natans*; TAUI 1 ♂; same data as for preceding; FSUNS ID 04956 (TAUI) 3 ♀♀; same data as for preceding; FSUNS ID 04894, 04953, 04954 (TAUI) 1 ♂; same data as for preceding; A. Freidberg leg.; FSUNS ID 04952 (TAUI) 1 ♂; Tel Aviv; 32.0780°N, 34.8128°E; 7 Nov. 1977; M. Kaplan leg.; det. W. Hurkmans as *Merodon natans*; TAUI 1 ♂; Ben-Shemen; 31.9516°N, 34.9353°E; 13 Nov. 1982; Ben-Shahar leg.; TAUI 1 ♂, 1 ♀; Jerusalem; 31.7784°N, 35.2080°E; 18 Oct. 1988; R. Kasher leg.; det. W. Hurkmans as *Merodon natans*; TAUI 1 ♂; Ayalon Park Canada; 31.8362°N, 34.9955°E; 4 Nov. 1996; L. Friedman leg.; TAUI 1 ♀; same data as for preceding; FSUNS ID 04895 (TAUI) 1 ♀; Yakum; 32.2508°N, 34.8383°E; 19 Oct. 1996; Hofman leg.; TAUI. — SOMALIA: 1 ♀; Galgala Oasis; 11.000°N, 49.050°E; 14 Oct. 1973; collected by the Spedizione Biologica in Somalia, 1973; MZUF 1 ♀; plateau between Hongolo and Bur Inaoski; 9.250°N, 50.330°E; 1924; G. Stefanini, N. Puccioni leg.; MZUF.

**Diagnosis.** Morphological features such as a large fossette (Fig. 2E) and golden erect pile on terga in male (Fig. 7A); position of fossette close to base of arista (Fig. 2I:f); and dense white pile on eyes in both sexes separate this species from other species of the *Merodon natans* group.

**Taxonomic notes.** *Merodon makrisi* sp. nov. is a medium sized species (9–13 mm). Morphological features such as a longer basoflagellomere (Fig. 2E, F); and broader metafemur (Fig. 4E, F) in both sexes, and large, rounded posterior surstyle lobe (Figs 8A:p, B:p, 10D) of male genitalia, easily separate this species from the related *M. calcaratus* (in *M. calcaratus* posterior surstyle lobe narrow, fingerlike (Fig. 5A–G)). *Merodon makrisi* sp. nov. is very similar to both *M. natans* and *M. pulveris* from which males can be distinguished by a set of characters of antenna, shape of the male genitalia and pile on terga and eyes: fossette in *M. makrisi* sp. nov. large, extending from the base of arista to the apex of basoflagellomere (Fig. 2E) (fossette in *M. natans* and *M. pulveris* smaller, never extending to the apex of basoflagellomere (Fig. 2A, C)); posterior surstyle lobe narrower and more elongated (Figs 8A:p, B:p, 10D) (in *M. natans* and *M. pulveris* posterior surstyle lobe broader (Fig. 10A–C)); ventral margin of posterior surstyle lobe with distinct triangular prominence (Figs 8A:v, B:v, 10D:v), which is not visible from lateral view in *M. natans* (Fig. 10A, B); pile on terga longer, erect, predominantly pale, some black adpressed pile may present near posterior margin of terga 2–3 (in *M. natans* and *M. pulveris* pile on terga shorter, semi adpressed, black pile present in anterior and posterior part of terga 2–3). Females of *M. makrisi* sp. nov., *M. natans* and *M. pulveris* are very similar, but fossette position is near to the base of arista in *M. makrisi* sp. nov. (Fig. 2F, I:f) can differentiate this species from *M. pulveris* and *M. natans* (Fig. 2B, D, J:f, K:f) (in *M. natans* and *M. pulveris* fossette position medially between the base of the arista and apex of basoflagellomere).

**Description. MALE** (Fig. 7A). **Head:** *Antenna:* dark brown; basal part of arista light brown; in some specimens basoflagellomere ventrally light brown; basoflagellomere two times as long as wide with acute apex; large fossette extending from base of arista to apex of basoflagellomere (Fig. 2E); lunule dark brown. *Face:* Black, white pollinose; covered with long white pile as long as pedicel, except for medial vitta extending from base of antenna to lower part of face without long white pile; ventral part of face and anteroventral part of gena black, shiny; frontal triangle black, white pollinose, covered with dense long white pile as long as pedicel; eyes holoptic, covered with dense white pile; in specimens from Israel and Somalia eyes covered with scarce, white pile as long as scapus; eye contiguity about 10 ommatidia long; vertical triangle isosceles black, shiny except for anterior part to anterior ocellus and posterior part to posterior ocelli white pollinose; vertical triangle covered with long white pile as long as pile on frontal triangle and intermixed black pile on ocellar triangle; ocellar triangle equilateral; occiput white pollinose covered with white

pile as long as pile on vertical triangle. **Thorax:** Scutum black golden-bronze lustered with five white pollinose vittae; covered with yellow erect pile as long as pile on occiput and short black adpressed pile between transverse suture and scutellum; short black bristles present on area beyond transverse suture and above wing base; scutellum black, covered with long white pile as long as pile on scutum; pleura black, white pollinose; dorsal part of anterior anepisternum, posterior anepisternum, anterior anepimeron, dorsomedial part of anepimeron with long dense white pile as long as pile on scutum; long white pile on katepisternum broadly separated with bare area between; proepimeron and katatergum with some white pile. *Legs:* Femora black, yellow only at base and apex, covered with white pile; metafemur swollen with serrated triangular lamina (Fig. 4E); tibiae of pro-, meso- and metaleg reddish-brown, medially darkened, covered with white pile; colour of basitarsomere, second and third tarsomeres of pro-, meso- and metaleg varies from yellow to dark brown; fourth and fifth tarsomeres always darkened - light to dark brown; tarsomeres mainly covered with white pile, intermixed with some black pile. *Wing:* Hyaline, covered with microtrichia except for some bare areas in first and second basal cells; stigma light yellow; wing veins dark brown, basally yellowish; halter and calypter yellow. **Abdomen:** Black with golden-bronze luster, slightly tapering; tergum 2 without antero-lateral reddish maculae; terga 2–4 with white pollinose fasciae; pollinose fascia on tergum 2 widely separated; lateral margin of abdomen blackish and white pollinose, posterior margin of terga 3–4 broadly yellowish; terga covered with long golden erect pile as long as pile on mesonotum and some short, black, adpressed pile may be present near posterior margin of terga 2–3; sternum 1 dark brown to blackish; colour of sterna 2–4 varies from dark brown to light brown; sterna covered with long, white, erect pile longer than pile on terga. **Male genitalia** (Figs 8, 10D): *Epandrium* (Fig. 8A:a, p, B:a, p): anterior surstyle lobe on inner side oval shaped, covered with dense, short, white pile (Fig. 8A:a, B:a); ventral margin of posterior surstyle lobe with distinct triangular prominence (Figs 8A:v, B:v, 10D:v); cercus square-like, in some specimens rounded (Fig. 8A:c). *Hypandrium* (Fig. 8C, E): Broad medially (Fig. 8C); aedeagus and associated structures as in Fig. 8D: ae, la, aa, ea, n; lateral sclerite of aedeagus elongate with small protuberance in posteroventral part, covered with short, white dense microtrichia (Fig. 8D: la). — **FEMALE** (Fig. 7B): Differs from male by normal sexual dimorphism and following characters: colours clearly different on mesoscutum and abdomen, golden luster lacks (Fig. 7A, B); body pilosity distinctly shorter (Fig. 7A, B); fossette smaller, never extending to apex of basoflagellomere (Fig. 2F); frons black, white pollinose except shiny ocellar triangle and medial vitta extending from anterior part of anterior ocellus to lunule; pile on terga shorter and adpressed; terga 3–4 with short black adpressed pile on anterior and posterior parts.

**Variability.** The population of *Merodon makrisi* sp. nov. in Cyprus is characterized by some stable morphological

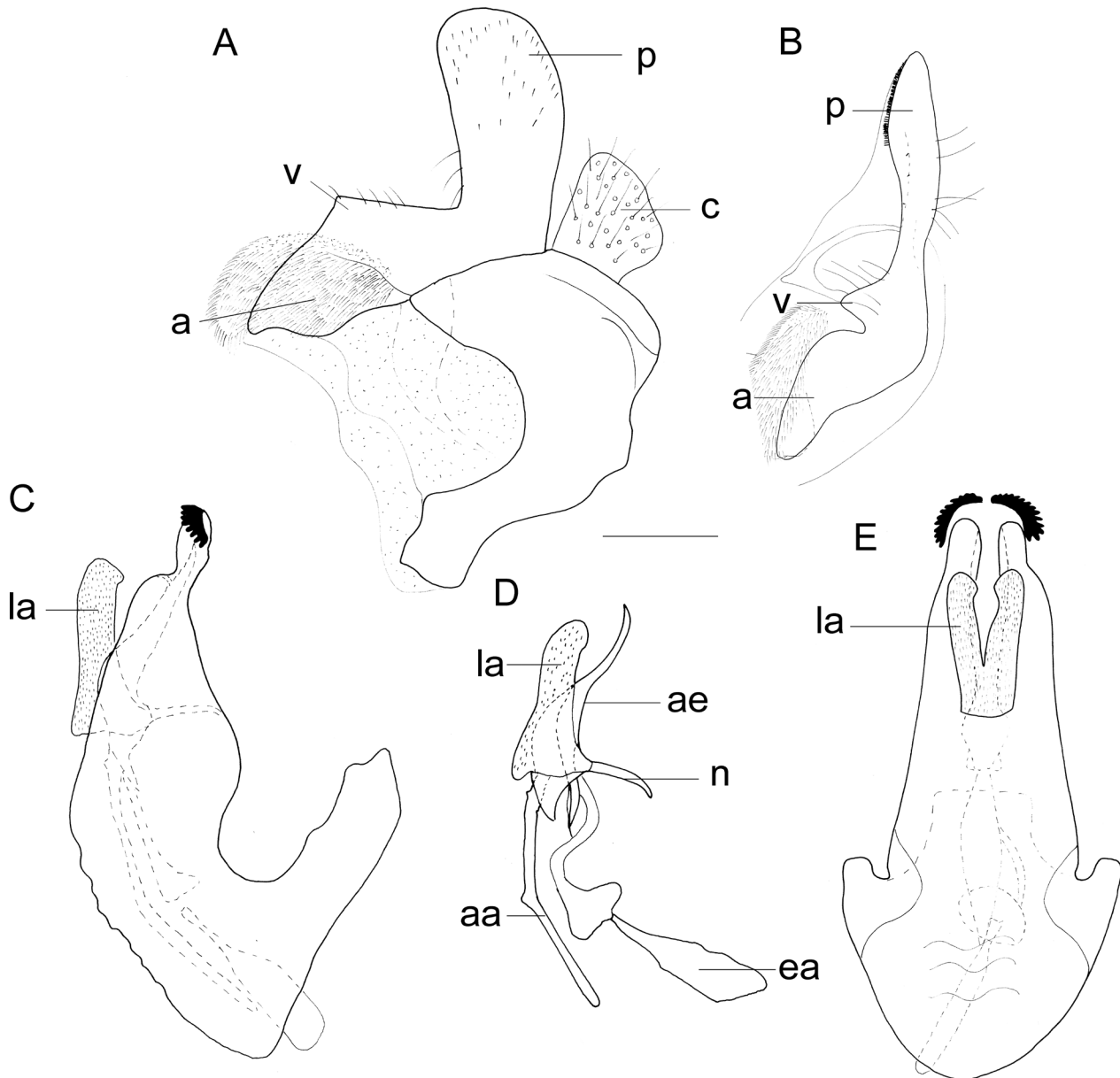


**Figure 8.** *Merodon makrisi* Vujić, Radenković & Tot sp. nov. male genitalia, Cyprus. **A** epandrium **B** left surstyle **C**, **E** hypandrium **D** aedeagus and associated structures; **A**, **C**, **D** lateral view **B**, **E** ventral view. Abbreviations: a - anterior surstyle lobe, aa - aedeagal apodeme, ae - aedeagus, c - cercus, ea - ejaculatory apodeme, la - lateral sclerite of aedeagus, n - notch on theca to which is attached the aedeagal apodeme, p - posterior surstyle lobe, v - triangular prominence on ventral margin of posterior surstyle lobe. Scale bar: 0.2 mm.

characters: eyes with dense white pile; tergum 2 without anterolateral reddish maculae; lateral margin of abdomen blackish; fasciae on terga smaller and narrower than in mainland specimens of *M. makrisi* sp. nov. and Autumn generation specimens of *M. pulveris*, while in specimens from mainland (Israel) these features are variable. The population of *M. makrisi* nov. from Cyprus shares very similar characteristics of its fasciae with the spring generation of *M. pulveris*: their smaller and narrower fasciae on terga, medially pointed at least on tergum 3, not reaching the lateral margin of terga are present also in the spring generation of *M. pulveris*.

**Etymology.** The specific epithet is derived from the personal name Makris (a noun in genitive case). The species

is dedicated to Christodoulos Makris, who collected the main part of the type series of the new species. He is an excellent observer, ecologist, photographer and author of Cyprus wildlife, insects and plants.

**Distribution.** *Merodon makrisi* sp. nov. is found in Cyprus, Israel and Somalia (Fig. 6).

**Biology.** In Cyprus, this species is commonly found on or near calcareous soils in rocky habitats with bulbs and orchids, around patches with open vegetation (Fig. 7C). Besides *Prospero autumnale*, flowers and plants such as *Narcissus* sp., *Cistus* sp., *Colchicum troodi* Kotschy, *Juniperus* sp., *Pistacia* sp., *Asphodelus ramosus* L., *Drimia aphylla* (Forssk.) J.C. Manning & Goldblatt are found

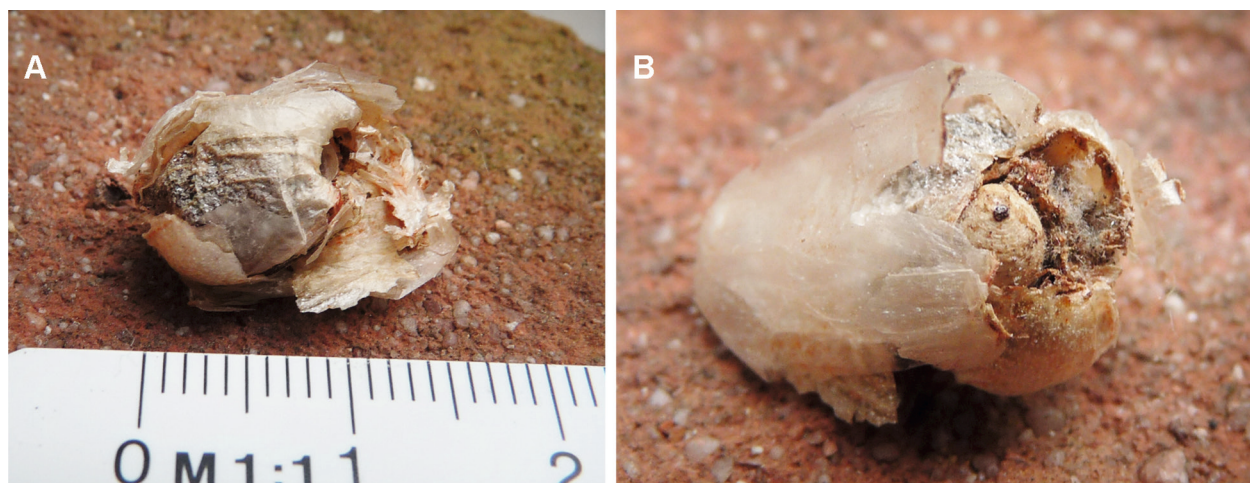


**Figure 9.** Bulb of *Prospero autumnale* (A, B), from which one male specimen of *Merodon makrasi* Vujić, Radenković & Tot sp. nov. was reared. Photo: A. van Eck.

here, as well as *Pinus brutia* Ten. as the dominant tree. The fly is most abundant at lower altitudes up to about 200 m a.s.l., but also found higher up in the mountains. Flies found higher up (740 m a.s.l.), fly around swiftly, and often rest on low vegetation or on the ground. Flower visits have been observed on *Prospero autumnale*. Flight period is in Autumn (October/November). The puparium was found in *Prospero autumnale* and described here. On 7 Feb. 2016 bulbs of *P. autumnale* were collected (Fig. 7C) and reared at ambient temperature. One adult male emerged on 21 Oct. 2016. The puparium remained in the bulb (Fig. 9A, B).

### *Merodon natans* (Fabricius, 1794)

*Syrphus natans* Fabricius, 1794: 283.

*Syrphus annulatus* Fabricius, 1794: 296. syn. nov.

*Syrphus melancholicus* Fabricius, 1794: 302.

**Diagnosis.** *Merodon natans* is a medium sized species (8–12 mm), which can be easily distinguished from *M. calcaratus* by its longer antenna (Fig. 2A, B), broader metafemur in both sexes (Fig. 4A, B) and the large, rounded posterior surstyle lobe of the male genitalia (Fig. 10A, B) (in *M. calcaratus* posterior surstyle lobe narrow, fingerlike (Fig. 5A–G)). Morphologically it is closely related to *M. makrasi* sp. nov. and *M. pulveris*. Males of these species can be distinguished by the structure of the male terminalia: ventral margin of posterior surstyle lobe without visible triangular prominence from lateral view, although present in some specimens, but it is small and visible only from ventral view in *M. natans* (Fig. 10A, B) (ventral margin of posterior surstyle lobe with clearly visible triangular prominence present in *M. makrasi* sp. nov. (Figs 8A:v, B:v, 10D:v) and *M. pulveris* (Fig. 10C:v)). Females of *M. natans* and *M. pulveris* are very similar, but the yellow pile, intermixed with some black pile on tarsomeres of proleg in *M. natans* can differentiate this species from *M. pulveris* (in *M. pulveris* tarsomeres of proleg covered with yellow pile only, except in some

specimens with a very few black pile on the fifth tarsomere). Females of *M. natans* and *M. makrasi* sp. nov. can be separated based on the position of fossette, which is near the base of arista in *M. makrasi* sp. nov. (Fig. 2E, I:f) (in *M. natans* fossette position medially between the base of the arista and apex of basofagellomere (Fig. 2B, J:f)).

**Type material.** *Syrphus natans* Fabricius: Type locality: Italy. Original description was based on an unspecified number of specimens. One appropriately labelled type was located in J.C. Fabricius collection (ZMUC), but only a pin without any remaining parts of the specimen is present in the collection (“193.20”). Consequently, we decided to designate a neotype because the type material has been destroyed. **Neotype** (designated here): ITALY: 1 ♂, Colli Berici, Unknown leg. (DS coll.), genitalia in a separate microvial with glycerine. Both basofagellomere with arista glued to the locality label. Original labels: “Colli Berici (VI) / Viliaga - Pr. N. 132 / 45.384722°N 11.510000°E / 10-22 Aug. 2011”, “*Merodon* / ♂ / *natans* / Det. Sommaggio 2011”, “AU1861”, “24944”. — ***Syrphus annulatus* Fabricius:** Type locality: “Gallia” [France]. Original description was based on an unspecified number of specimens. Two syntypes were found in J.C. Fabricius collection (ZMUC). Both specimens are partly destroyed, except for the remaining part of thorax and wings. Characters of both specimens match the definition of *Merodon natans* and we designated one of these specimens with a label as lectotype and the second specimen with a label as paralectotype. Designation of *Syrphus annulatus* lectotype was based on syntypes deposited in Copenhagen Museum (ZMUC). The syntypes are partly destroyed, but the pilosity and pilosity of the mesoscutum clearly demonstrated that these specimens belong to the *Merodon natans* group. The synonymy with *M. natans* is based on distribution (France), where no other species from the *M. natans* group occur. **Lectotype** (designated here): FRANCE: sex unknown, original labels: “Gallia”, “*annulatus*”, “P 198.7 Bosc” [based on remaining body parts sex unclear] (ZMUC). **Paralectotype** (designated here): FRANCE: sex unknown, original labels: “Gallia”, “*annulatus*”, “P 198.7 Bosc” [based on remaining body parts sex unclear] (ZMUC). — ***Syrphus melancholicus* Fabricius:** Type locality: Italy. Original description was based on an unspecified number of specimens. One syntype was found in J.C. Fabricius collection (ZMUC). Characters of the syntype match *M. natans* and it is designated as lectotype. **Lectotype** (designated here): ITALY: 1 ♂,

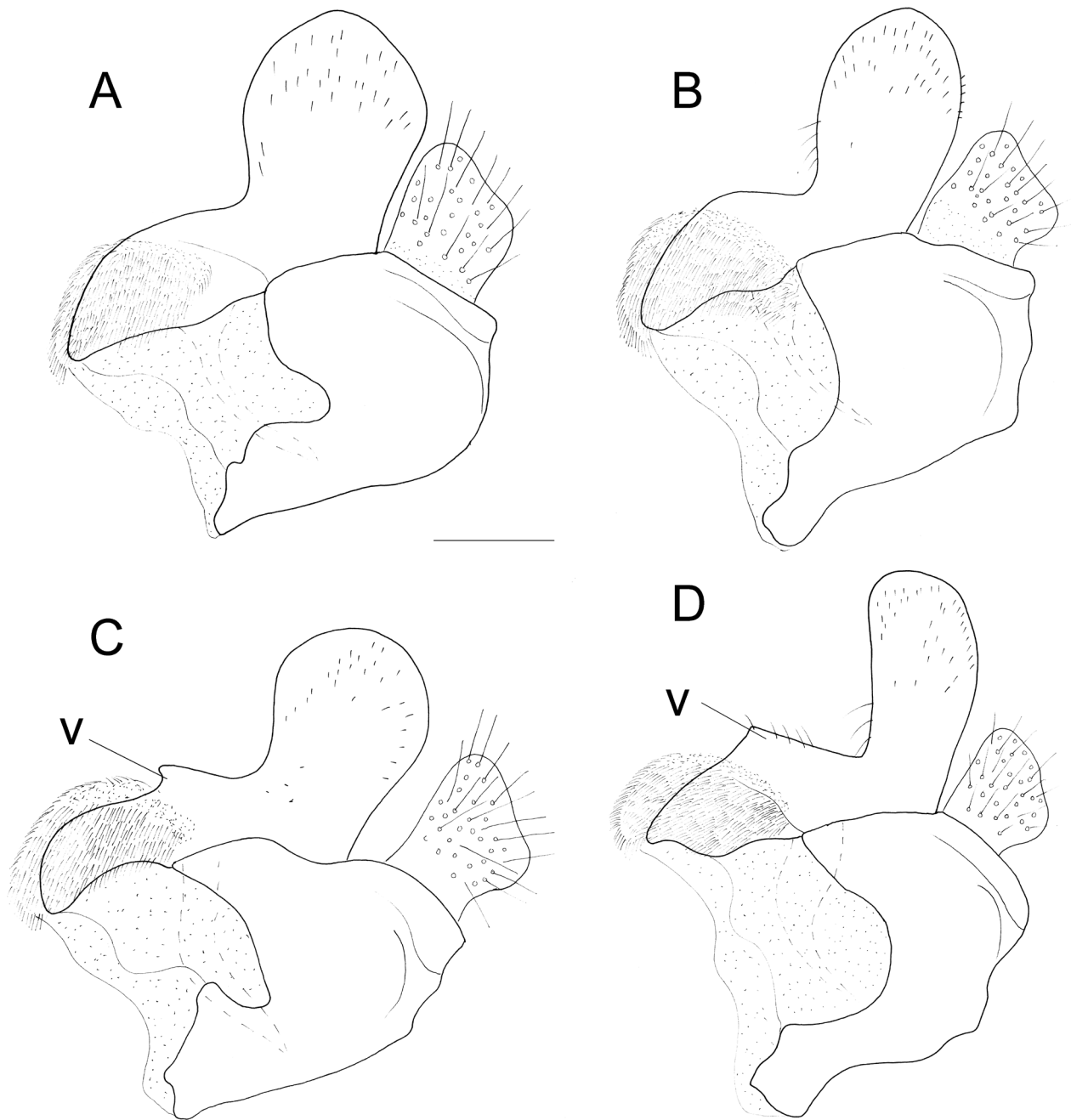


**Figure 10.** Epandrium, lateral view. **A, B** *Merodon natans* **C** *M. pulveris* **D** *M. makrisi* Vujić, Radenković & Tot sp. nov. Abbreviation: v – triangular prominence on ventral margin of posterior surstyle lobe; **A** Greece (Achaia) **B** Montenegro **C** Greece (Rhodes) **D** Cyprus. Scale bar: 0.2 mm.

original labels: “*melancholicus*”, “245.58” (ZMUC). — **Other studied material.** Published in Arok et al. (2019); SPAIN: 1 ♂; Soria, Miño de Medinaceli; 28 Aug. 1984; M.A. Marcos-García leg.; published in Marcos-García (1988). — **Additional material examined.** CROATIA: 1 ♀; Island Cres, env. Cres; 8–10 Sep. 2009; J. Halada leg.; FSUNS ID 25463 (MB coll.) 1 ♀; Nos Kalik, Krka N.P.; 43.8175°N, 15.9913°E; 130 m a.s.l.; 1 Oct. 2017; A. van Eck leg.; AvE coll. — GREECE: 1 ♂; Iraklia, Ageli; 36.8420°N, 25.4609°E; 21 Oct. 2018; J. Gavalas leg.; FSUNS ID 25448 (MAegean) 6 ♀♀; same data as for preceding; FSUNS ID 25449 to 25454 (MAegean) 1 ♀; Iraklia, Merichas; 36.8284°N, 25.4686°E; 28 Oct. 2018; J. Gavalas leg.; FSUNS ID 25455 (MAegean) 1 ♀; Crete, Asteri near Skala-Elos; 23–25 Apr. 1956; Brochmann leg.; ZFMK-DIP-00076213 (ZFMK) 1 ♀; Crete, Agia Galini, Fourfouras; 9 Oct. 1992; N. Chalwatzis leg.; ZFMK-DIP-00076212 (ZFMK) 2 ♂♂;

Kefalonia, 1 km W of Fiskardo; 50 m a.s.l.; 5 Oct. 1994; S.M. Blank leg.; ZFMK-DIP-00076209, ZFMK-DIP-00076210 (ZFMK) 1 ♂; Kefalonia, 1 km W of Poriarata, near Vlachata; 150 m a.s.l.; 9 Oct. 1994; S.M. Blank leg.; ZFMK-DIP-00076206 (ZFMK) 2 ♀♀; same data as for preceding; ZFMK-DIP-00076207, ZFMK-DIP-00076208 (ZFMK) 1 ♂; 42 km SW of Gythio, Cape Tenaro; 16 Oct. 1994; S.M. Blank leg.; ZFMK-DIP-00076211 (ZFMK). — ITALY: 1 ♀; Sardinia, Siniscola, Pineta; Apr. 1989; M. Hauser leg.; ZFMK-DIP-00069590 (ZFMK). — SERBIA: 1 ♀; Pčinja, Vogance; 42.3451°N, 21.9159°E; 513 m a.s.l.; 11 Sep. 2020; A. Vujić, L. Likov, T. Tot, M. Ranković leg.; on *Mentha* sp.; FSUNS ID 32714 (FSUNS) 2 ♂♂, Pčinja, Donja Trnica; 42.3840°N, 22.0525°E; 11 Sep. 2020; A. Vujić, L. Likov, T. Tot, M. Ranković leg.; on/near *Prospero autumnale*; FSUNS ID 32720, 32724 (FSUNS) 3 ♀♀; same data as for preceding; FSUNS ID 32721 to 32723 (FSUNS) 1 ♀;

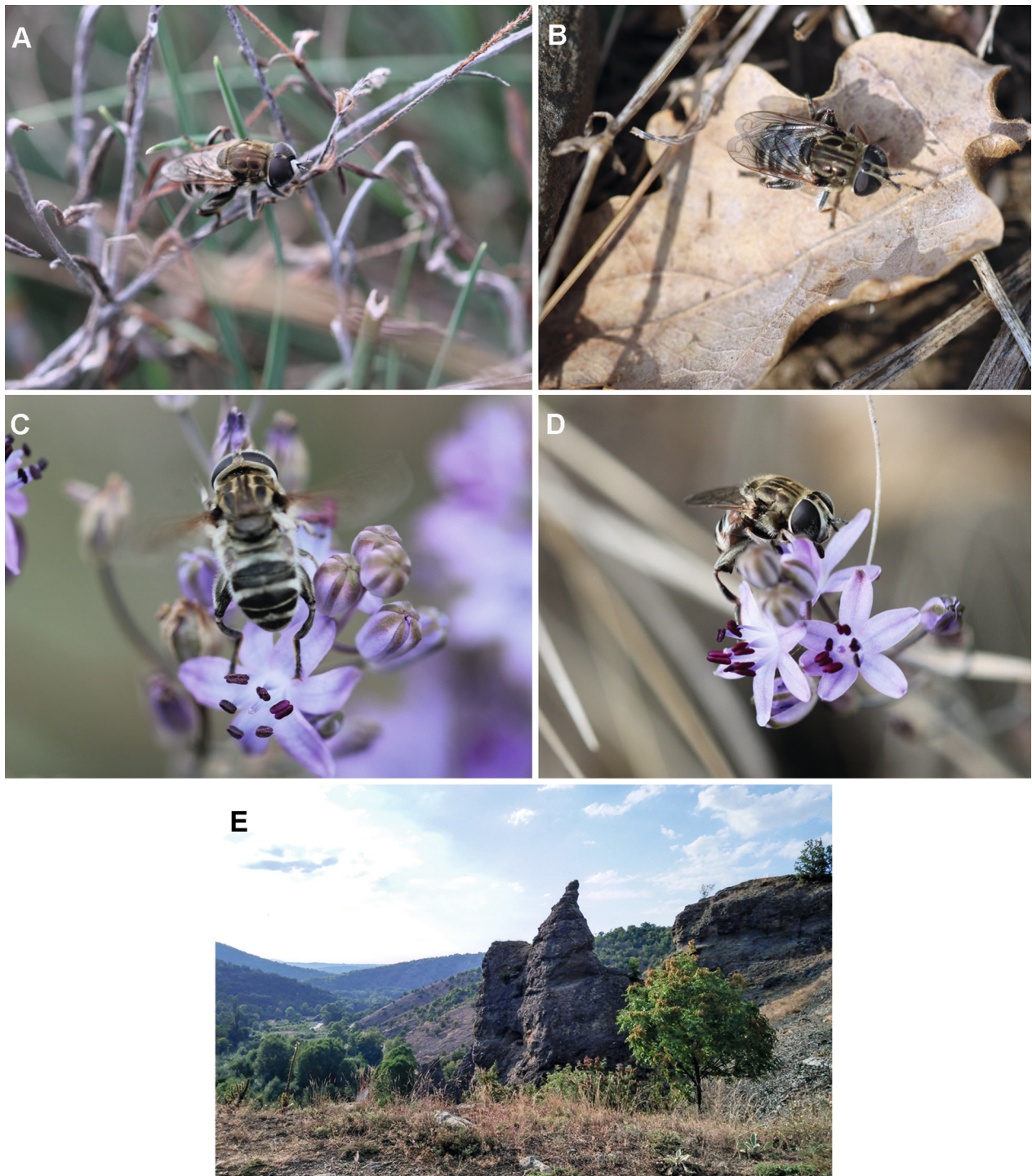


**Figure 11.** *Merodon natans* in a Serbian habitat. **A, C** male **B, D** female **E** typical habitat where *M. natans* can be collected. Photos: T. Tot, 11 Sep. 2020.

same data as for preceding; 15 Sep. 2020 a female reared from pupa collected 11 Sep. 2020 in *Prospero autumnale* bulb by A. Vujić; FSUNS ID 34373 (FSUNS).

**Redescription. MALE** (Fig. 11A, C). **Head:** *Antenna:* dark brown; basal part of arista light brown; in some specimens basoflagellomere light brown; basoflagellomere two times as long as wide. *Face:* Black, white pollinose; covered with long white pile as long as pedicel, except for medial vitta extending from base of antenna to lower part of face without long white pile; ventral

part of face and anteroventral part of gena black, shiny; frontal triangle black, white pollinose, covered with long white pile as long as pedicel; eyes holoptic, covered with white pile; vertical triangle isosceles black, shiny except for anterior part to anterior ocellus and posterior part to posterior ocelli white pollinose; vertical triangle covered with long white pile as long as pile on frontal triangle and intermixed black pile on ocellar triangle; ocellar triangle equilateral; occiput black, white pollinose covered with white pile as long as pile on vertical triangle. **Thorax:** Scutum black, with five white pollinose vittae; covered

with white erect pile as long as pile on occiput and short, black adpressed pile on area between transverse suture and scutellum; short black bristles present above wing base; scutellum black, covered with long white pile as long as pile on scutum; pleura black, white pollinose; dorsal part of anterior anepisternum, posterior anepisternum, anterior anepimeron, dorsomedial part of anepimeron with long, dense white pile as long as pile on scutum; long white pile on katapisternum broadly separated with bare area between; proepimeron and katatergum with some white pile. **Legs:** Femora black, yellow only at base and apex, covered with white pile, some black pile presented on its apical part; metafemur swollen with serrated triangular lamina (Fig. 4A); tibiae yellow medially darkened, covered with white pile; colour of tarsomere dorsally varies from yellow to dark brown, ventrally yellowish; tarsomeres mainly covered with white pile, intermixed with some black pile. **Wing:** Hyaline, covered with microtrichia except for some bare areas in first and second basal cells; stigma light yellow; wing veins dark brown, basally yellowish; halter and calypter yellow. **Abdomen:** Black, slightly tapering; tergum 2 with anterolateral reddish maculae, in some specimens anterolateral reddish maculae on tergum 2 absent; terga 2–4 with white pollinose fasciae; pollinose fasciae on tergum 2 widely separated, on terga 3–4 in some specimens may merge; lateral margin of abdomen blackish covered with white pollinosity, in some specimens lateral margin of abdomen yellowish; posterior margin of terga 3–4 yellowish; terga covered with adpressed black and white pile, shorter than pile on scutum; white pile on lateral margin of abdomen longer than pile on terga; sternum 1 dark brown; colour of sterna 2–4 varies from dark brown to light brown; sterna covered with long, white erect pile longer than pile on terga. **Male genitalia:** *Epandrium* (Fig. 10A, B): posterior surstyle lobe rounded, ventral margin of posterior surstyle lobe without visible triangular prominence from lateral view, although it can be present in some specimens, but it is small and visible only from ventral view; anterior surstyle lobe on inner side oval shaped, covered with dense, short white pile. *Hypandrium:* as in other members of *Merodon natans* group, hypandrium broadened medially. **FEMALE** (Fig. 11B, D): Similar to male except for normal sexual dimorphism. Frons black covered with white pollinosity, except for black shiny vitta extending from lunule to anterior ocellus.

**Variability.** The posterior surstyle lobe in males of *M. natans* varies in shape, as in the case of *M. calcaratus*, but is less distinct. In the Montenegro (Boka Kotorska) population of *M. natans* and in a single specimen from Spain, the posterior surstyle lobe is narrower (Fig. 10B).

**Distribution.** *Merodon natans* occurs in most countries of southern Europe (Spain, Italy, Croatia, Serbia, Bulgaria, North Macedonia, Montenegro, Greece) and part of western Europe (France) (Fig. 6). According to Marcos-García et al. (2007) and Speight (2020), *M. natans* is recorded from Israel and the Caucasus. However, the records of *M. natans* from Israel refer to *M. neolydicus*

Vujić in Vujić et al. (2018b) and *M. makrisi* sp. nov. described in this paper. We can here anticipate that specimens from the Caucasus will also likely refer to another *Merodon* species.

**Biology.** Preferred environments are forests with open ground; herb-rich open areas in thermophilous *Quercus* forest and phrygana with *Cistus* scrub; also in orchards in southern Europe (Speight 2020). Adults prefer open areas with tall herbs and scrub (Fig. 11A, B, E), within dry woodland; a secretive species, as easily collected by use of Malaise traps as by direct observation (Speight 2020). Flowers visited include: *Prospero autumnale* (Fig. 11C, D), *Foeniculum* sp., *Mentha* sp., *Solidago* sp., *Drimys maritima*. The flight period is in Spring (April/May) and Autumn (end August/beginning October). The puparium, described here, is found in the host plant *Prospero autumnale* in Serbia (Fig. 11C, D).

**Additional remark.** This study revealed that records from Portugal (van Eck 2016) were based on incorrect identifications. At present, *M. natans* is not confirmed for the Portuguese fauna and should be removed from its checklist.

### *Merodon pulveris* Vujić & Radenković in Radenković et al. 2011

Fig. 12A, B

*Merodon pulveris* Vujić & Radenković in Radenković et al. 2011: 41.

**Diagnosis.** *Merodon pulveris* is a medium sized species (11–12 mm). It can be separated from *M. calcaratus* by its longer antenna (Fig. 2C, D), broader metafemur in both sexes (Fig. 4C, D) and the large, rounded posterior surstyle lobe (Fig. 10C) of the male genitalia (in *M. calcaratus* narrow, fingerlike; Fig. 5A–G). *Merodon pulveris* is closely related to *M. natans* and *M. makrisi* sp. nov., but differs by the following characters of the male genitalia: ventral margin of posterior surstyle lobe with distinct triangular prominence (Fig. 10C:v), in *M. natans* without visible triangular prominence from lateral view (Fig. 10A, B), it can be present in some specimens, but it is small and visible only from ventral view (Fig. 10A, B); posterior surstyle lobe broader and shorter (Fig. 10C), narrower and more elongated in *M. makrisi* sp. nov. (Figs 8A:p, B:p, 10D). Fossette position medially between the base of the arista and apex of basoflagellomere distinguishes females of this species from *M. makrisi* sp. nov. (in *M. makrisi* sp. nov. position of fossette is near base of arista (Fig. 21:f)). From *M. natans*, females of *M. pulveris* can be separated by the presence of only yellow pile on the proleg tarsomeres, except in some specimens only, where the fifth tarsomere has sparse black pile (in *M. natans* proleg tarsomeres covered with yellow pile but also with some intermixed black pile).



**Figure 12.** *Merodon pulveris*. **A** male on *Drimia aphylla*, in Cyprus, photo: C. Makris, 6 Oct. 2016 **B** female in Cyprus, photo: C. Makris, 20 Oct. 2013 **C** typical habitat in Agiassos (Lesvos, Greece) where *M. pulveris* can be collected, photo: D. Vujanović.

**Type material.** We studied the type material published in Radenković et al. (2011). — **Other studied material.** Published in Arok et al. (2019); CYPRUS: 1 ♂, 1 ♀; Limassol, Episkopi Ancient Kourion stadium; 34.6708°N, 32.8744°E; 112 m a.s.l.; 7 Oct. 2017; J. van Steenis leg.; JvS coll.; published in van Steenis et al. (2019). — **Additional material examined.** CYPRUS: 2 ♀♀; Limassol, Eftagonya; 550 m a.s.l.; 25 Oct. 1951; G. Mavromoustakis leg.; KBIN (R.I.Sc.N.B. 24.236) 1 ♂; Limassol, Episkopi, Kourion; 4 Nov. 2016; A. van Eck leg.; FSUNS ID 25390 (FSUNS) 1 ♀; same data as for preceding; FSUNS ID 25389 (FSUNS) 1 ♀; Pera Pedi; 34.8658°N, 32.8489°E; 881 m a.s.l.; 2 Oct. 2017; X. Mengual leg.; ZFMK-DIP-00028080 (ZFMK) 1 ♂; same data as for preceding; 2–7 Oct. 2017; Malaise trap; ZFMK-DIP-00027945 (DNA-voucher D401) (ZFMK) 1 ♀; same data as for preceding; ZFMK-DIP-00027945 (DNA-voucher D399) (ZFMK) 1 ♀; same data as for preceding; 8–12 Oct. 2017; ZFMK-DIP-00027916 (DNA-voucher D397) (ZFMK) 1 ♂; Episkopi, near Ancient Kourion stadium, across road; 34.6695°N, 32.8743°E; 106 m a.s.l.; 4 Oct. 2017; C. Makris leg.; ZFMK-DIP-00028071 (ZFMK) 7 ♂♂; Episkopi, near Ancient Kourion stadium; 34.6709°N, 32.87453°E; 112 m a.s.l.; 7 Oct. 2017; X. Mengual leg.; ZFMK-DIP-00027868 (DNA-voucher D394), ZFMK-DIP-00028072 to ZFMK-DIP-00028074, ZFMK-DIP-00028075 (DNA-voucher D365), ZFMK-DIP-00028076, ZFMK-DIP-00028077 (ZFMK) 2 ♀♀; same data as for preceding; ZFMK-DIP-00028078, ZFMK-DIP-00028079 (ZFMK) 4 ♂♂; same data as for preceding; 10 Oct. 2017; ZFMK-DIP-00027874 (DNA-voucher D396), ZFMK-DIP-00028081 to ZFMK-DIP-00028083 (ZFMK) 2 ♀♀; same data as

for preceding; ZFMK-DIP-00028084, ZFMK-DIP-00028085 (ZFMK) 2 ♀♀; S of Kelefos Bridge, N of Arminou Reservoir; 34.8866°N, 32.7463°E; 460 m a.s.l.; 11 Oct. 2017; ZFMK-DIP-00028087, ZFMK-DIP-00028086 (ZFMK). — GREECE: 1 ♂; Rhodes, Lindos; 6 Apr. 1971; V.S. van der Goot leg.; ZFMK-DIP-00076341 (ZFMK) 1 ♀; Rhodes; 18 Apr. 1970; A.C. Ellis, W.N. Ellis leg.; ZFMK-DIP-00076205 (ZFMK). — TURKEY: 1 ♀; Mugla, University campus; 37.1617°N, 28.3703°E; 720 m a.s.l.; 26 May–26 Jun. 2015; H. Kavak leg.; MT (Malaise trap); FSUNS ID 25366 (MB coll.) 4 ♂♂; Mugla, University campus; 37.1606°N, 28.3697°E; 730 m a.s.l.; Nov. 2015–Apr. 2016; M. Barták, S. Kubik leg.; MT (Malaise trap); FSUNS ID 25367 to 25369, 25371 (MB coll.) 2 ♂♂; Kizilyaka; 37.0225°N, 28.4383°E; 105 m a.s.l.; 27 Apr.–4 May 2016; M. Barták, S. Kubik leg.; FSUNS ID 25363, 25365 (MB coll.) 2 ♀♀; same data as for preceding; FSUNS ID 25362, 25364 (MB coll.) 1 ♀; 8km S of Çine, river bank; 37.5428°N, 28.0628°E; 68 m a.s.l.; 29 Apr.–1 May 2016; M. Barták, S. Kubik leg.; SW (Sweeping); FSUNS ID 25370 (MB coll.).

**Distribution.** *Merodon pulveris* inhabits the Anatolian Peninsula, the eastern Mediterranean islands (Lesvos, Samos, Rhodes) and Cyprus, but is absent from southern and western Europe as opposed to *M. natans* (Fig. 6).

**Biology.** Preferred environments (Fig. 12C) are open areas in Eastern European maquis on limestone near coniferous forests with large populations of its host plant *Pros-*

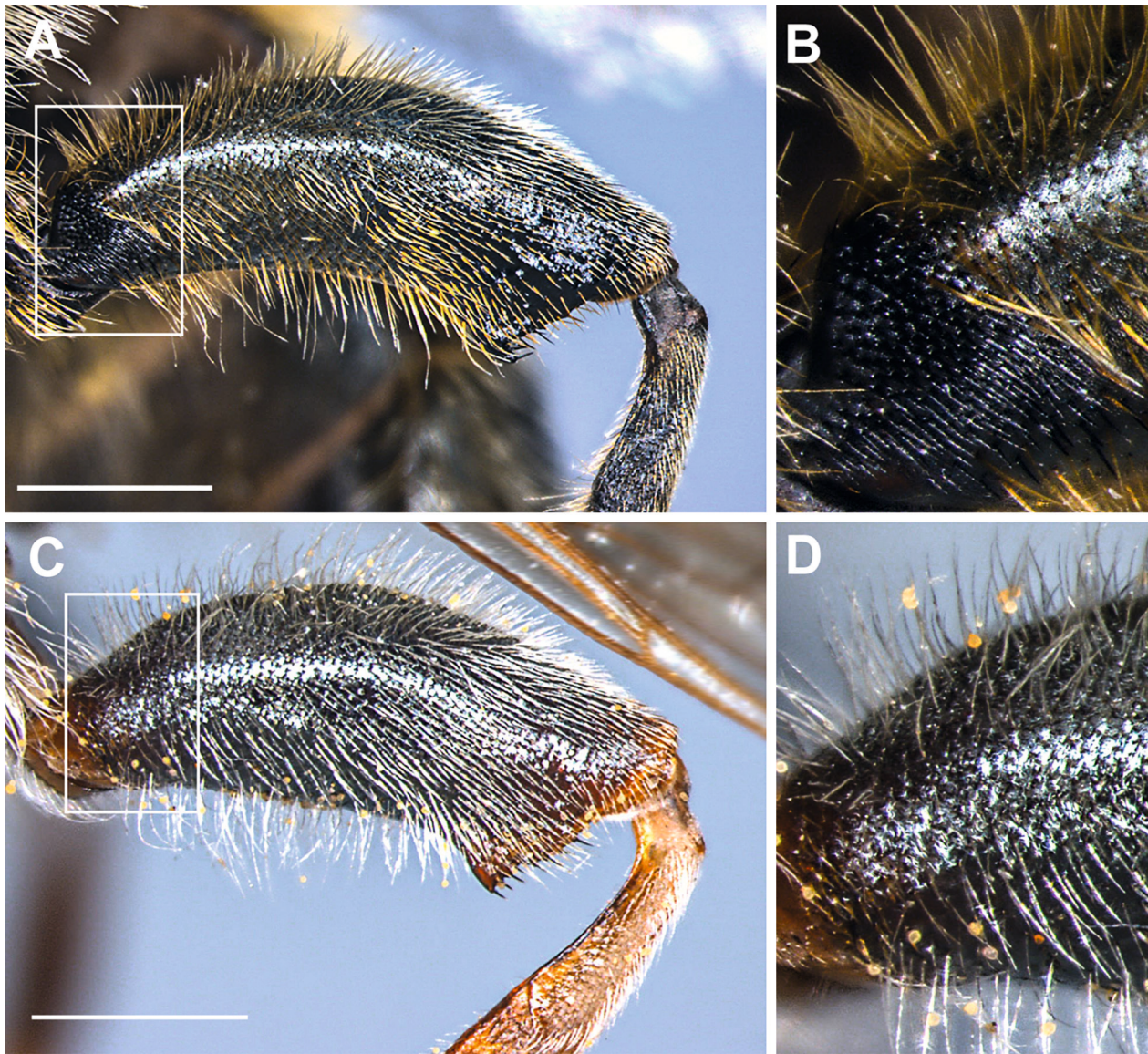


**Figure 13.** Metafemur, lateral view. **A, B** *Merodon segetum* **C, D** *M. pulveris*, rectangle marks enlarged basal part of metafemur; **A, B** Spain **C, D** Turkey; **A–D** male. Scale bar: 1 mm.

*pero autumnale* (Radenković et al. 2011). Flowers visited include: *Foeniculum* sp., *Prospero autumnale* (van Steenis et al. 2019), *Drimia aphylla* (Fig. 12A). Flight period

is in spring (April–May) and autumn (late September/mid October). The larva described here was found in *Prospero autumnale* on Lesvos island in Greece.

### 3.2. Identification key to *Merodon natans* lineage

1. Area of short black pile present on antero-basal ~1/4 of profemur, ~1/5 of mesofemur and ~1/6–1/7 of metafemur (Fig. 13A, B). Antenna with sensory pit on inner side of basoflagellomere large, at least 3 times as long as basal diameter of first aristomere (in females sensory pit smaller). Male genitalia: surstyle lobe with more or less straight ventral margin (Fig. 14A); hypandrium medially not broadened, with setulae in ventral view (Fig. 14B). Large species (15–18 mm) ..... *M. segetum*
- Pro-, meso- and metafemora antero-basally without area of short black pile (Fig. 13C, D). Antenna with sensory pit on inner side of basoflagellomere smaller, as long as basal diameter of first aristomere. Male genitalia: ventral margin of surstyle lobe invaginated (Figs 5A–D, F, G, 8A, 10A–D (invagination on ventral margin of surstyle marked on Fig. 5A)); hypandrium medially broadened (Fig. 8B), ventrally without setulae (Fig. 8C, E). Medium sized species (8–13 mm) ..... **2** (*M. natans* group)
2. Antenna shorter, less than 2 times (approx. 1.75) longer than broad (Fig. 2G, H); basoflagellomere with curved dorsal margin (Fig. 2G, H); small fossette present near apex of basoflagellomere. Metafemur not swollen (Fig. 4G, H). Male genitalia: posterior surstyle lobe narrow, fingerlike (Fig. 5A–G).....*M. calcaratus*

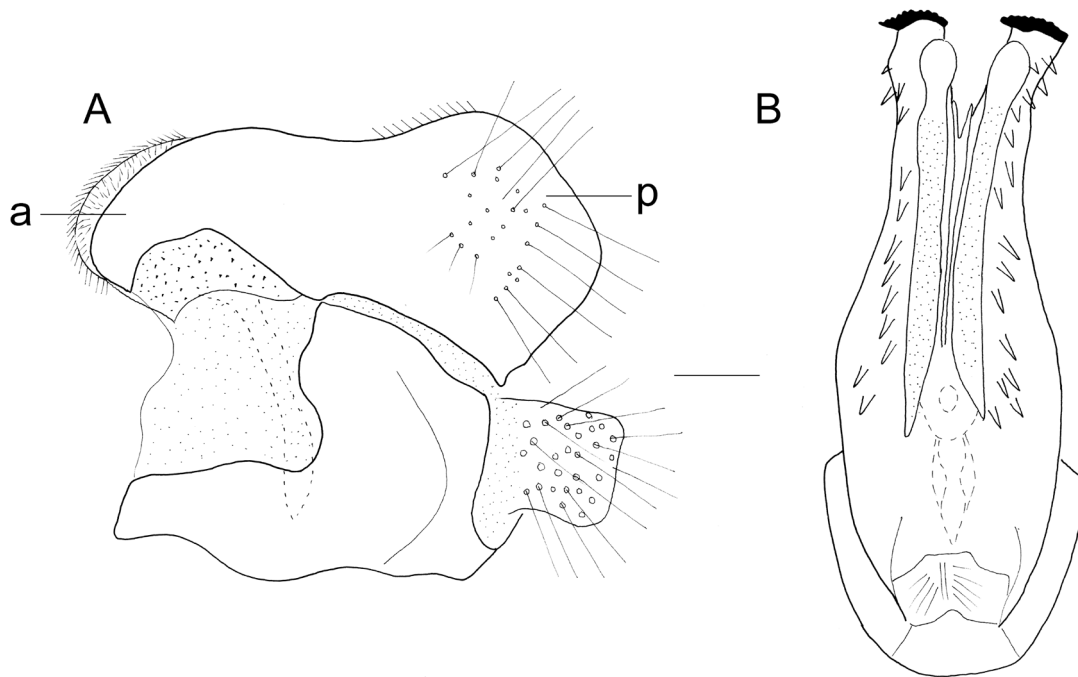


**Figure 14.** *Merodon segetum* (Spain), genitalia. **A** epandrium **B** hypandrium; **A** lateral view **B** ventral view. Abbreviations: a – anterior surstyle lobe, p – posterior surstyle lobe. Scale bar: 0.2 mm.

- Antenna longer, at least 2 times longer than broad (Fig. 2A–F); basoflagellomere without curved dorsal margin (Fig. 2A–F); fossette larger in size, its position medianly or near to base of basoflagellomere (Fig. 2A–F). Metafemur swollen (Fig. 4A–F). Male genitalia: posterior surstyle lobe broader (Fig. 10A–D).....**3**
- 3. Eyes holoptic (males).....**4**
- Eyes dichoptic (females).....**6**
- 4. Male genitalia: ventral margin of posterior surstyle lobe without visible triangular prominence in lateral view (Fig. 10A, B); if present, small and visible only from ventral view.....*M. natans*
- Male genitalia: ventral margin of posterior surstyle lobe with clearly visible triangular prominence in lateral view (Fig. 10C:v, D:v).....**5**
- 5. Fossette large, extending from base of arista to apex of basoflagellomere (Fig. 2E). Pile on terga longer, erect, predominantly pale, some black adpressed pile may be present near posterior margin of terga 2–3.....*M. makrasi* Vujić, Radenković & Tot sp. nov.
- Fossette smaller, never extending from base of arista to apex of basoflagellomere (Fig. 2C). Pile on terga shorter, semi adpressed, black pile present in anterior and posterior parts of terga 2–3.....*M. pulveris*
- 6. Position of fossette close to base of arista (Fig. 2I:f).....*M. makrasi* sp. nov.
- Fossette position medially between base of arista and apex of basoflagellomere (Fig. 2J, K:f).....**7**
- 7. Tarsomeres of proleg covered with yellow pile, with some intermixed black pile. Distribution: Southern Europe (Spain, Italy, Croatia, Serbia, Bulgaria, North Macedonia, Montenegro, Greece) and parts of western Europe (France).....*M. natans*
- Tarsomeres of proleg with yellow pile, in some specimens only fifth tarsomere with sparse black pile. Distribution: Anatolian Peninsula, the eastern Mediterranean islands (Lesvos, Samos, Rhodes) and Cyprus....*M. pulveris*

### 3.3. Description of preimaginal morphology of *Merodon natans* species group

#### 3.3.1. Puparium description of *Merodon makrasi* sp. nov.

Most morphological characters of the puparia of *M. makrasi* sp. nov. and *M. natans* appear to be very similar, however the single specimen of *M. natans* is damaged and morphological analysis using electron microscopy could not be performed. Therefore, although the follow-

ing description refers to both species, most of the characters have been described for *M. makrasi* sp. nov., but the features that seem to be different between them have been emphasized.

**Puparium description** (*Merodon makrasi* sp. nov. n=2; *M. natans* n=1): Dimensions and shape (Fig. 15A). Length × width: 11 mm × 5 mm in *M. makrasi* sp. nov., and 10 mm × 5 mm (ca., puparium damaged) in *M. natans*; brownish in colour; sub-cylindrical; rough integument with larval segmentation persisting as transverse folds and wrinkles; integumental vestiture well-developed, with small

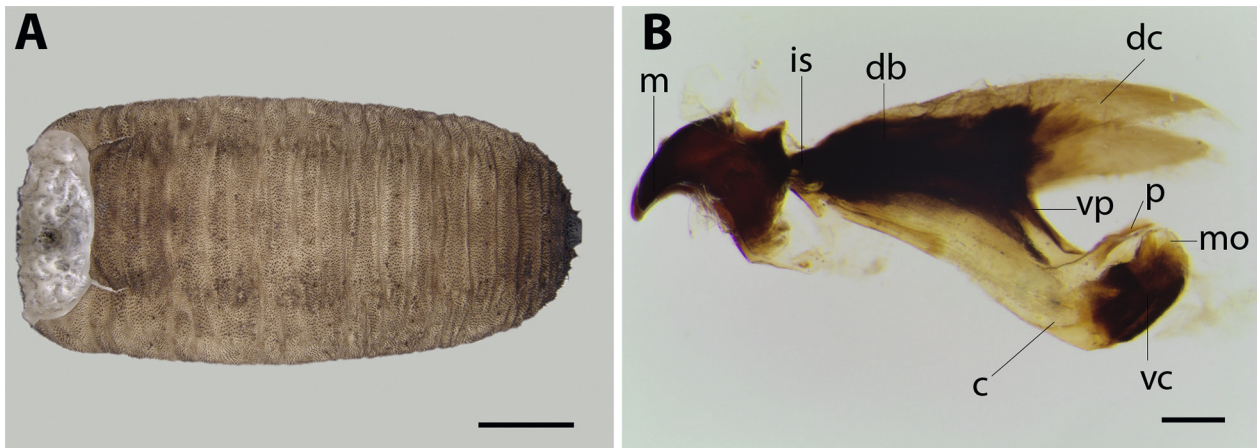


**Figure 15.** Light micrographs of *Merodon makrisi* Vujić, Radenković & Tot sp. nov. puparium. **A** puparium in dorsal view **B** head skeleton in lateral view. Abbreviations: c – cibarium, db – dorsal bridge, dc – dorsal cornu, is – intermediate sclerite, m – mandibles, mo – mortar, p – pestle, vc – ventral cornu, vp – vertical plate. Scale bars: 2 mm (**A**); 200  $\mu$ m (**B**).

domes and short slightly pointed and sclerotized spicules (Figs 15A, 16A); slightly pronounced segmental sensilla, bearing long seta (Figs 15A, 16B); dorsal surface of prothorax with pair of anterior spiracles (Figs 16C, 17C), about twice as long as broad at base, sclerotized, cylindrical in shape, brownish in colour, apex with two short linear spiracular openings (Fig. 16C); two different pairs of lappets on anal segment (Figs 16D, E, 17E), ventrolateral pair represented by well-developed fleshy papilla with one sensillum bearing single seta, dorsolateral pair with very poorly developed basal papilla, apically divided bearing one sensillum with long seta on top of each division. — **Head skeleton** (Figs 15B, 17A): Mandibles with dark sclerotized hooks, without accessory teeth, fused to external heavily sclerotized mandibular lobes; dorsal cornu narrowed and tapered slightly downwards towards sharp apex, representing whole length of ventral cornu (in *M. natans*) and slightly exceeding it (in *M. makrisi* sp. nov.); dorsal bridge, vertical plate and intermediate sclerite apparently fused together and all highly sclerotized (in *M. natans*, vertical plate slightly less sclerotized); ventral cornu elongate and narrow in profile view, wider and more heavily sclerotized at posterior end, with cibarium located at base, forming grinding mill of (not so sclerotized) pestle and (more sclerotized) mortar construction, at posterior end of cibarium. — **Puparial spiracles**: Sclerotized, dark brown in colour, stout, cylindrical in shape, gradually tapered, slightly pointed at end (Figs 16A, 17B), apex with shallow indentation visible on ventral side in *M. makrisi* sp. nov. (Fig. 16B); length  $\approx$  0.3 mm, twice as long as broad; separated by distance of five times their length; whole ventral and lateral surfaces (except apex) covered with irregularly-spaced, oval-shaped domed tubercles; whole spiracular surface (between tubercles, at base, and at apex) reticulate with polygonal pattern (Fig. 16A, B), more irregular on ventral side, with polygons noticeably smaller in apical part; 5–7 radially-arranged spiracular openings on each tubercle in *M. makrisi* sp. nov. (Fig. 16B). — **Posterior respiratory process (prp)**: Dark-red to black in colour, short, wider than long (visible from dorsal view, Figs 15A, 16D) in

*M. makrisi* sp. nov. and slightly longer in *M. natans* (Fig. 17D), with annular groove at base; base wider than apex, prp in shape of truncated cone, although more cylindrical in *M. natans*; entirely coriaceous (Figs 16D, 17D), lateral surface with slightly undulate longitudinal indentations in basal half and with small dents from base to apex, somewhat smoother in area just below spiracular plate in *M. makrisi* sp. nov. (Fig. 16D); outline of spiracular plate sub-elliptical and only slightly irregular, undulate with small indentations; spiracular plate with 4 pairs of spiracular openings (around 2 central scars in shallow depressions), clearly separated from each other, sinuous and irregularly curved (Figs 16E, F, 17E); 4–7 very small circular nodules on each side of surface of spiracular plate in area of spiracular openings in *M. makrisi* sp. nov. (in both examined specimens); 4 pairs of well-developed branched inter-spiracular setae (Figs 16F, 17E).

**Material examined:** *Merodon makrisi* sp. nov.: CYPRUS, Episkopi, Kourion; 34.6699°N, 32.8754°E; A. van Eck leg.; 2 puparia (1 whole, 1 in parts) in bulbs of *Prospero autumnale*, 7 Feb. 2016, reared, 1 male emerged 21 Oct. 2016; FSUNS. *M. natans*: SERBIA, Pčinja, Donja Trnica; 42.3840°N, 22.0525°E; A. Vujić leg.; 1 puparium in bulb of *P. autumnale*, 11 Sep. 2020, reared, 1 female emerged 15 Sep. 2020; FSUNS.

### 3.3.2. Third instar larva of *Merodon pulveris*

**Larva dimensions and shape:** Length: 9 mm, width: 3 mm; sub-cylindrical; roundly arched dorsally and slightly flattened ventrally; anterior end truncated, inclined ventrally; uniformly yellowish to light brown in colour; rough integument with segmentation as transverse wrinkles, anterior segments corrugated with conspicuous folds; integumental vestiture well-developed, with short slightly pointed and sclerotized yellowish-brown spicules; segmental sensilla all conspicuous, consisting of wider basal papilla bearing very long needle-like terminal setae (Fig. 18). — **Head:** Mandibles with black sclerotized hooks (Fig. 19A, B), with large accessory teeth on basal outer side of hooks, clearly visible in lateral view (Fig. 19B), and another pair of very small accessory teeth

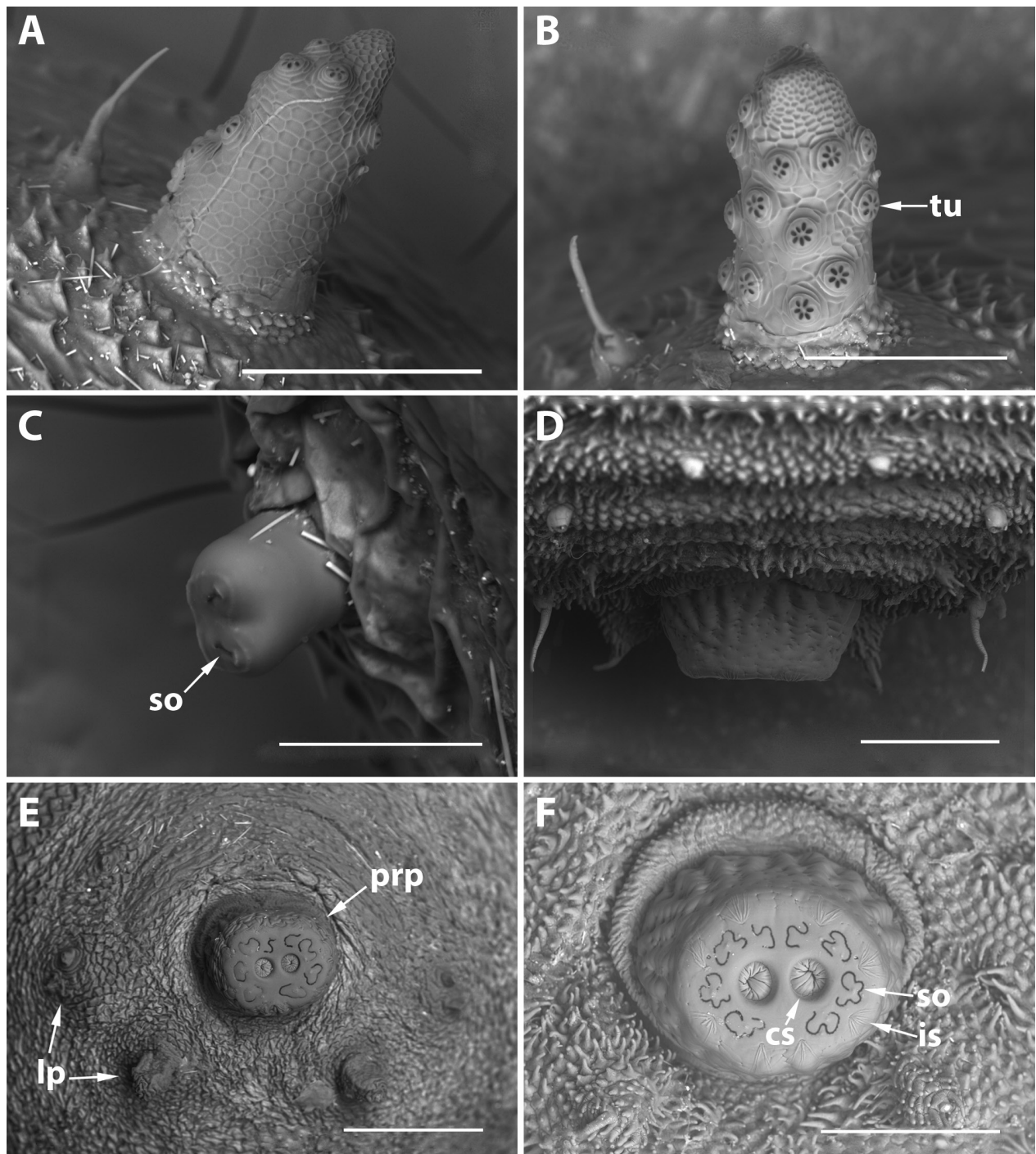


**Figure 16.** SEM micrographs of *Merodon makrisi* Vujić, Radenković & Tot sp. nov. puparium. **A** pupal spiracle in dorsal view **B** pupal spiracle in ventral view **C** anterior spiracle **D** posterior respiratory process (prp) in dorsal view **E** anal segment **F** prp showing the spiracular plate. Abbreviations: cs – central scar, is – inter-spiracular setae, lp – lappets, prp – posterior respiratory process, so – spiracular opening, tu – tubercle. Scale bars: 200  $\mu$ m (**A**, **B**); 100  $\mu$ m (**C**); 500  $\mu$ m (**D**, **E**, **F**).

on inner side of hooks, visible in frontal view (Fig. 19A); mouthhooks projecting downwards along each side of mouth, fused to brownish-black sclerotized external mandibular lobes at base; well-developed and sclerotized antenno-maxillary organs (Fig. 19A, B), located on pair of fleshy rounded projections between mouth and dorsal surface of prothorax, consisting of 2 pairs of cylindrical to conical-shaped structures tipped with different types of sensilla, antennae with single antennal sensory cone and one small sensilla on top surface; dorsal lip smooth with-

out ornamentation. — **Thorax:** Lateral lips flat and coated in long, clearly pointed and slightly sclerotized spicules; dorsal surface of prothorax with five longitudinal grooves, with conspicuous, clearly pointed and yellowish-brown spicules distributed on grooves, with dome-shaped, very aggregated spicules on folds; dorsal surface of prothorax with pair of anterior spiracles (Fig. 19B) about twice as long as broad at base, sclerotized, cylindrical in shape, reddish-brown in colour, bilobulated at apex and completely retractile within inverted integumental pockets;

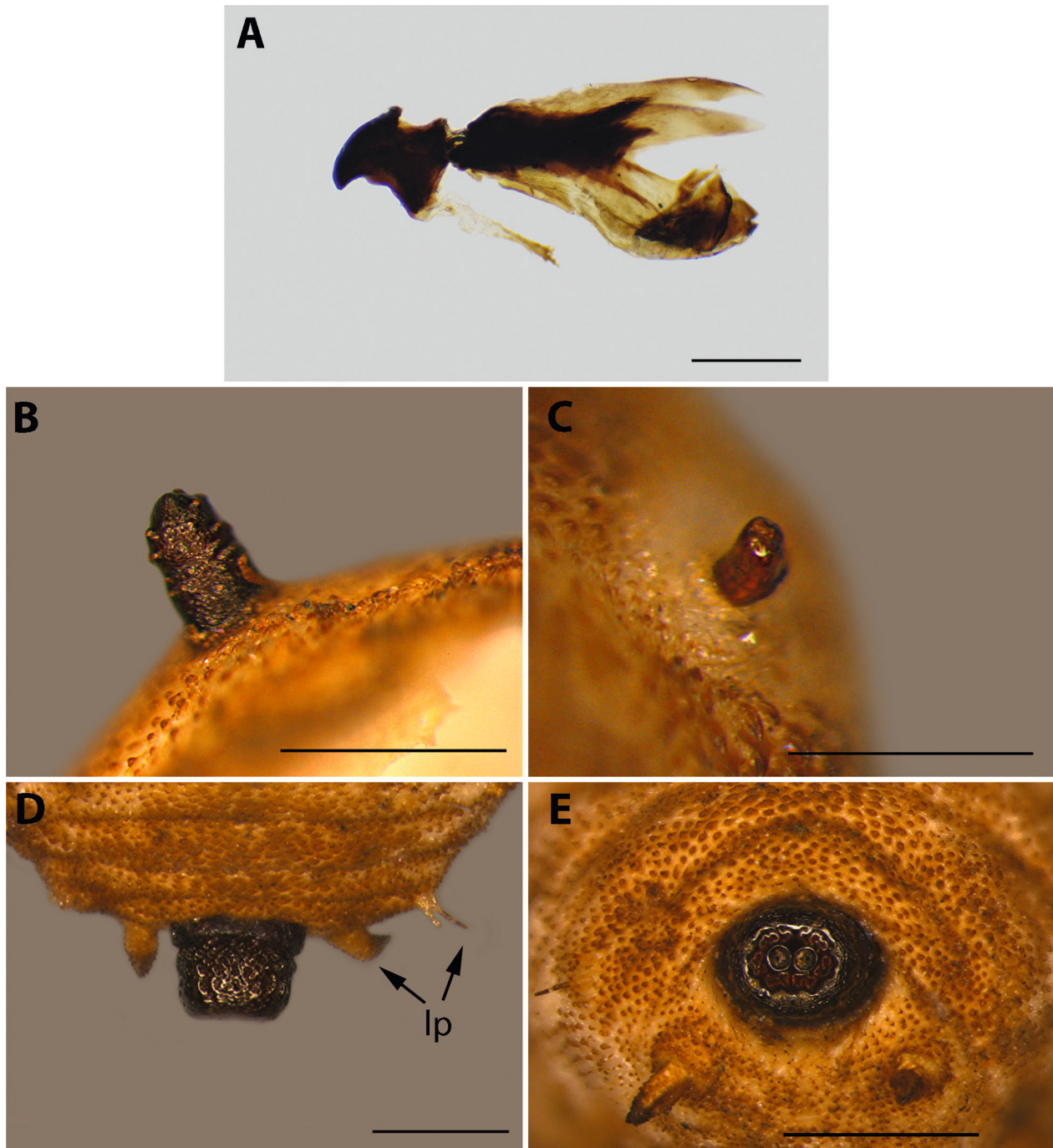


**Figure 17.** Light micrographs of *Merodon natans* puparium. **A** head skeleton in lateral view **B** pupal spiracle **C** anterior spiracle **D** posterior respiratory process (prp) in dorsal view **E** anal segment with prp. Abbreviation: lp - lappets. Scale bars: 500  $\mu$ m (A, B, C, D, E).

mesothoracic prolegs absent. — **Abdomen:** Primordia of pupal spiracles (Fig. 19C) present on dorsal surface of first abdominal segment (indicating third larval stage); pronounced segmental sensilla all bearing setae; locomotory organs poorly developed, visible as pairs of raised domes on abdominal segments, located between segmental sensilla number 8 and 9, lacking crochets, having same type of ventral ornamentation but more developed and less sclerotized; two different pairs of lappets (Fig. 19D, E) on anal segment, ventro-lateral pair represented by longer fleshy papilla with one sensillum bearing seta, dorso-lateral pair with poorly developed basal papilla,

apically divided, bearing one sensillum with long seta on top of each division; prp dark reddish-black and shiny, short (but clearly visible from dorsal view, Figs 18B, 19D), in shape of truncated cone, with annular groove at base, slightly wider than long, with base slightly groove wider than apex; entirely coriaceous, lateral surface with longitudinal indentations, with small dents, conspicuously ornamented from base to apex, differently in its (slightly narrowed) apical third (below spiracular plate); outline of spiracular plate sub-elliptical and slightly irregular, with indentations, bearing groove in joining point of two parts of plate, on both dorsal and ventral sides, visible in polar

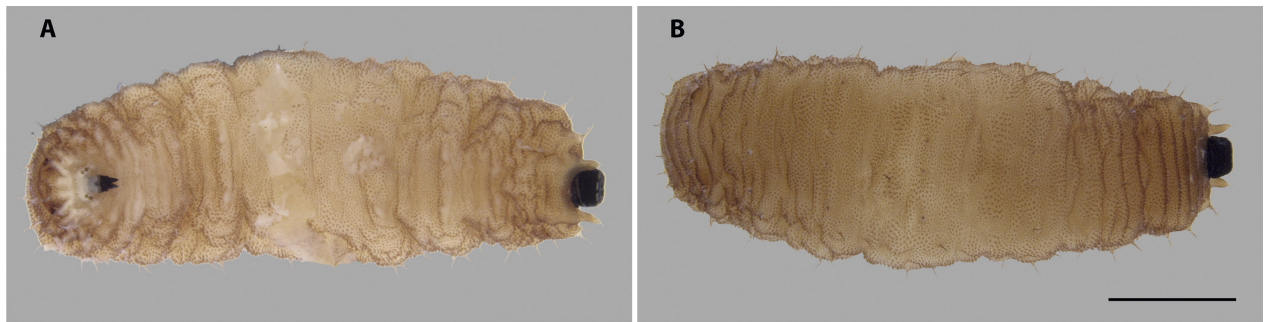


**Figure 18.** Light micrographs of *Merodon pulveris* larva general view. **A** larva in ventral view (Note: The central part of the specimen has been damaged in the process of tissue sampling for the DNA extraction.) **B** larva in dorsal view. Scale bar: 2 mm.

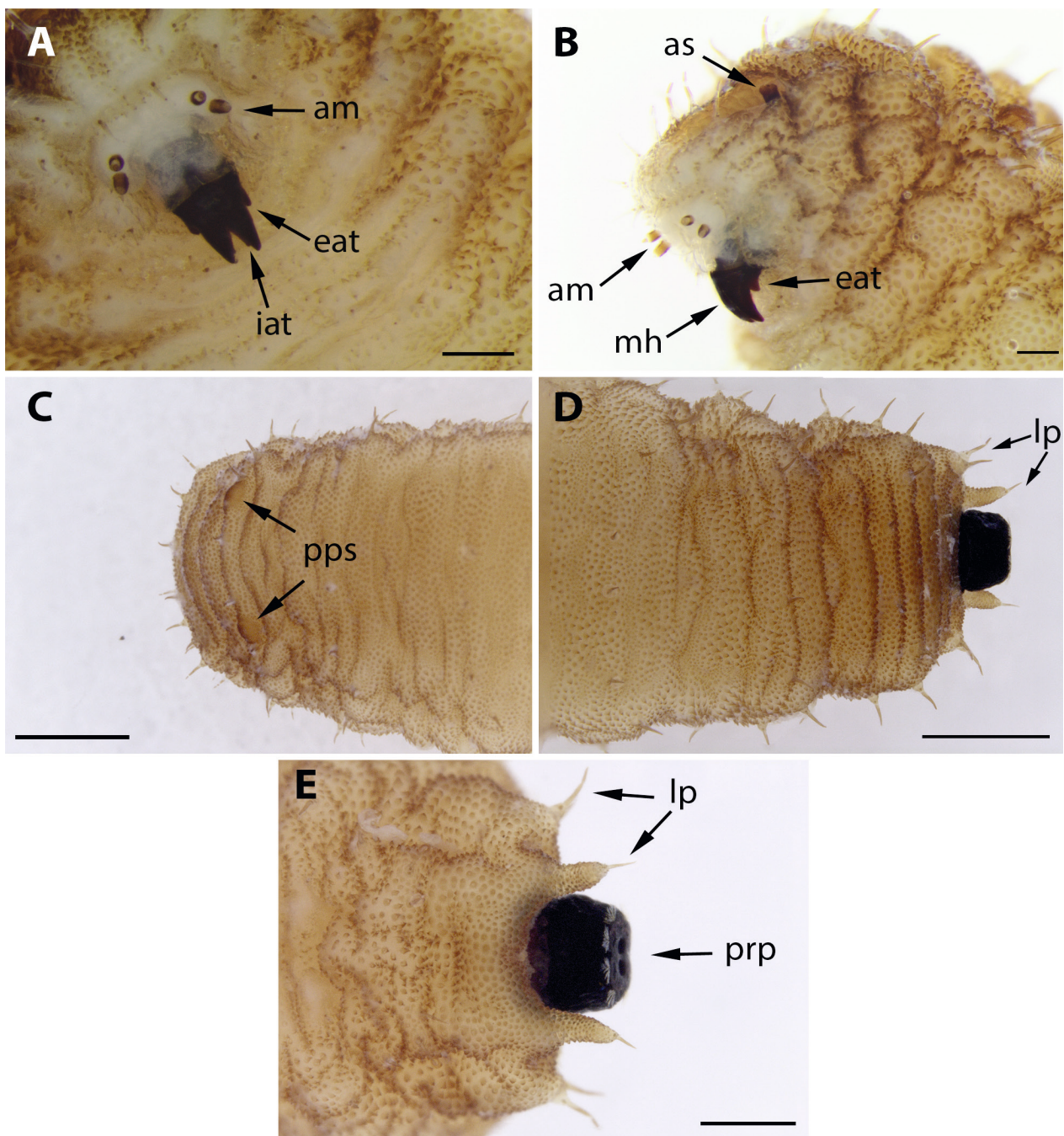


**Figure 19.** Light micrographs of *Merodon pulveris* larva. **A** mandibles **B** head **C** primordia of pupal spiracles **D** posterior part of the abdomen in dorsal view **E** posterior part of the abdomen in ventral view. Abbreviations: am – antenno-maxillary organs, as – anterior spiracle, eat – external accessory teeth, iat – internal accessory teeth, lp – lappets, mh – mouthhooks, pps – primordia of pupal spiracles, prp – posterior respiratory process. Scale bars: 200  $\mu$ m (A, B); 1 mm (C, D); 500  $\mu$ m (E).

**Table 1.** Genetic distances\* based on concatenated 5'-end and 3'-end COI gene sequences between species within the *M. natans* species group.

Species	<i>M. natans</i>	<i>M. pulveris</i>	<i>M. calcaratus</i>
<i>M. natans</i>			
<i>M. pulveris</i>	5.1		
<i>M. calcaratus</i>	5.3	5.9	
<i>M. makrisi</i> sp. nov.	5.4	6.4	5.6

\*Average uncorrected *p* distances expressed as percentages.

view; spiracular plate with 4 pairs of slightly curved and convoluted irregularly-shaped spiracular openings around two central scars; spiracular scars in pair of abrupt cavities, two sunken depressions in middle of spiracular plate; 4 pairs of very well-developed branched inter-spiracular setae emerging from edge of spiracular plate (Fig. 19E).

**Material examined.** GREECE, Lesvos Island, Loutra; 39.0510°N, 26.5312°E; Apr. 2018; A. Vujić leg.; 1 (L3 instar) larva in bulb of *Prospero autumnale* (Lp in FSUNS).

### 3.4. Molecular data

The concatenated 5'-end and 3'-end COI gene sequence matrix contains 61 sequences of 1,358 bp length. The total number of the variable positions is 429, while 331 are parsimony informative. As a result of MP analysis, we inferred a strict consensus tree (length=1,242, consistency index=0.45, retention index=0.78) of four equally parsimonious trees (see Supplementary file 2: Figure S1). ML and MP analyses resulted in similar tree topologies (Fig. 20, Supplementary file 2: Figure S1). The *Merodon natans* species group is resolved as monophyletic with high bootstrap support (99 and 97) on both MP and ML trees. Species clades of *M. natans*, *M. pulveris*, *M. calcaratus* and *M. makrisi* sp. nov. are also well supported, each with a bootstrap value of 100. Immature specimen AU1590 (larva) from Lesvos island belongs to the *M. pulveris* clade. Within *M. pulveris* two clades can be distinguished, one which corresponds to specimens from Cyprus and the second which contains specimens from Greek islands (Samos, Rhodes and Lesvos) and from Turkey (see Supplementary file 1: Table S1). Both these clades are well supported (bootstrap values: ML=100 and 87; MP=99).

Genetic distances based on concatenated 5'-end and 3'-end COI gene sequences between species pairs within the *M. natans* species group are in the range from 5.1% between *M. natans* and *M. pulveris* to 6.4% between *M. pulveris* and *M. makrisi* sp. nov. (Table 1). The average *p* distance between the two *M. pulveris* clades is 2.2%.

The combined COI+28S rRNA gene sequence matrix contains 48 sequences. The total length is 1,957 bp and there are 515 variable positions from which 377 are parsimony informative. *Merodon makrisi* sp. nov. is present with only one specimen due to lower sequencing success of 28S rRNA gene compared to COI gene. MP analysis resulted in a strict consensus tree (length=1,358 bp, con-

sistency index=0.48, retention index=0.76) of two equally parsimonious trees and had similar topology as ML tree (Fig. 21, Supplementary file 3: Figure S2). The *M. natans* species group is recovered as monophyletic, as well as the species *M. natans*, *M. pulveris* and *M. calcaratus* (bootstrap support value of 100). The single specimen of *M. makrisi* sp. nov. is resolved in a separate branch, clearly divergent from all other species of the *M. natans* group.

### 3.5. Geometric morphometric analysis

Wing shape variation among specimens was quantified using PCA, which produced 18 principal components (PCs) in total within both males and females. First two principal components (PCs) described 35% of wing-shape variation among male specimens and 36% among female specimens. In the space defined by the first two PCs groupings of conspecific specimens is clearly noticeable within both males and females (Fig. 22). In both cases, PC1 depicts wing shape differences between *M. natans* and *M. pulveris*, whereas PC2 differentiates *M. calcaratus* from *M. natans* and *M. pulveris* (Fig. 22).

Discriminant analysis provided evidence for highly significant wing shape differences among all species pairs ( $P < 0.01$ ; males: *M. natans* - *M. pulveris*  $F_{18,129}=41.67$ ; *M. natans* - *M. calcaratus*  $F_{18,129}=13.43$ ; *M. calcaratus* - *M. pulveris*  $F_{18,129}=18.57$ . Females: *M. natans* - *M. pulveris*  $F_{18,116}=30.43$ ; *M. natans* - *M. calcaratus*  $F_{18,116}=40.53$ ; *M. calcaratus* - *M. pulveris*  $F_{18,116}=27.86$ ). Additionally, DA with cross-validation based on wing shape showed correct species assignment for 97.32% male specimens and 98.53% for female specimens. Among the 149 male specimens, four were misclassified, one *M. pulveris* and two *M. calcaratus* as *M. natans*, and one specimen of *M. natans* as *M. pulveris*. Within 136 female specimens, only two specimens of *M. natans* were misclassified as *M. pulveris*. All female specimens of *M. pulveris* and *M. calcaratus* were correctly classified.

CVA conducted on wing shape parameters gave two highly significant canonical axes within both males and females (Males: CV1: Wilks'=0.0520,  $\chi^2=406.5518$ ,  $p < .01$ ; CV2: Wilks'=0.3607,  $\chi^2=140.2089$ ,  $p < .01$ ; Females: CV1: Wilks'=0.0293,  $\chi^2=439.3760$ ,  $p < .01$ ; CV2: Wilks'=0.2190,  $\chi^2=189.0509$ ,  $p < .01$ ).

Within males, CV1 with 77% of wing shape variation clearly differentiates *M. pulveris* from *M. natans* and *M. calcaratus*, while CV2 with 23% of shape variation clearly separated *M. calcaratus* from *M. natans* and *M. pul-*

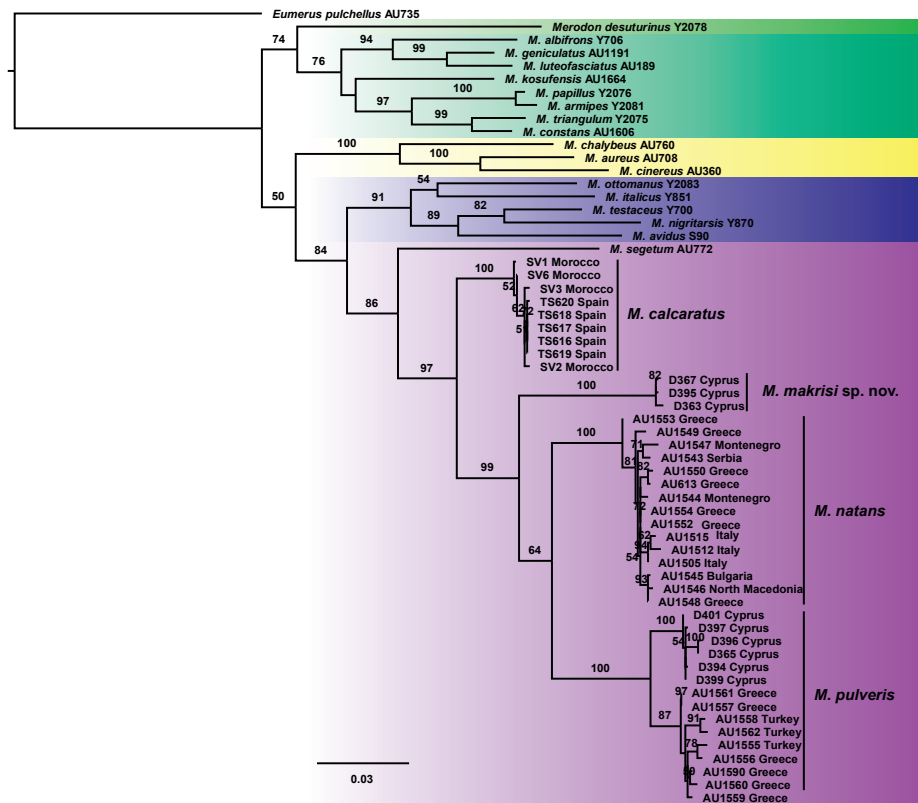


**Figure 20.** Maximum likelihood tree of *Merodon natans* species group based on COI gene sequence analysis. Bootstrap values  $\geq 50$  are presented near nodes. Coloured sections indicate different *Merodon* lineages (yellow – *aureus* lineage, light green – *desuturinus* lineage, dark green – *albifrons* lineage, blue – *avidus* lineage, purple – *natans* lineage).

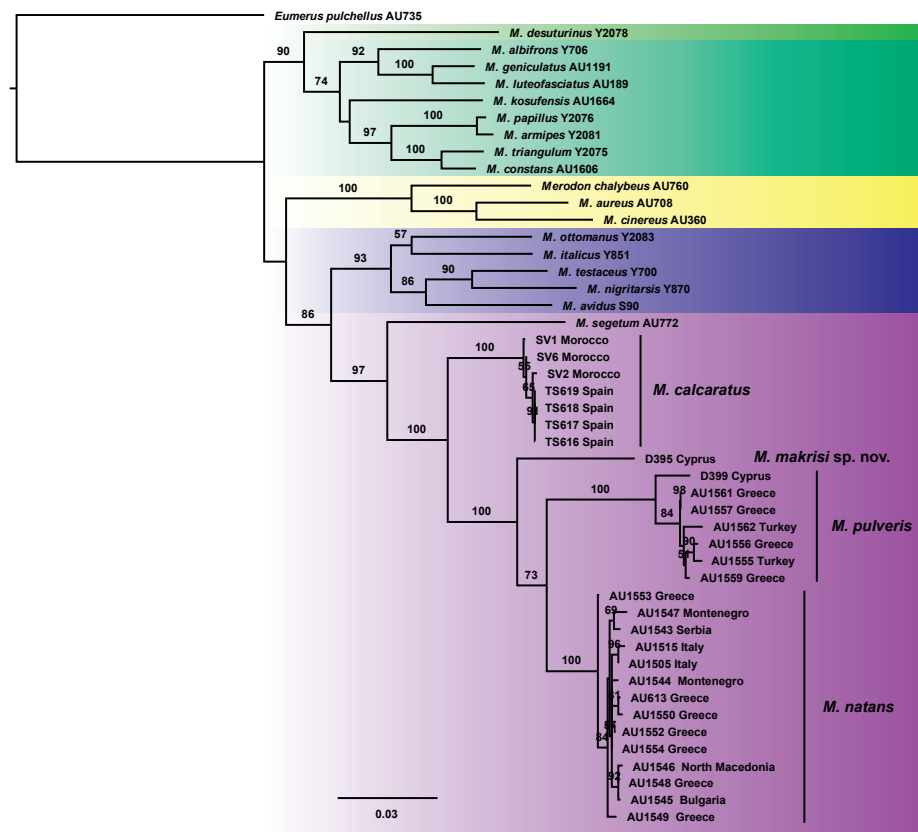


**Figure 21.** Maximum likelihood tree of *Merodon natans* species group based on combined COI+28S rRNA gene sequence analysis. Bootstrap values  $\geq 50$  are presented near nodes. Coloured sections indicate different *Merodon* lineages (yellow - *aureus* lineage, light green - *desuturinus* lineage, dark green - *albifrons* lineage, blue - *avidus* lineage, purple - *natans* lineage).

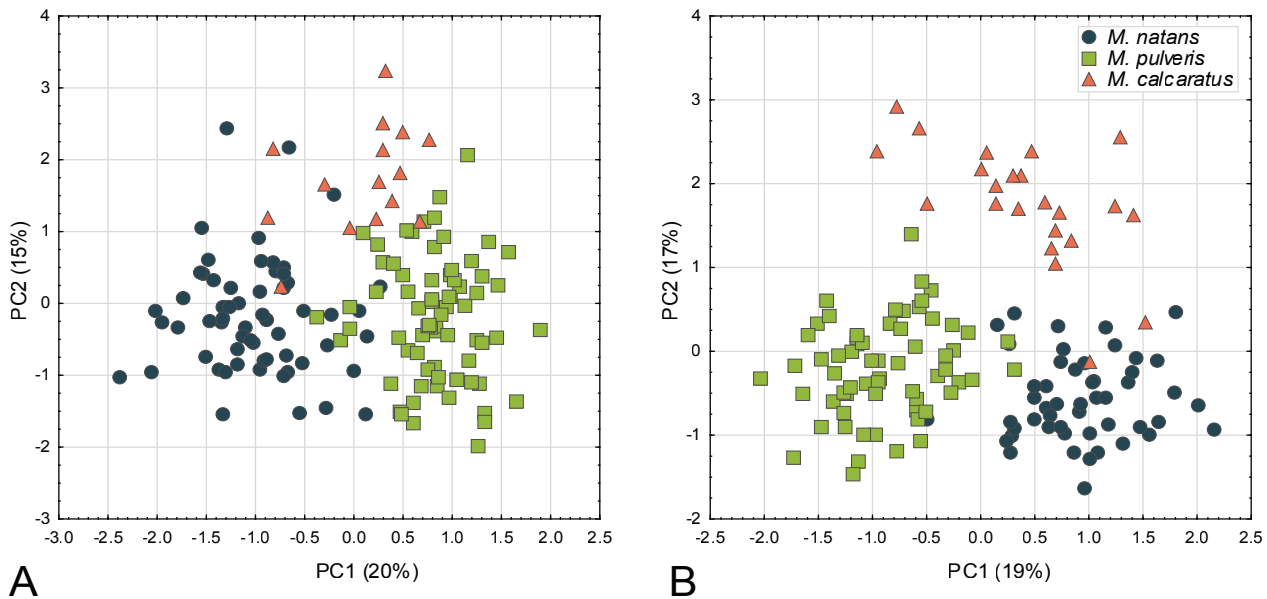


**Figure 22.** Scatter plot of individual scores of the two first principal components showing wing shape variation within the specimens of the *M. natans* group. PCA **A** Wing shape variation among male specimens **B** Wing shape variation among female specimens.

*veris* (Fig. 23A). Within females, CV1 with 64% of total wing shape variation points out the difference between *M. natans* and *M. calcaratus* and CV2 with 36% of total wing shape variation depicts the separation of *M. pulveris* from *M. natans* and *M. calcaratus* (Fig. 24A).

Phenogram based on squared Mahalanobis distances showed different phenetic relationships within males and females (Figs 23E, 24E). In males, *M. natans* and *M. calcaratus* had the most similar wing shape (Fig. 23E), whereas in females phenetic relationships were consistent with our molecular results, with *M. natans* and *M. pulveris* having the most similar wing shape (Fig. 24E).

Pairwise differences in average wing shape were visualised using superimposed outline drawings which allows recognition of wing regions that are contributing to the species discrimination (Figs 23B–D, 24B–D). Within males, differences between species pair *M. natans* and *M. calcaratus* were associated with most prominent landmark displacements in the central and distal parts of their wings (Fig. 23B). Differences in wing shape between *M. pulveris* and *M. calcaratus* males were most obvious in distal part of the wing (Fig. 23C), while the differences between *M. natans* and *M. pulveris* were associated with landmark shifts in the proximal part of the wing (Fig. 23D). Contrary to males, wing shape differences between females of *M. natans* and *M. calcaratus* were mainly in the distal part (Fig. 24B). Major differences in wing shape between females of *M. pulveris* and *M. calcaratus* were found in the central and distal parts of the wing (Fig. 24C). Differences in wing shape between females of *M. pulveris* and *M. natans* were associated with landmark displacements in the central and proximal parts of wings (Fig. 24D).

### 3.5.1. Population-level analysis

Wing shape variation among populations was measured using discriminant and canonical variate analysis. DA

showed correct classification for 81.85% of the specimens. Out of 270 specimens, 49 are misclassified, 46 into other conspecific populations, and only three as other species. Based on the UPGMA cluster analysis constructed with the Mahalanobis square distances, *M. natans* populations were the closest to each other, forming a cluster. Within this cluster, the population from Greece, Crete had the most distinct wing shape (Fig. 25B). The second cluster consists of two isolated branches, first with two western Mediterranean populations of *M. calcaratus*, and second one with conspecific populations of *M. pulveris* (Fig. 25B). According to topology, within *M. pulveris* branch specimens from Greece, Lesvos have the most distinct wing shape.

CVA produced eight significant CV axes, from which the first two were describing 72% of total shape variation (Fig. 25A). In the scatter plot described with these two CV axes, all conspecific populations were grouped together following the pattern of species delimitation results. First CV with 45% of total shape variation indicates separation of *M. pulveris* populations from *M. natans* populations, while CV2 with 27% of shape variation clearly separated populations of *M. calcaratus* from *M. natans* and *M. pulveris* (Fig. 25A).

### 3.6. Correlation among wing shape, genetic and spatial differentiation

Simple two-tailed Mantel tests revealed that geographical distance was not significantly correlated with wing shape differentiation nor with genetic differentiation among *M. natans*, *M. pulveris* and *M. calcaratus* (wing – geography:  $p=0.63474$ ,  $r=0.76691$ ; genetic- geography:  $p=0.14519$ ,  $r=0.97433$ ).

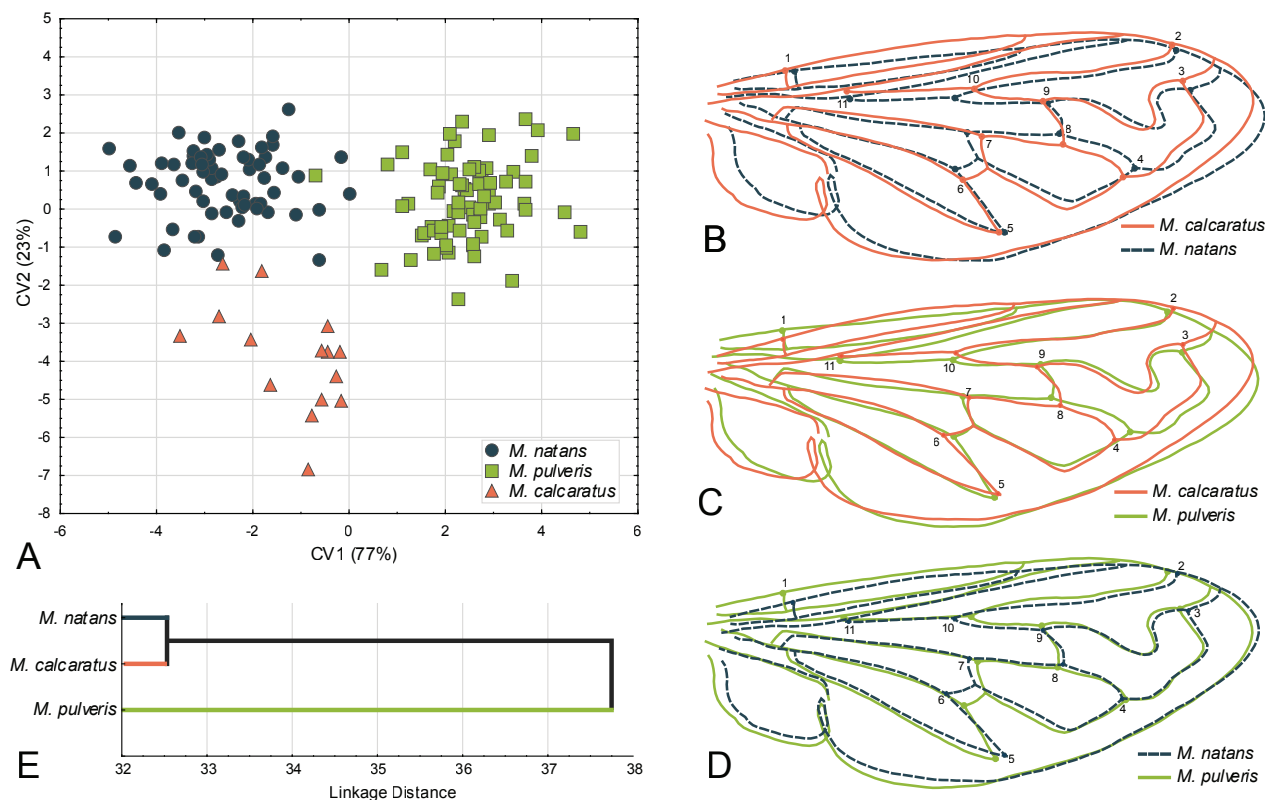


**Figure 23.** Wing shape differences among males of *Merodon natans*, *M. pulveris* and *M. calcaratus*. **A** Scatter plot of individual scores of CV1 and CV2 **B, C, D** Superimposed outline drawings showing differences in average wing shape for each species pair. Differences between the species were exaggerated 3-fold to make them more visible **E** UPGMA phenogram constructed using squared Mahalanobis distances of wing shape.

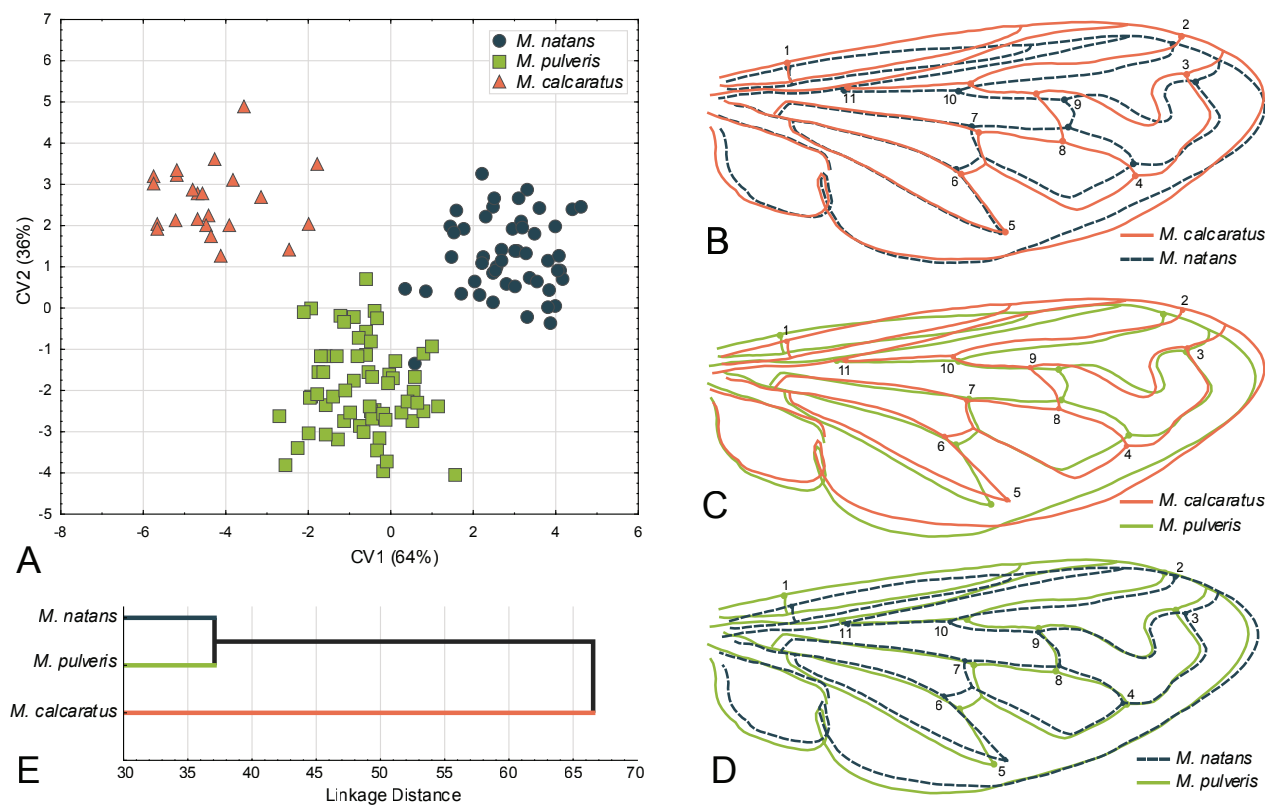


**Figure 24.** Wing shape differences among females of *Merodon natans*, *M. pulveris* and *M. calcaratus*. **A** Scatter plot of individual scores of CV1 and CV2 **B, C, D** Superimposed outline drawings showing differences in average wing shape for each species pair. Differences between the species were exaggerated 3-fold to make them more visible **E** UPGMA phenogram constructed using squared Mahalanobis distances of wing shape.

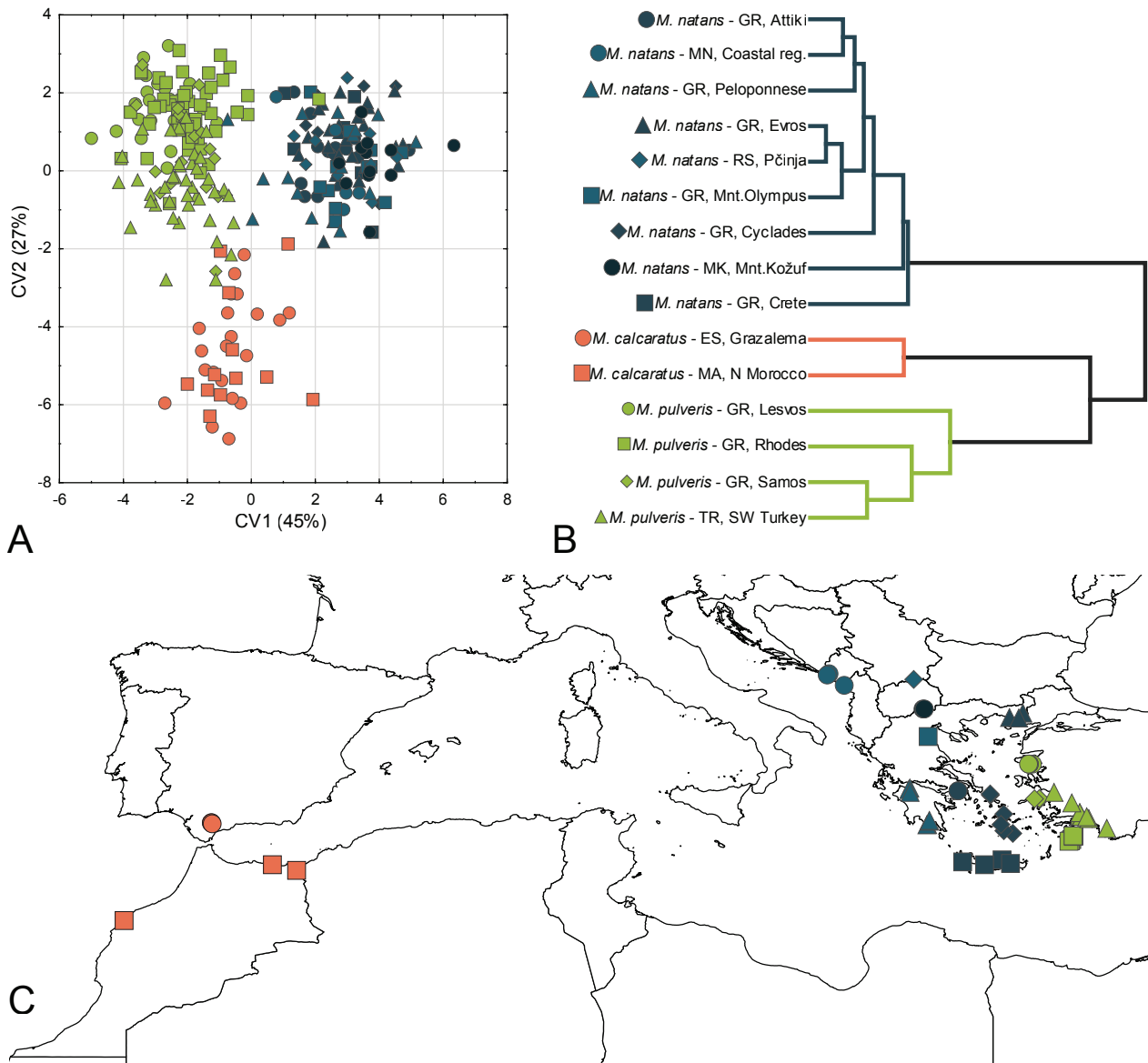


**Figure 25.** Wing shape differences among populations of *Merodon natans*, *M. pulveris* and *M. calcaratus*. **A** Scatter plot of individual scores of CV1 and CV2 **B** UPGMA phenogram constructed using squared Mahalanobis distances of wing shape **C** Map of Mediterranean basin showing the distribution of populations used in the analysis.

## 4. Discussion

### 4.1. Integrative taxonomy

The *Merodon natans* lineage as an independent evolutionary clade was first established by Radenković et al. (2018b) and here we have confirmed its monophyly on both COI and COI +28S trees.

The integrative taxonomy approach using multiple data sources implemented in this study supports species delimitation based on morphological differences within the *M. natans* group. Thus, it has proved useful in taxonomy of the group, as it has been in many previous studies on the genus *Merodon* (e.g., Popović et al. 2014, 2015; Ačanski et al. 2016; Šašić et al. 2016; Kočiš Tubić et al. 2018; Radenković et al. 2018a; Šašić Zorić et al. 2020; Vujić et al. 2020a, 2020b, 2020c). Morphological

descriptions combined with molecular data resolved four species of the *M. natans* species group: *M. calcaratus*, *M. pulveris*, *M. natans* and *M. makrasi* sp. nov. The first three species are also supported by the results of geometric morphometry analysis. Additionally, species distribution data proved useful for discriminating among species as they are mostly allopatric, except on the island of Cyprus where both *M. pulveris* and *M. makrasi* sp. nov. can be found in sympatry.

The four closely related species of the *Merodon natans* group have diagnostic morphological differences. Although *M. calcaratus* has exhibited high intraspecific variability, this species has diagnostic characters which make it morphologically the most divergent within the *M. natans* group. This is also supported by the *M. calcaratus* specimens resolved as sister to the other three species clades on the COI and COI+28S trees. *Merodon makrasi* sp. nov. is morphologically similar to both *M.*

*natans* and *M. pulveris*, while the latter two species are the most similar. Characters of antenna and male genitalia structure are the most stable features for delimiting *M. natans*, *M. pulveris* and *M. makrisi* sp. nov. Characters of the basoflagellomere are also very important for species delimitation.

The pattern of morphological relatedness between species of the *M. natans* group is supported by COI and COI+28S trees and in wing geometric morphometric analysis of *M. calcaratus*, *M. pulveris* and *M. natans* females, while in males *M. calcaratus* and *M. natans* have the most similar wing shape. Arok et al. (2019) provided evidence for *M. pulveris* and *M. natans* delimitation based on wing parameters. Here, we strengthened this evidence with the use of additional specimens of *M. natans* and *M. pulveris* from a broader geographical area, as well as including *M. calcaratus* in the analysis. These three species are significantly divergent based on wing shape. In both males and females, the percentage of correct species classification in discriminant function analysis is excellent (males: 97.32%, females: 98.53%). This segregation is also noticeable in CVA scatterplots, as well as in clear conspecific clustering in population analysis, which clearly illustrates the division of these three species. In addition, based on Mantel tests there is no significant correlation of wing and genetic differentiation with geographical proximity among *M. calcaratus*, *M. natans* and *M. pulveris*. As mentioned above, an interesting wing-shape pattern among male specimens is observed. Although it would be expected due to morphological and molecular results, males of *M. natans* and *M. pulveris* do not have the most similar wing shape in the UPGMA phenogram. Similar findings were recorded between sympatric species from e.g., the *M. aureus* group: *M. aureus* and *M. calidus* Šašić Zorić, Ačanski & Vujić, 2020 (Vujić et al. 2020c). However, according to our findings *M. natans* and *M. pulveris* do not occur in sympatry, and we can only assume that the most different wing shape between males can be the result of sympatry or secondary contact in the past. *Merodon makrisi* sp. nov. was not included in the geometric morphometric analysis, but molecular data and morphological characters clearly delineate it from other taxa within the *M. natans* group. This species was not included in the geometric morphometric analysis due to an insufficient number of available specimens with intact and undamaged wings that were available for analysis. Considering that *M. makrisi* sp. nov. can be separated from other investigated species based on morphology, its exclusion from the geometric morphometric analysis does not affect the strength of the provided results.

Despite their adult morphological resemblance, COI genetic distance between *M. natans* and *M. pulveris* is relatively high (5.1%) and similar to values between more distant species pairs (5.3–6.4%). The specimens of *M. pulveris* from Cyprus, based on COI and COI+28S analyses, segregate as reciprocally monophyletic within the *M. pulveris* clade. This population is morphologically indistinguishable from other analysed *M. pulveris* populations despite a genetic distance value of 2.2%, while the data on geometric morphometry is limited due to a

small sample size. Previous studies documented genetic distances between morphologically cryptic *Merodon* species mostly in the range 0.3–2.5% (Marcos-García et al. 2011; Popović et al. 2015; Šašić et al. 2016; Radenković et al. 2018a; Vujić et al. 2020c). Island speciation occurs often in the *M. aureus* species group, where endemic species are recorded on Andros, Crete, Cyprus, Naxos, Peloponnese and Rhodes (Vujić et al. 2016; Radenković et al. 2018a; Šašić Zorić et al. 2018). However, lack of additional data and relatively high genetic distance among the other species within the *M. natans* species group prevent us from any further conclusion about possible speciation on Cyprus. Furthermore, variation in morphological characters is present between populations of *M. makrisi* sp. nov. on the mainland and Cyprus. The Cyprus population of this species is characterized by stable morphological characters, while in populations from the mainland (Israel, Somalia) these features are variable. Thus, it is possible that the population of *M. makrisi* sp. nov. from Cyprus belongs to a distinct taxon, but no genetic data for mainland specimens of this species are available. Additional molecular and morphometric studies would certainly help to clarify the taxonomic status of populations of *M. pulveris* and *M. makrisi* sp. nov. from Cyprus (subspecies or small populations with limited variability).

## 4.2. Morphological characters of the immature stages

The shared character of the three species of the *Merodon natans* group examined in our study is the presence of two different pairs of lappets on the anal segment, the dorsolateral pair being apically divided. This trait was also reported in two species of the *avidus-nigritarsis* lineage: *M. avidus* larva (Andrić et al. 2014) and in *M. opacus* Vujić, Likov & Radenković, 2020 puparium (Vujić et al. 2020a). Other species, that belong to the *albifrons* lineage (i.e., *M. geniculatus*, *M. hurkmansi* Marcos-García, Vujić & Mengual, 2007 (larva described as *M. constans* in Ricarte et al. (2008), redefined in Andrić et al. (2014)), *M. luteihumerus* Marcos-García, Vujić & Mengual, 2007, *M. equestris* (Fabricius, 1794)) were described as having three pairs of lappets with the middle one consisting of two projections (Ricarte et al. 2008, 2017).

One of the most striking characters of the larva of *M. pulveris* is the possession of two sets of accessory teeth, a large pair on the basal outer side of the mandibular hooks and a small pair on the inner side of the hooks. Among all immature stages of *Merodon* species for which this character has been described, accessory teeth of the mandibular hooks were reported only for *M. equestris* and *M. avidus* larvae (Ricarte et al. 2008; Andrić et al. 2014), but only on the inner side of hooks. Nevertheless, accessory teeth were not recorded in puparia, either the ones examined here or those of other studied species including *M. avidus*. Furthermore, it has been suggested that there is mouthhook wear during larval development, making characters related to its shape deceptive in puparia (Preradović et al. 2018). The notable feature of the head skel-

eton of *M. makrasi* sp. nov. is that the dorsal cornu slightly exceeds the ventral cornu in its length, whereas in *M. natans* both cornua are approximately the same length; in other species of the genus the dorsal cornu is usually more or less shorter than the ventral. Anterior spiracles of *M. pulveris* larva are bilobulated at the apex, the same shape as for the other two species of the *M. natans* group. The two spiracular openings at the apex of the anterior spiracle of *M. makrasi* sp. nov. and *M. natans* is a feature previously reported for the anterior respiratory process of *M. geniculatus*, *M. avidus*, *M. opacus* and *M. hurkman-si*, whereas *M. luteihumerus* and *M. equestris* exhibit 3–5 spiracular openings (Ricarte et al. 2008, 2017; Andrić et al. 2014; Vujić et al. 2020a).

Shared characters of the three species examined in our study are the general shape and ornamentation of the posterior respiratory process (prp). The prp shape varies among *Merodon* species; for instance, very short cylinder (button-shaped) in *M. avidus* and *M. opacus*, barrel-shaped in *M. calidus* (puparium described as *M. aureus* in Preradović et al. (2018), redefined in Vujić et al. (2020c)) and markedly narrowed in the apical third in *M. rufus* Meigen, 1838 (Andrić et al. 2014; Preradović et al. 2018; Vujić et al. 2020a). In the *M. natans* group, the prp shape is a truncated cone, with a groove at the base. The prp being wider than long with base wider than apex is notable in *M. makrasi* sp. nov., however, these features are somewhat less pronounced in *M. pulveris* and even less in *M. natans*, with a slightly longer and more cylindrical prp. The lateral surface of the prp is entirely coriaceous, with small dents from base to apex and with slightly undulate longitudinal indentations in the basal part, somewhat resembling the prp of *M. geniculatus* (see figs 5D, 6D in Ricarte et al. (2017)). The part just below the spiracular plate is conspicuously ornamented in *M. pulveris* and *M. natans*, while it is smoother in *M. makrasi* sp. nov. Other species have different ornamentation of the prp surface; e.g., very smooth from base to apex in *M. rufus* (with small dents only in the area below spiracular plate) and with a network of small rounded protuberances in *M. calidus* (Preradović et al. 2018).

One of the problems in the morphological research of *Merodon* immature stages is the difficulty of finding specimens in the field, since the larval food-plants and the breeding and oviposition sites have not been recorded for most *Merodon* species (Hurkmans 1993; Rotheray 1993; Speight 2020). Another important handicap is the proper species identification of immature stages. Rearing phytophagous syrphid is not particularly complicated (Rotheray 1993) but can take months (Rotheray and Gilbert 2011). In our study, pupae of *M. makrasi* sp. nov. and *M. natans* were successfully reared. An identification of immature stages based on DNA COI barcode libraries generated for *Merodon* adults was suggested by Ståhls et al. (2009) and was successfully employed for larvae of *M. avidus* by Andrić et al. (2014), as well as for larva of *M. pulveris* in our study. Nevertheless, sequencing analysis is not possible in cases of rotten or parasitoidised specimens, as has been shown by Preradović et al. (2018). Furthermore, species-level illustrations are limited and

a comprehensive identification key has been published only recently (Ricarte et al. 2017). The immature stages of only nine out of 234 species of *Merodon* have been described so far (Heiss 1938; Stuckenberg 1956; Ricarte et al. 2008, 2017; Andrić et al. 2014; Preradović et al. 2018; Vujić et al. 2020a).

### 4.3. Diversity and distribution

The four species of the *Merodon natans* group are mostly distributed within the Mediterranean Basin, but we report the first records of the presence of this species group in the Afrotropical Region, with the distributional range of two species reaching the easternmost parts of Sub-Saharan Africa. *Merodon natans* has been described geographically as a “Balkan” species, occurring throughout the Balkans and the eastern Mediterranean islands, except Dodecanese, North Aegean islands and Cyprus (Arok et al. 2019). Additional data in the present work confirm a broader distribution to the west, including records from Spain, Italy and France. Although there are records in the literature of *M. natans* from Gibraltar (Ebejer and Bensusan 2010) and Portugal (van Eck 2016), voucher specimens were examined by the authors in the work frame of this survey and identified as *M. obscuritarsis* Strobl in Czerny & Strobl, 1909. *Merodon pulveris* is characterized as having an “Anatolian” distribution, being found in western and southwestern Turkey, and on Dodecanese, North Aegean islands and Cyprus. A second species from the *M. natans* group occurring on the island of Cyprus is *M. makrasi* sp. nov., primarily distributed in Israel, but also with records from Somalia. The southernmost record of the *M. natans* group is one for *M. calcaratus* from Kenya. However, this species is mostly distributed along the northwestern (Mediterranean) coast of the African continent and on the Iberian Peninsula.

The regions with the highest diversity of *Merodon* taxa, such as the Mediterranean Basin, are characterized with flora rich in species of geophytes, as the bulbs and other underground storage organs of these plants are food sources for *Merodon* larvae (Ricarte et al. 2008, 2017). Therefore, the current geographical distributions of *Merodon* taxa are probably connected to areas with high diversity of this distinctive flora (Vujić et al. 2011, 2013). Since the Afrotropical Region is rich in bulbous plants, it is assumed that the *Merodon* species diversity in this region is underestimated (Djan et al. 2020), with only 16 species (out of a total number of 234) described for this region to date (Vujić et al. 2021). The genus *Merodon* has been classified into over 20 monophyletic species groups (Vujić et al. 2021), with a vast majority of species present in the Palaearctic Region and only two species groups (prior to *M. natans* species group), *M. aureus* and *M. desuturinus*, known to have representatives in the Afrotropical Region as well (Radenković et al. 2018b). The *M. desuturinus* species group has been found to represent an important link between the Palaearctic and Afrotropical faunas, consisting of two clearly separate lineages, i.e., a Palaearctic and an Afrotropical lineage (the latter includ-

ing *M. melanocerus* and *M. planifacies* subgroups and the species *M. cuthbertsoni* Curran, 1939, all from southern Africa (Radenković et al. 2018b). The results of our research show the presence of yet another *Merodon* species group in the Afrotropical Region, the *M. natans* species group, with the first published records of this genus in eastern Africa.

Out of the four species of the *Merodon natans* group, descriptions of immature stages are presented for three species: *M. pulveris* based on larva, and *M. natans* and *M. makrisi* sp. nov. based on puparia, all found in the bulbs of the same plant species, *Prospero autumnale*. With the small size of one such bulb in mind, it could be speculated that these larvae grow at a slow rate, but it is possible that larvae move from one bulb to another while they grow, since *P. autumnale* can be found in dense patches. However, in the locality where the puparium of *M. makrisi* sp. nov. was found, the loamy soil can be very dried out and hard, making it seemingly difficult to move from one bulb to another. On the other hand, bulbs of *P. autumnale* are found quite superficially, making it possible for the larva to migrate to another bulb over the ground. This plant had previously been recorded as a possible larval host-plant for *M. natans* and *M. pulveris* in Greece (Vujić et al. 2020d), and also for *M. calcaratus* in Portugal (van Eck 2016). Most of the known larval host-plants of *Merodon* species belong to the same plant family, Asparagaceae (Ricarte et al. 2008; Andrić et al. 2014; Preradović et al. 2018), although some are recorded within Amaryllidaceae (Heiss 1938; Ricarte et al. 2017; Popov and Mishustin pers. comm.) and Iridaceae (Stuckenberg 1956). In a recent study by Vujić et al. (2020a) it has been speculated that groups of related *Merodon* species might have the same host plant genus. Considering both our extant records and fitting distributions with *Prospero* Salisb. (WCSP 2019), *M. natans* species group could therefore be connected to this genus throughout most of its range. However, *Prospero* is not present in the Afrotropical Region, so larval development is most likely associated with other bulbous geophytes in this area, probably also from Asparagaceae subfamily Scilloideae (alternatively regarded as Hyacinthaceae). Moreover, it could be assumed that cases of aberrant distribution records may have been the result of plant introductions. More data are needed to obtain better supported conclusions about relations with food-plants. Furthermore, additional material and molecular analyses of *Merodon* populations from Somalia and Kenya will be useful to confirm their taxonomic identification or to reveal if they belong to a separate species. The male genitalia of *M. calcaratus* have very variable morphological features, even on an intrapopulation level. Nonetheless, all studied specimens are characterized with the same apomorphic characters, which clearly differentiate this taxon from other species of the *M. natans* group.

## 5. Authors' contributions

AV, TT, XM, AvanE, SRad performed the sampling; AV, TT, SRad conceived and designed the study; AV, TT, AAnd, JA, LjŠZ, CP-B, AAra,

SV, MA, XM performed the experimental analysis; AV, TT, AAnd, JA, LjŠZ, CP-B participated in data analyses. AV, TT, AAnd, JA, LjŠZ, CP-B, AAra, MA, XM, AvanE, SRoj took part in draft preparation, contributed to discussions during preparation of the paper, as well as read and commented on. All authors approved the final version of the manuscript.

## 6. Acknowledgements

We are sincerely grateful to Martin Ebejer (Wales, United Kingdom) and Antonio Ricarte (Alicante, Spain) for sharing photos of *Merodon natans* from Gibraltar and Spain, which helped a lot to understand the distribution of this species. Christodoulos Makris (Limassol, Cyprus) collected many specimens in Cyprus, shared information on flower visits and generously offered photos for this paper. The Department of Environment (ref. no's 02.15.001.003 and 04.05.002.005.006) and the Department of Forests (ref. no. 2.15.05.3) of the Ministry of Agriculture, Rural Development and Environment of the Republic of Cyprus (Nicosia, Cyprus) kindly permitted us (AvE and XM) to collect in Cyprus. We thank Claudia Eitzbauer (ZFMK, Germany) for her support to obtain molecular data. Chris Palmer (Portsmouth, UK) is thanked for checking the English language of the manuscript. The authors acknowledge financial support of the Ministry of Education, Science and Technological Development of the Republic of Serbia (Grant No. 451-03-9/2021-14/200125 and Grant No. 451-03-9/2021-14/200358). André van Eck was financially supported for research in Cyprus by the Dutch Uyttenboogaart-Eliassen Foundation (UES), with grant nrs. SUB.2016.12.12 and SUB.2018.12.03. The authors declare that no competing interests exist.

## 7. References

- Ačanski J, Vujić A, Djan M, Obreht-Vidaković D, Ståhls G, Radenković S (2016) Defining species boundaries in the *Merodon avidus* complex (Diptera, Syrphidae) using integrative taxonomy, with the description of a new species. *European Journal of Taxonomy* 237: 1–25. <https://doi.org/10.5852/ejt.2016.237>
- Andrić A, Šikoparija B, Obreht D, Đan M, Preradović J, Radenković S, Pérez-Bañón C, Vujić A (2014) DNA barcoding applied: identification of the larva of *Merodon avidus* (Diptera: Syrphidae). *Acta Entomologica Musei Nationalis Pragae* 54(2): 741–757. <https://biotaxa.org/AEMNP/article/view/9167/10927>
- Arok M, Ačanski J, Tot T, Radenković S, Vujić A (2019) *Merodon natans* and *M. pulveris* (Diptera: Syrphidae): Delimitating cryptic hoverfly species using the geometric morphometric method. *Acta Entomologica Serbica* 24(2): 63–84. <https://doi.org/10.5281/zenodo.3379973>
- Belshaw R, Lopez-Vaamonde C, Degerli N, Quicke DLJ (2001) Phylogenetic taxa and taxonomic chaining: evaluating the classification of braconine wasps (Hymenoptera: Braconidae) using 28S D2-3 rDNA sequences and morphological characters. *Biological Journal of the Linnean Society* 73(4): 411–424. <https://doi.org/10.1006/bjpl.2001.0539>
- Chen H, Rangasamy M, Tan SY, Wang H, Siegfried BD (2010) Evaluation of five methods for total DNA extraction from western corn rootworm beetles. *PLoS ONE* 5(8): e11963. <https://doi.org/10.1371/journal.pone.0011963>
- Courtney GW, Sinclair BJ, Meier R (2000) Morphology and terminology of Diptera larvae. In: Papp L, Darvas B (Eds) *Contributions to*

- a Manual of Palaearctic Diptera (with Special Reference to Flies of Economic Importance). Science Herald, Budapest, 85–161.
- Curran CH (1939) Records and descriptions of African Syrphidae.—III (Diptera). American Museum Novitates 1025: 1–11.
- Czerny L, Strobl PG (1909) Spanische Dipteren. III. Verhandlungen der Zoologisch-Botanischen Gesellschaft in Wien 59: 121–301.
- Djan M, Ståhls G, Veličković N, Ačanski J, Obreht Vidaković D, Rojo S, Pérez-Bañón C, Radenković S, Vujić A (2020) The *Merodon planifacies* subgroup (Diptera, Syrphidae): congruence of molecular and morphometric evidences reveal new taxa in Drakensberg mountain valleys (Republic of South Africa). Zoologischer Anzeiger 287(2020): 105–120. <https://doi.org/10.1016/j.jcz.2020.05.010>
- Doczkal D, Pape T (2009) *Lyneborgimyia magnifica* gen. et sp. n. (Diptera: Syrphidae) from Tanzania, with a phylogenetic analysis of the Eumerini using new morphological characters. Systematic Entomology 34(3): 559–573. <https://doi.org/10.1111/j.1365-3113.2009.00478.x>
- Ebejer MJ, Bensusan K (2010) Hoverflies (Diptera, Syrphidae) recently encountered on Gibraltar, with two species new for Iberia. Dipterists Digest 17: 123–139.
- Fabricius JC (1794) Entomologia systematica emendata et aucta. Vol. 4. Christian Gottlob Proft, Copenhagen, 472 pp.
- Fabricius JC (1805) Systema antliatorum secundum ordines, genera, species, adiectis synonymis, locis, observationibus, descriptionibus. Apud Carolum Reichard, Brunswick, 372 + 30 pp.
- Folmer O, Black M, Hoeh W, Lutz R, Vrijenhoek R (1994) DNA primers for amplification of mitochondrial cytochrome c oxidase subunit I from diverse metazoan invertebrates. Molecular Marine Biology and Biotechnology 3(5): 294–299. <https://www.ncbi.nlm.nih.gov/pubmed/7881515>
- Goloboff PA (1999) NONA computer program. Version 2.0. Tucuman (Argentina). Available from <https://www.softpedia.com/get/Science-CAD/NONA.shtml> [Accessed on 22.01.2019]
- Haarto A, Ståhls G (2014) When mtDNA COI is misleading: congruent signal of ITS2 molecular marker and morphology for North European *Melanostoma Schiner, 1860* (Diptera, Syrphidae). ZooKeys 431: 93–134. <https://doi.org/10.3897/zookeys.431.7207>
- Hadley A (2006) CombineZ5. Available from <http://www.hadleyweb.pwp.blueyonder.co.uk/CZ5/combinez5.htm> [Accessed on 13.11.2020]
- Hall TA (1999) BioEdit: a user-friendly biological sequence alignment editor and analysis program for Windows 95/98/ NT. Nucleic Acids Symposium Series 41: 95–98. <http://brownlab.mbio.ncsu.edu/JWB/papers/1999Hall1.pdf>
- Haffaessas B, Djellab S, Samraoui F, Alfarhan AH, Gilbert F, Ricarte A, Samraoui B (2017) Hoverflies of the Guelma district, with species new to Algeria and North Africa (Diptera: Syrphidae). Annales de la Société entomologique de France (N.S.) 53(5): 324–333. <https://doi.org/10.1080/00379271.2017.1355262>
- Heiss EM (1938) A classification of the larvae and puparia of the Syrphidae of Illinois exclusive of aquatic forms. Illinois Biological Monographs 16(4): 1–142. <https://doi.org/10.5962/bhl.title.50277>
- Hijmans RJ, Guarino L, Mathur P (2012) DIVA GIS. Version 7.5. A geographic information system for the analysis of species distribution data. Available from <https://www.diva-gis.org> [Accessed on 13.08.2020]
- Hurkmans W (1993) A monograph of *Merodon* (Diptera: Syrphidae). Part 1. Tijdschrift Voor Entomologie 136: 147–234.
- Katoh K, Standley DM (2013) MAFFT multiple sequence alignment software version 7: improvements in performance and usability. Molecular Biology and Evolution 30(4): 772–780. <https://doi.org/10.1093/molbev/mst010>
- Klingenberg CP (2011) MorphoJ: an integrated software package for geometric morphometrics. Molecular Ecology Resources 11: 353–357. <https://doi.org/10.1111/j.1755-0998.2010.02924.x>
- Kočiš Tubić N, Ståhls G, Ačanski J, Djan M, Obreht Vidaković D, Hayat R, Khaghaninia S, Vujić A, Radenković S (2018) An integrative approach in the assessment of species delimitation and structure of the *Merodon nanus* species group (Diptera: Syrphidae). Organisms Diversity & Evolution 18(4): 479–497. <https://doi.org/10.1007/s13127-018-0381-7>
- Kumar S, Stecher G, Tamura K (2016) MEGA7: Molecular Evolutionary Genetics Analysis version 7.0 for bigger datasets. Molecular Biology and Evolution 33(7): 1870–1874. <https://doi.org/10.1093/molbev/msw054>
- Loew H (1848) Ueber die europäischen Arten der Gattung *Eumerus*. Stettiner Entomologische Zeitung 9(4): 108–128.
- Mantel NA (1967) The detection of disease clustering and a generalized regression approach. Cancer Research 27: 209–220.
- Marcos-García MÁ, Vujić A, Mengual X (2007) Revision of Iberian species of the genus *Merodon* (Diptera: Syrphidae). European Journal of Entomology 104: 531–572. <https://doi.org/10.14411/eje.2007.073>
- Marcos-García MÁ, Vujić A, Ricarte A, Ståhls G (2011) Towards an integrated taxonomy of the *Merodon equestris* species complex (Diptera: Syrphidae) including description of a new species, with additional data on Iberian *Merodon*. The Canadian Entomologist 143(4): 332–348. <https://doi.org/10.4039/n11-013>
- McAlpine JF (1981) Morphology and terminology—Adults. In: McAlpine JF, Peterson BV, Shewell GE, Teskey HJ, Vockeroth JR, Wood DM (Eds) Manual of Nearctic Diptera. Vol. 1. Research Branch, Agriculture Canada, Ottawa, 9–63.
- Meigen JW (1822) Systematische Beschreibung der bekannten europäischen zweiflügeligen Insekten. Dritter Theil. Schulz-Wundermann, Hamm, x + 416 pp.
- Meigen JW (1838) Systematische Beschreibung der bekannten europäischen zweiflügeligen Insekten. Siebenter Theil oder Supplementband. Schultz, Hamm, xii + 434 pp.
- Mengual X, Ståhls G, Vujić A, Marcos-García MÁ (2006) Integrative taxonomy of Iberian *Merodon* species (Diptera: Syrphidae). Zootaxa 1377: 1–26.
- Mengual X, Ståhls G, Láska P, Mazánek L, Rojo S (2018) Molecular phylogenetics of the predatory lineage of flower flies *Eupeodes-Scaeva* (Diptera: Syrphidae), with the description of the Neotropical genus *Austroscaeva* gen. nov. Journal of Zoological Systematics and Evolutionary Research 56(2): 148–69. <https://doi.org/10.1111/jzs.12212>
- Miller MA, Pfeiffer W, Schwartz T (2010) Creating the CIPRES Science Gateway for inference of large phylogenetic trees. In: Proceedings of the Gateway Computing Environments Workshop (GCE), New Orleans, Louisiana (USA), November 2010. Institute of Electrical and Electronics Engineers, Piscataway, New Jersey, 1–8. <https://doi.org/10.1109/GCE.2010.5676129>
- Nedeljković Z, Ačanski J, Vujić A, Obreht D, Đan M, Ståhls G, Radenković S (2013) Taxonomy of *Chrysotoxum festivum* Linnaeus, 1758 (Diptera: Syrphidae) – an integrative approach. Zoological Journal of the Linnean Society 169(1): 84–102. <https://doi.org/10.1111/zoj.12052>
- Nedeljković Z, Ačanski J, Đan M, Obreht-Vidaković D, Ricarte A, Vujić A (2015) An integrated approach to delimiting species borders

- in the genus *Chrysotoxum* Meigen, 1803 (Diptera: Syrphidae), with description of two new species. *Contributions to Zoology* 84(4): 285–304. <https://doi.org/10.1163/18759866-08404002>
- Nedeljković Z, Ricarte A, Šašić Zorić Lj, Djan M, Hayat R, Vujić A, Marcos-García MÁ (2020) Integrative taxonomy confirms two new West-Palaearctic species allied with *Chrysotoxum vernale* Loew, 1841 (Diptera: Syrphidae). *Organisms Diversity & Evolution* 20: 821–833. <https://doi.org/10.1007/s13127-020-00465-w>
- Nixon KC (2008) ASADO, version 1.85 TNT-MrBayes Slaver version 2; mxram 200 (v1 5.30). Made available through the author (previously named WinClada, version 1.00.08 (2002). Available from <http://www.diversityoflife.org/winclada> [Accessed on 22.01.2019]
- Pehlivan E, Akbulut N (1991) Some investigations on the syrphid species attacking on *Narcissus* in Karaburun (Izmir) and the biology and control measures of *Merodon eques* (F.) (Diptera). *Turkish Journal of Agriculture and Forestry* 15: 47–81.
- Popov GV (2010) *Merodon alexandri* spec. nov.—a new species of hoverfly (Diptera: Syrphidae) from the northern Black Sea Region. *Studia Dipterologica* 16: 133–151.
- Popović D, Djan M, Šašić Lj, Šnjegota D, Obreht D, Vujić A (2014) Usage of Different Molecular Markers in Delimitation of Cryptic Taxa of *Merodon avidus* species complex (Diptera: Syrphidae). *Acta Zoologica Bulgarica Supplement 7*: 33–38. <http://acta-zoologica-bulgarica.eu/downloads/acta-zoologica-bulgarica/2014/supplement-7-33-38.pdf>
- Popović D, Ačanski J, Đan M, Obreht D, Vujić A, Radenković S (2015) Sibling species delimitation and nomenclature of the *Merodon avidus* complex (Diptera: Syrphidae). *European Journal of Entomology* 112(4): 790–809. <https://doi.org/10.14411/eje.2015.100>
- Preradović J, Andrić A, Radenković S, Šašić Zorić Lj, Pérez-Bañón C, Campoy A, Vujić A (2018) Pupal stages of three species of the phytophagous genus *Merodon* Meigen (Diptera: Syrphidae). *Zootaxa* 4420(2): 229–242. <https://doi.org/10.11646/zootaxa.4420.2.5>
- Quantum GIS Development Team (2012) Quantum GIS Geographic Information System. Open Source Geospatial Foundation Project. Available from <https://qgis.org/en/site> [Accessed on 13.12.2020]
- Radenković S, Vujić A, Ståhls G, Pérez-Bañón C, Rojo S, Petanidou T, Šimić S (2011) Three new cryptic species of the genus *Merodon* Meigen (Diptera: Syrphidae) from the island of Lesbos (Greece). *Zootaxa* 2735: 35–56. <https://doi.org/10.11646/zootaxa.2735.1.5>
- Radenković S, Šašić Zorić Lj, Djan M, Obreht Vidaković D, Ačanski J, Ståhls G, Veličković N, Markov Z, Petanidou T, Kociš Tubić N, Vujić A (2018a) Cryptic speciation in the *Merodon luteomaculatus* complex (Diptera: Syrphidae) from the eastern Mediterranean. *Journal of Zoological Systematics and Evolutionary Research* 56(2): 170–191. <https://doi.org/10.1111/jzs.12193>
- Radenković S, Veličković N, Ssymank A, Obreht Vidaković D, Djan M, Ståhls G, Veselić S, Vujić A (2018b) Close relatives of Mediterranean endemo-relict hoverflies (Diptera, Syrphidae) in South Africa: Morphological and molecular evidence in the *Merodon melanoceurus* subgroup. *PLoS ONE* 13(7): e0200805. <https://doi.org/10.1371/journal.pone.0200805>
- Radenković S, Vujić A, Obreht Vidaković D, Djan M, Milić D, Veselić S, Ståhls G, Petanidou T (2020) Sky island diversification in the *Merodon rufus* group (Diptera, Syrphidae)—recent vicariance in south-east Europe. *Organisms Diversity & Evolution* 20: 345–368. <https://doi.org/10.1007/s13127-020-00440-5>
- Reemer M, Goudsmits K (2004) Oviposition observed in *Chrysotoxum cautum*, *C. vernale* and *Merodon avidus* (Diptera, Syrphidae). *Volucella* 7: 217–218.
- Ricarte A, Marcos-García MÁ, Rotheray GE (2008) The early stages and life histories of three *Eumerus* and two *Merodon* species (Diptera: Syrphidae) from the Mediterranean region. *Entomologica Fennica* 19: 129–141. <https://doi.org/10.33338/ef.84424>
- Ricarte A, Souba-Dols GJ, Hauser M, Marcos-García MÁ (2017) A review of the early stages and host plants of the genera *Eumerus* and *Merodon* (Diptera: Syrphidae), with new data on four species. *PLoS ONE* 12(12): e0189852. <https://doi.org/10.1371/journal.pone.0189852>
- Rodríguez FJLOJ, Oliver JL, Marín A, Medina JR (1990) The general stochastic model of nucleotide substitution. *Journal of Theoretical Biology* 142(4): 485–501. [https://doi.org/10.1016/S0022-5193\(05\)80104-3](https://doi.org/10.1016/S0022-5193(05)80104-3)
- Rohlf FJ (2017a) TpsDig—digitize landmarks and outlines. Ver. 2.31. [Computer software and manual] Department of Ecology, Evolution and Anthropology, Stony Brook University.
- Rohlf FJ (2017b) TpsRelv. Ver. 1.69. Department of Ecology, Evolution and Anthropology, Stony Brook University.
- Rohlf FJ, Slice DE (1990) Extensions of the Procrustes method for the optimal superimposition of landmarks. *Systematic Zoology* 39(1): 40–59. <https://doi.org/10.2307/2992207>
- Rondani C (1843) Diptères nouveaux d’Italie. *Revue Zoologique par la Société Cuvierienne* 6: 43–44.
- Rondani C (1845) Sulle specie Italiane del genere *Merodon*. *Memoria decimaquarta per servire alla ditterologia Italiana. Nuovi Annali delle Scienze naturali Bologna* 4: 254–267.
- Rosenberg MS, Anderson CD (2011) PASSaGE: pattern analysis, spatial statistics and geographic exegesis. Version 2. *Methods in Ecology and Evolution* 2: 229–232. <https://doi.org/10.1111/j.2041-210X.2010.00081.x>
- Rossi P (1790) *Fauna Etrusca. Sistens insecta quae in provinciis Florentina et Pisana praesertim collegit*. Vol. 2. Masi, Livorno, 348 pp.
- Rossi P (1794) *Mantissa insectorum, exhibens species nuper in Etruria collectas, adiectis Faunae Etruscae illustrationibus, ac emendationibus*. Vol. 2. Polloni, Pisa, 154 pp.
- Rotheray GE (1993) Colour guide to hoverfly larvae (Diptera, Syrphidae) in Britain and Europe. *Dipterist Digest* 9: 1–156.
- Rotheray GE (2019) *Ecomorphology of Cyclorrhaphan Larvae* (Diptera). Springer, Cham, Switzerland, 286 pp.
- Rotheray GE, Gilbert FS (1999) Phylogeny of Palaearctic Syrphidae (Diptera): evidence from larval stages. *Zoological Journal of the Linnean Society* 127(1): 1–112. <https://doi.org/10.1006/zjls.1998.0156>
- Rotheray GE, Gilbert F (2008) Phylogenetic relationships and the larval head of the lower Cyclorrhapha (Diptera). *Zoological Journal of the Linnean Society* 153(2): 287–323. <https://doi.org/10.1111/j.1096-3642.2008.00395.x>
- Rotheray GE, Gilbert FS (2011) *The Natural History of Hoverflies*. Forest text, UK, 334 pp.
- Rozo-Lopez P, Mengual X (2015) Mosquito species (Diptera, Culicidae) in three ecosystems from the Colombian Andes: identification through DNA barcoding and adult morphology. *ZooKeys* 513: 39–64. <https://doi.org/10.3897/zookeys.513.9561>
- Sack P (1913) Die Gattung *Merodon* Meigen (*Lampetia* Meig. olim). *Abhandlungen der Senckenbergischen Naturforschenden Gesellschaft* 31(4): 427–462.
- Simon C, Frati F, Beckenbach A, Crespi B, Liu H, Flook P (1994) Evolution, weighting, and phylogenetic utility of mitochondrial gene sequences and a compilation of conserved polymerase chain reaction primers. *Annals of the Entomological Society of America* 87(6): 651–701. <https://doi.org/10.1093/aesa/87.6.651>

- Speight MCD (2020) Species accounts of European Syrphidae, 2020. Syrph the Net, the database of European Syrphidae (Diptera), vol. 104. Syrph the Net publications, Dublin, 314 pp.
- Ståhls G, Vujić A, Pérez-Bañón C, Radenković S, Rojo S, Petanidou T (2009) COI barcodes for identification of *Merodon* hoverflies (Diptera, Syrphidae) of Lesvos Island, Greece. *Molecular Ecology Resources* 9(6): 1431–1438. <https://doi.org/10.1111/j.1755-0998.2009.02592.x>
- Stamatakis A (2014) RAxML version 8: a tool for phylogenetic analysis and post-analysis of large phylogenies. *Bioinformatics* 30(9): 1312–1313. <https://doi.org/10.1093/bioinformatics/btu033>
- Stepanenko OV, Popov GV (1997) On the immature stages biology of *Merodon nigratarsis*. *Rondani*, 1845 (Diptera: Syrphidae). *The Kharkov Entomological Society Gazette* 5(2): 40–43.
- Stuckenberg BR (1956) The immature stages of *Merodon bombiformis* Hull, a potential pest of bulbs in South Africa. *Journal of Entomological Society of South Africa* 19(2): 219–224. [https://journals.co.za/content/JESSA/19/2/AJA00128789\\_4333](https://journals.co.za/content/JESSA/19/2/AJA00128789_4333)
- Šašić Lj, Ačanski J, Vujić A, Ståhls G, Radenković S, Milić D, Obreht-Vidaković D, Đan M (2016) Molecular and morphological inference of three cryptic species within the *Merodon aureus* species group (Diptera: Syrphidae). *PLoS ONE* 11(8): e0160001. <https://doi.org/10.1371/journal.pone.0160001>
- Šašić Zorić LjZ, Ačanski JM, Đan MR, Kočiš Tubić NS, Veličković NN, Radenković SR, Vujić AA (2018) Integrative taxonomy of *Merodon caerulescens* complex (Diptera: Syrphidae) – evidence of cryptic speciation. *Matica Srpska Journal for Natural Sciences* 135: 103–118. <https://doi.org/10.2298/ZMSPN1835103S>
- Šašić Zorić Lj, Ačanski J, Vujić A, Ståhls G, Djan M, Radenković S (2020) Resolving the taxonomy of the *Merodon dobrogensis* species subgroup (Diptera: Syrphidae), with the description of a new species. *Canadian Entomologist* 152(1): 36–59. <https://doi.org/10.4039/tce.2019.72>
- Thompson FC (1999) A key to the genera of the flower flies of the Neotropical Region including the descriptions of genera and species and a glossary of taxonomic terms. *Contributions on Entomology, International* 3: 319–378.
- TIBCO Software Inc. (2018) Statistica (data analysis software system), version 13. Available from <http://tibco.com>
- van Eck A (2016) Hoverflies (Diptera, Syrphidae) new to the fauna of mainland Portugal, with an updated hoverfly checklist. *Boletín de la Sociedad Entomológica Aragonesa* 59: 187–203.
- van Eck A, Andrade RAM, van Steenis W, van der Ent L-J (2020a) New additions to the hoverflies of mainland Portugal (Diptera, Syrphidae) with some observations on flower visits. *Boletín de la Sociedad Entomológica Aragonesa* 66: 193–198.
- van Eck APW, van den Broek R, Özden Ö (2020b) Hoverflies (Diptera, Syrphidae), robber flies (Diptera, Asilidae) and soldier flies (Diptera, Stratiomyidae) along the Kyrenia Mountains of Cyprus. *Dipterists Digest* 27: 101–105.
- van Steenis J, van Zuijlen MP, van Steenis W, Makris C, van Eck A, Mengual X (2019) Hoverflies (Diptera: Syrphidae) of Cyprus: results from a collecting trip in October 2017. *Bonn zoological Bulletin* 68(1): 125–146. <https://doi.org/10.20363/BZB-2019.68.1.125>
- Veselić S, Vujić A, Radenković S (2017) Three new Eastern-Mediterranean endemic species of the *Merodon aureus* group (Diptera: Syrphidae). *Zootaxa* 4254(4): 401–434. <https://doi.org/10.11646/zootaxa.4254.4.1>
- Vujić A, Šimić S, Radenković S (1995) *Merodon desuturinus*, a new hoverfly (Diptera: Syrphidae) from the mountain Kopaonik (Serbia). *Ekologija* 30: 65–70.
- Vujić A, Pérez-Bañón C, Radenković S, Ståhls G, Rojo S, Petanidou T, Šimić S (2007) Two new species of the genus *Merodon* Meigen 1803 (Diptera: Syrphidae) from the island of Lesvos (Greece), the eastern Mediterranean. *Annales de la Société Entomologie de France* 43(3): 319–326. <https://doi.org/10.1080/00379271.2007.10697527>
- Vujić A, Marcos-García MÁ, Sarıbiyik S, Ricarte A (2011) New data for the *Merodon* Meigen 1803 fauna (Diptera: Syrphidae) of Turkey including a new species description and status changes in several taxa. *Annales de la Société Entomologique de France* 47: 78–88. <http://dx.doi.org/10.1080/00379271.2011.10697699>
- Vujić A, Radenković S, Ståhls G, Ačanski J, Stefanović A, Veselić S, Andrić A, Hayat R (2012) Systematics and taxonomy of the *ruficornis* group of genus *Merodon* (Diptera: Syrphidae). *Systematic Entomology* 37(3): 578–602. <https://doi.org/10.1111/j.1365-3113.2012.00631.x>
- Vujić A, Radenković S, Likov L, Trifunov S, Nikolić T (2013) Three new species of the *Merodon nigratarsis* group (Diptera: Syrphidae) from the Middle East. *Zootaxa* 3640(3): 442–464. <https://doi.org/10.11646/zootaxa.3640.3.7>
- Vujić A, Petanidou T, Tscheulin T, Cardoso P, Radenković S, Ståhls G, Baturan Ž, Mijatović G, Rojo S, Pérez-Bañón C, Devalez J (2016) Biogeographical patterns of the genus *Merodon* Meigen, 1803 (Diptera: Syrphidae) in islands of the eastern Mediterranean and adjacent mainland. *Insect Conservation and Diversity* 9(3): 181–191. <https://doi.org/10.1111/icad.12156>
- Vujić A, Ståhls G, Ačanski J, Rojo S, Pérez-Bañón C, Radenković S (2018a) Review of the *Merodon albifasciatus* Macquart species complex (Diptera: Syrphidae): the nomenclatural type located and its provenance discussed. *Zootaxa* 4374: 25–48.
- Vujić A, Radenković S, Likov L (2018b) Revision of the Palaearctic species of the *Merodon desuturinus* group (Diptera, Syrphidae). *Zookeys* 771: 105–138. <https://doi.org/10.3897/zookeys.771.20481>
- Vujić A, Radenković S, Likov L, Andrić A, Gilasian E, Barkalov A (2019) Two new enigmatic species of the genus *Merodon* Miegen (Diptera: Syrphidae) from the north-eastern Middle East. *Zootaxa* 4555(2): 187–208. <http://dx.doi.org/10.11646/zootaxa.4555.2.2>
- Vujić A, Likov L, Radenković S, Kočiš Tubić N, Djan M, Šebić A, Pérez-Bañón C, Barkalov A, Hayat R, Rojo S, Andrić A, Ståhls G (2020a) Revision of the *Merodon serrulatus* group (Diptera, Syrphidae). *ZooKeys* 909: 79–158. <https://doi.org/10.3897/zookeys.909.46838>
- Vujić A, Radenković S, Likov L, Andrić A, Janković M, Ačanski J, Popov G, de Courcy Williams M, Šašić Zorić Lj, Djan M (2020b) Conflict and congruence between morphological and molecular data: revision of the *Merodon constans* group (Diptera: Syrphidae). *Invertebrate Systematics* 34(4): 406–448. <https://doi.org/10.1071/IS19047>
- Vujić A, Šašić Zorić Lj, Ačanski J, Likov L, Radenković S, Djan M, Milić D, Šebić A, Ranković M, Khaghaninia S (2020c) Hide-and-seek with hoverflies: *Merodon aureus* – a species, a complex or a subgroup?. *Zoological Journal of the Linnean Society* 190(3): 974–1001. <https://doi.org/10.1093/zoolinnean/zlaa016>
- Vujić A, Speight M, de Courcy Williams M, Rojo S, Ståhls G, Radenković S, Likov L, Miličić M, Pérez-Bañón C, Falk S, Petanidou T (2020d) Atlas of the Hoverflies of Greece (Diptera: Syrphidae). Brill, Leiden / Boston, 384 pp.

Vujić A, Radenković S, Likov L, Veselić S (2021) Taxonomic complexity in the genus *Merodon* Meigen, 1803 (Diptera: Syrphidae). *Zookeys* 1031: 85–124. <https://doi.org/10.3897/zookeys.1031.62125>

WCSP (2019) World Checklist of Selected Plant Families. Facilitated by the Royal Botanic Gardens, Kew. Available from <http://wmsp.science.kew.org> [Accessed on 13.10.2020]

Zelditch ML, Swiderski DL, Sheets HD, Fink WL (2004) Geometric morphometrics for biologists: a primer. Elsevier Academic Press, London, 443 pp.

Zimsen E (1964) The type material of I. C. Fabricius. Munksgaard, Copenhagen, 656 pp.

## Supplementary material 1

### File 1

**Authors:** Vujić et al. (2021)

**Data type:** .xlsx

**Explanation note:** **Table S1.** List of hoverfly specimens used for molecular and geometric morphometric analyses.

**Copyright notice:** This dataset is made available under the Open Database License (<http://opendatacommons.org/licenses/odbl/1.0>). The Open Database License (ODbL) is a license agreement intended to allow users to freely share, modify, and use this Dataset while maintaining this same freedom for others, provided that the original source and author(s) are credited.

**Link:** <https://doi.org/10.3897/asp.79.e65861.suppl1>

## Supplementary material 2

### File 2

**Authors:** Vujić et al. (2021)

**Data type:** .pdf

**Explanation note:** **Figure S1.** Strict consensus tree of four equally parsimonious trees based on COI sequence analysis of *Merodon natans* species group. Filled circles stand for unique changes, open circles stand for non-unique changes; bootstrap values  $\geq 50$  are presented near nodes. Coloured sections indicate different *Merodon* lineages (yellow – *aureus* lineage, light green – *desuturinus* lineage, dark green – *albifrons* lineage, blue – *avidus* lineage, purple – *natans* lineage).

**Copyright notice:** This dataset is made available under the Open Database License (<http://opendatacommons.org/licenses/odbl/1.0>). The Open Database License (ODbL) is a license agreement intended to allow users to freely share, modify, and use this Dataset while maintaining this same freedom for others, provided that the original source and author(s) are credited.

**Link:** <https://doi.org/10.3897/asp.79.e65861.suppl2>

## Supplementary material 3

### File 3

**Authors:** Vujić et al. (2021)

**Data type:** .pdf

**Explanation note:** **Figure S2.** Strict consensus tree of two equally parsimonious trees based on combined COI+28S rRNA gene sequence analysis of *Merodon natans* species group. Filled circles stand for unique changes, open circles stand for non-unique changes; bootstrap values  $\geq 50$  are presented near nodes. Coloured sections indicate different *Merodon* lineages (yellow – *aureus* lineage, light green – *desuturinus* lineage, dark green – *albifrons* lineage, blue – *avidus* lineage, purple – *natans* lineage).

**Copyright notice:** This dataset is made available under the Open Database License (<http://opendatacommons.org/licenses/odbl/1.0>). The Open Database License (ODbL) is a license agreement intended to allow users to freely share, modify, and use this Dataset while maintaining this same freedom for others, provided that the original source and author(s) are credited.

**Link:** <https://doi.org/10.3897/asp.79.e65861.suppl3>